Exploring the dark universe with gravitational wave backgrounds.

PhD defense, October 14th 2024

Carlo Tasillo,
Deutsches Elektronen-Synchrotron (DESY)

Examination commission:
Dr. Kai Schmidt-Hoberg, Prof. Dr. Géraldine Servant,
Dr. Thomas Konstandin, Prof. Dr. Jochen Liske,
Prof. Dr. Oliver Gerberding

Contents.

Does NANOGrav observe a dark sector phase transition? #3

Torsten Bringmann (Oslo U.), Paul Frederik Depta (Heidelberg, Max Planck Inst.), Thomas Konstandin (DESY), Kai Schmidt-Hoberg (DESY), Carlo Tasillo (DESY) (Jun 15, 2023)

Published in: *JCAP* 11 (2023) 053 • e-Print: 2306.09411 [astro-ph.CO]

pdf DOI cite claim reference search 63 citations

Do pulsar timing arrays observe merging primordial black holes? #2

Paul Frederik Depta (Heidelberg, Max Planck Inst.), Kai Schmidt-Hoberg (DESY), Pedro Schwaller (Mainz U., Inst. Phys. and U. Mainz, PRISMA), Carlo Tasillo (DESY) (Jun 30, 2023)

e-Print: 2306.17836 [astro-ph.CO]

pdf cite claim reference search 51 citations

Hunting WIMPs with LISA: correlating dark matter and gravitational wave signals #1

Torsten Bringmann (Oslo U.), Tomás E. Gonzalo (KIT, Karlsruhe, TTP), Felix Kahlhoefer (KIT, Karlsruhe, TTP), Jonas Matuszak (KIT, Karlsruhe, TTP and RWTH Aachen U.), Carlo Tasillo (DESY) (Nov 10, 2023)

Published in: *JCAP* 05 (2024) 065 • e-Print: 2311.06346 [astro-ph.CO]

pdf DOI cite claim reference search 4 citations

Gravitational wave cosmology and dark matter

Conclusions

Gravitational wave cosmology
and dark matter.

The observable universe.

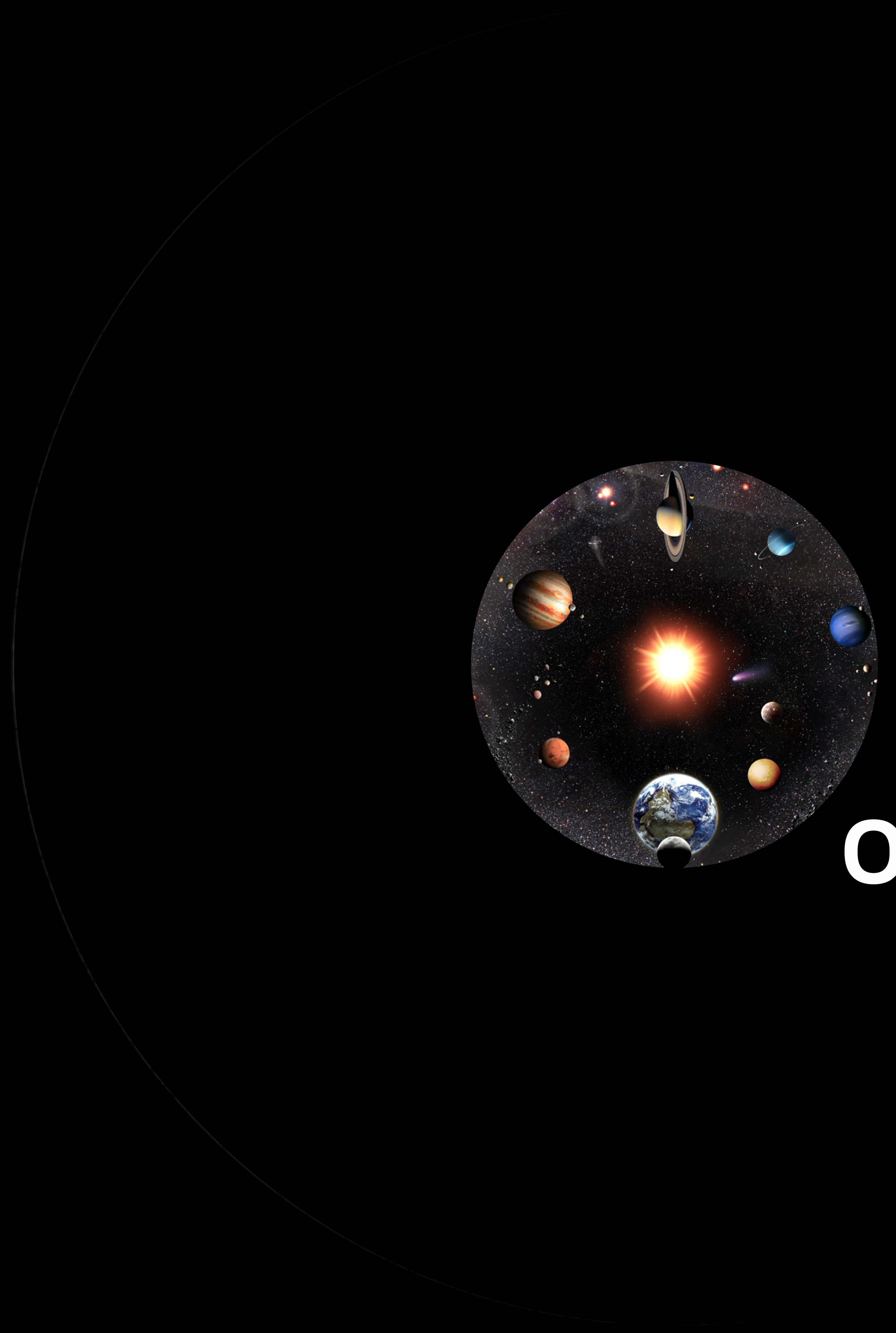

Our Solar System

[Pablo Carlos Budassi]

The observable universe.

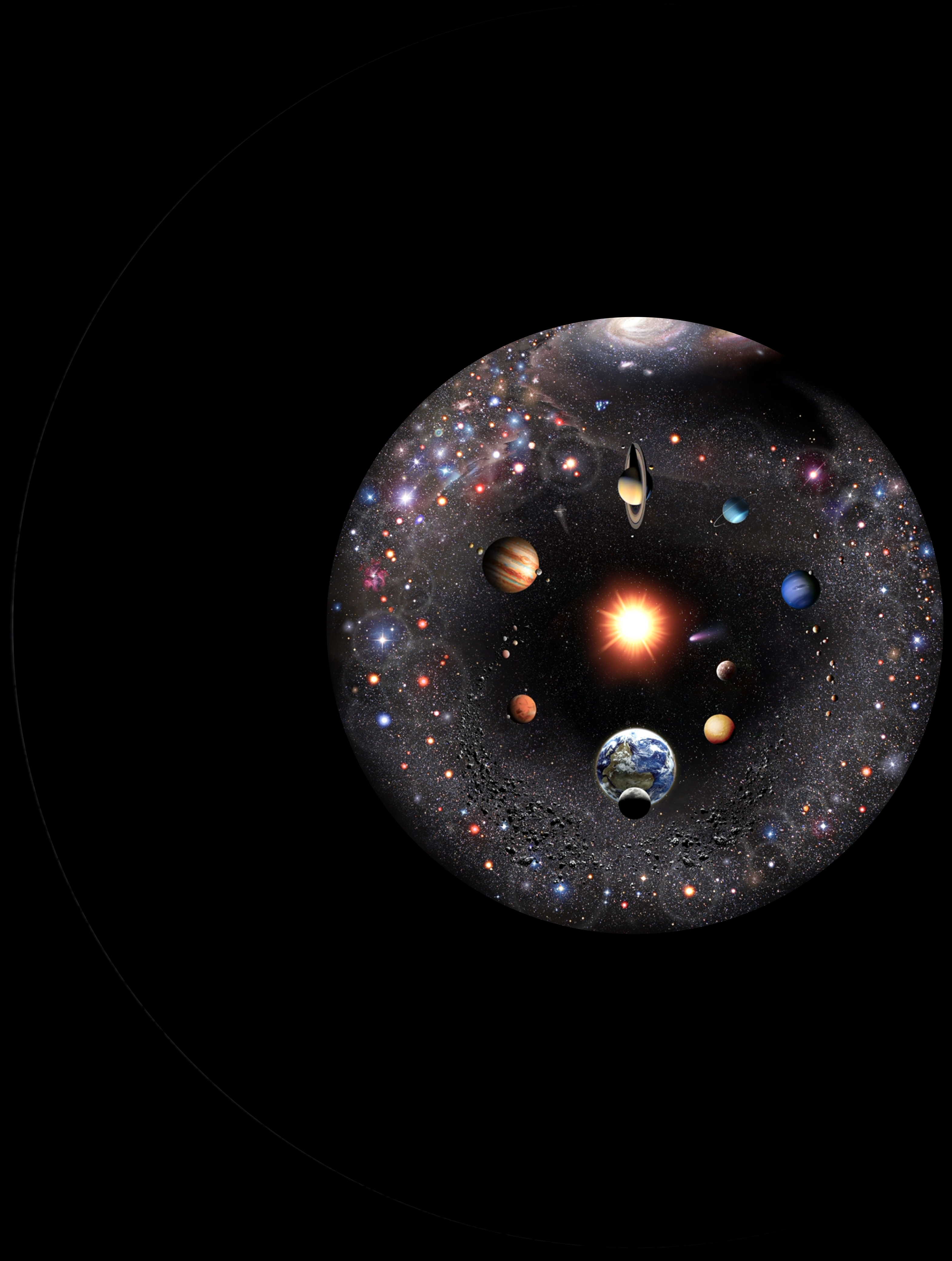

Our galaxy

[Pablo Carlos Budassi]

The observable universe.

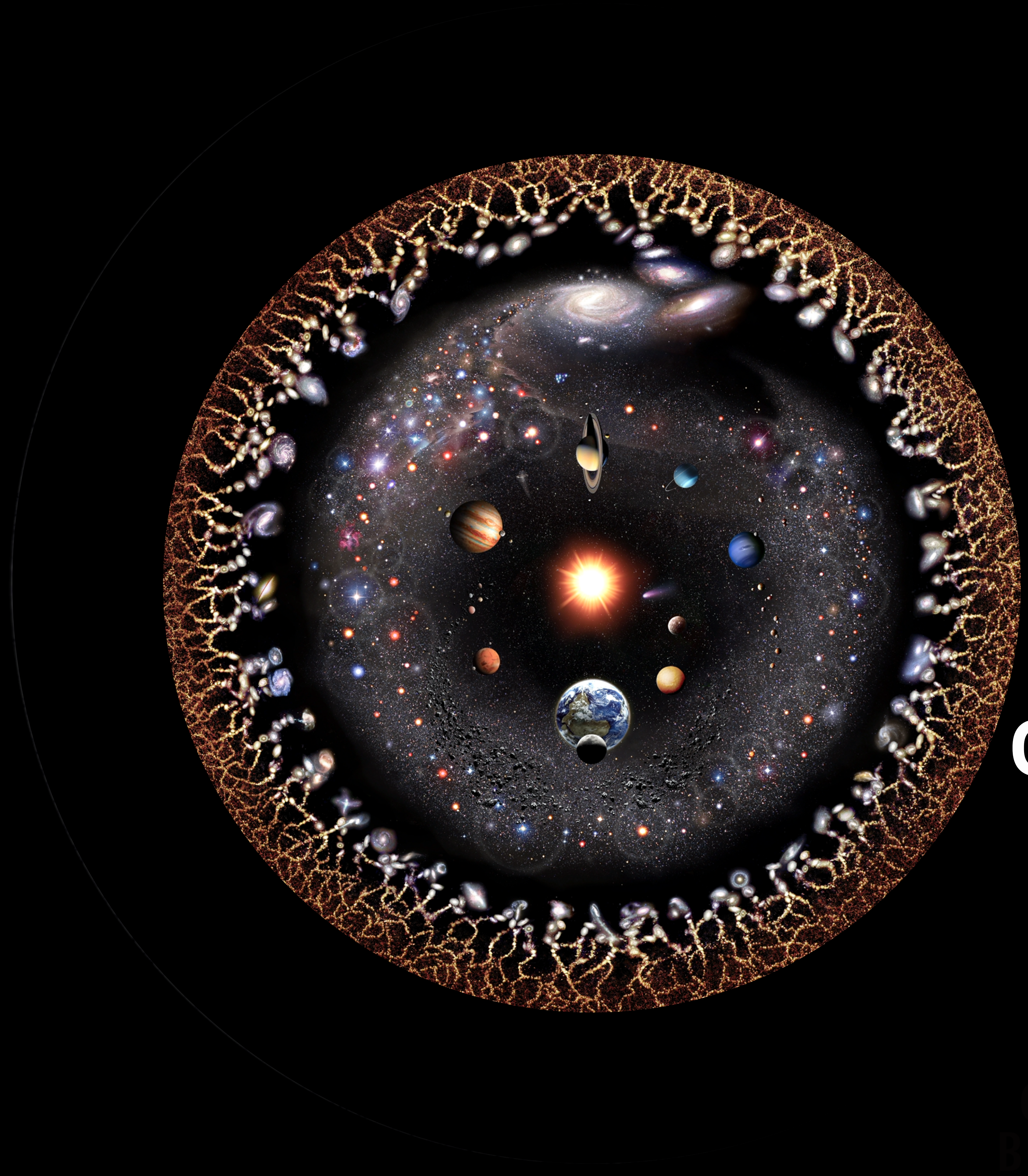

Other galaxies

[Pablo Carlos Budassi]

The observable universe.

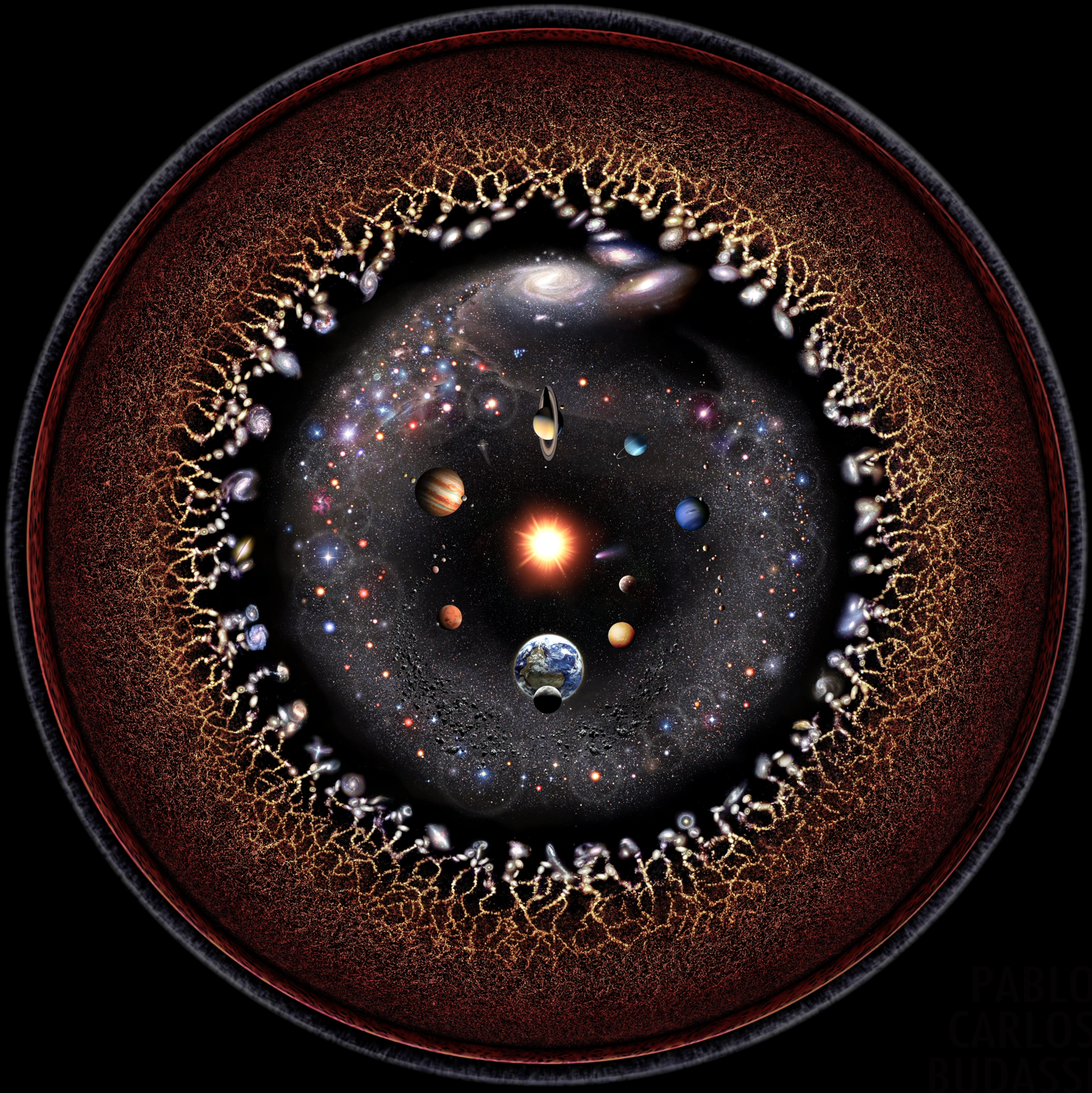

The CMB...
and the CGWB?

[Pablo Carlos Budassi]

We only understand 5%.

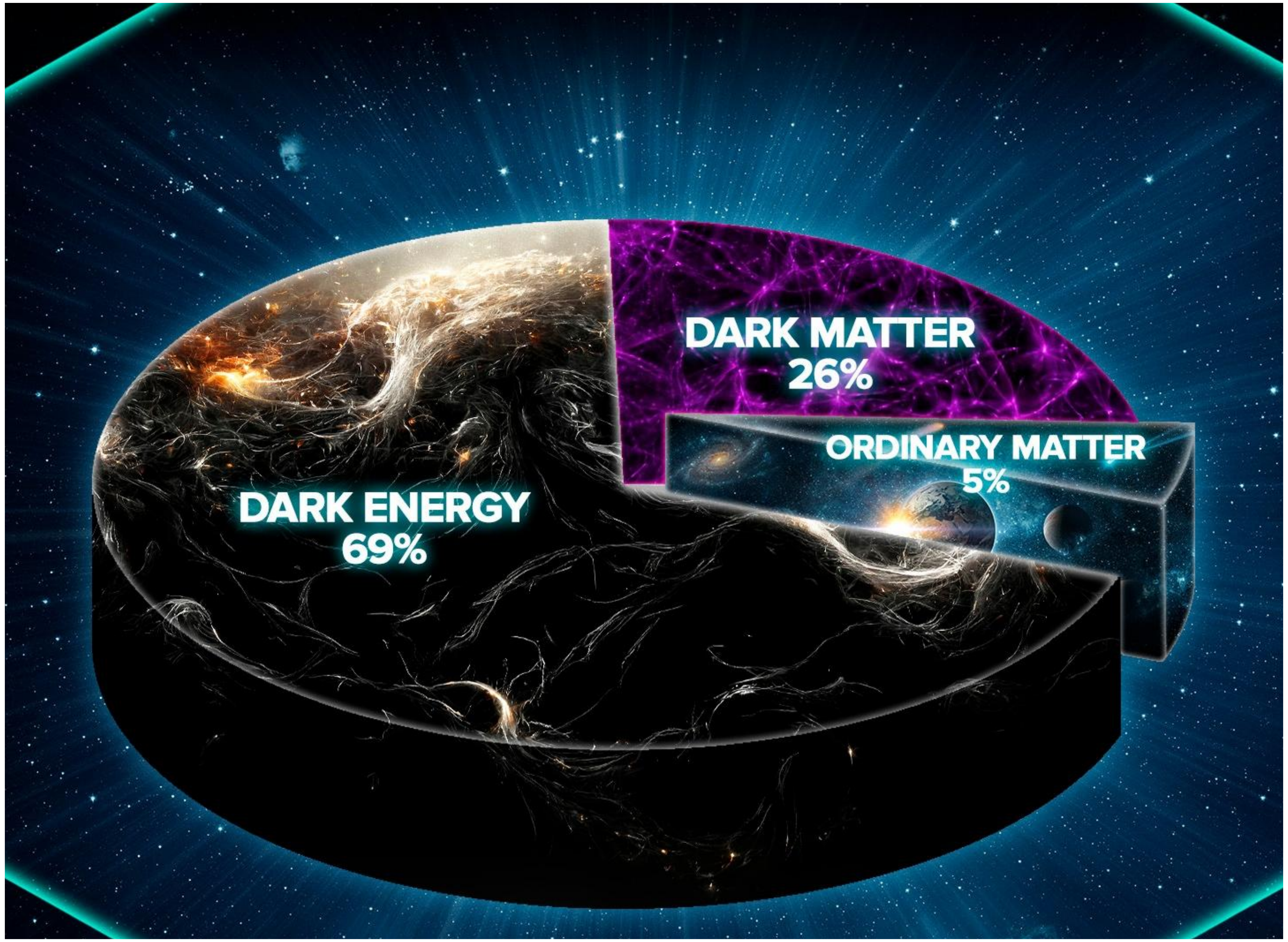

[PBS spacetime]

We need

$$\boxed{\Omega_{\rm DM} h^2 = 0.12}$$

of cold dark matter in order to explain the CMB, galaxy clustering, the bullet cluster, galactic rotation curves, …

Cirelli+ [2406.01705]


Astronomers detect 'cosmic bass note' of gravitational waves
Sound comes from the merging of supermassive black holes across the universe, according to scientists
Scientists 'hear' cosmic hum from gravitational waves
Scientists have finally 'heard' the chorus of gravitational waves that ripple through the universe
Scientists have observed for the first time the faint ripples caused by the motion of black holes that are gently stretching and squeezing everything in the universe
ASTROPHYSICS
A Background 'Hum' Pervades the Universe. Scientists Are Racing to Find Its Source
Astronomers are now seeking to pinpoint the origins of an exciting new form of gravitational waves that was announced earlier this year
For first time ever, scientists "hear" gravitational waves rippling through the universe
First Evidence of Giant Gravitational Waves Thrills Astronomers
The New York Times
The Cosmos Is Thrumming With Gravitational Waves, Astronomers Find
Radio telescopes around the world picked up a telltale hum reverberating across the cosmos, most likely from supermassive black holes merging in the early universe.
SCIENCE
Colossal gravitational waves—trillions of miles long—found for the first time
The Washington Post
In a major discovery, scientists say space-time churns like a choppy sea
Physics
Gravitational waves produce a background hum across the whole universe
After decades of searching, astronomers have found a distinctive pattern of light, from spinning stars called pulsars, that suggests huge gravitational waves are creating gentle ripples in space-time across the universe


We live in the age of GW cosmology!
Astronomers detect 'cosmic bass note' of gravitational waves
Sound comes from the merging of supermassive black holes across the universe, according to scientists
Scientists 'hear' cosmic hum from gravitational waves
Scientists have finally 'heard' the chorus of gravitational waves that ripple through the universe
For first time ever, scientists "hear" gravitational waves rippling through the universe
ASTROPHYSICS
Physics
Gravitational waves produce a background hum across the whole universe
After decades of searching, astronomers have found a distinctive pattern of light, from spinning stars called pulsars, that suggests huge gravitational waves are creating gentle ripples in space-time across the universe
In a major discovery, scientists say space-time churns like a choppy sea
The mind-bending finding suggests that everything around us is constantly being roiled by low-frequency gravitational waves
The Washington Post

Pulsar timing arrays.

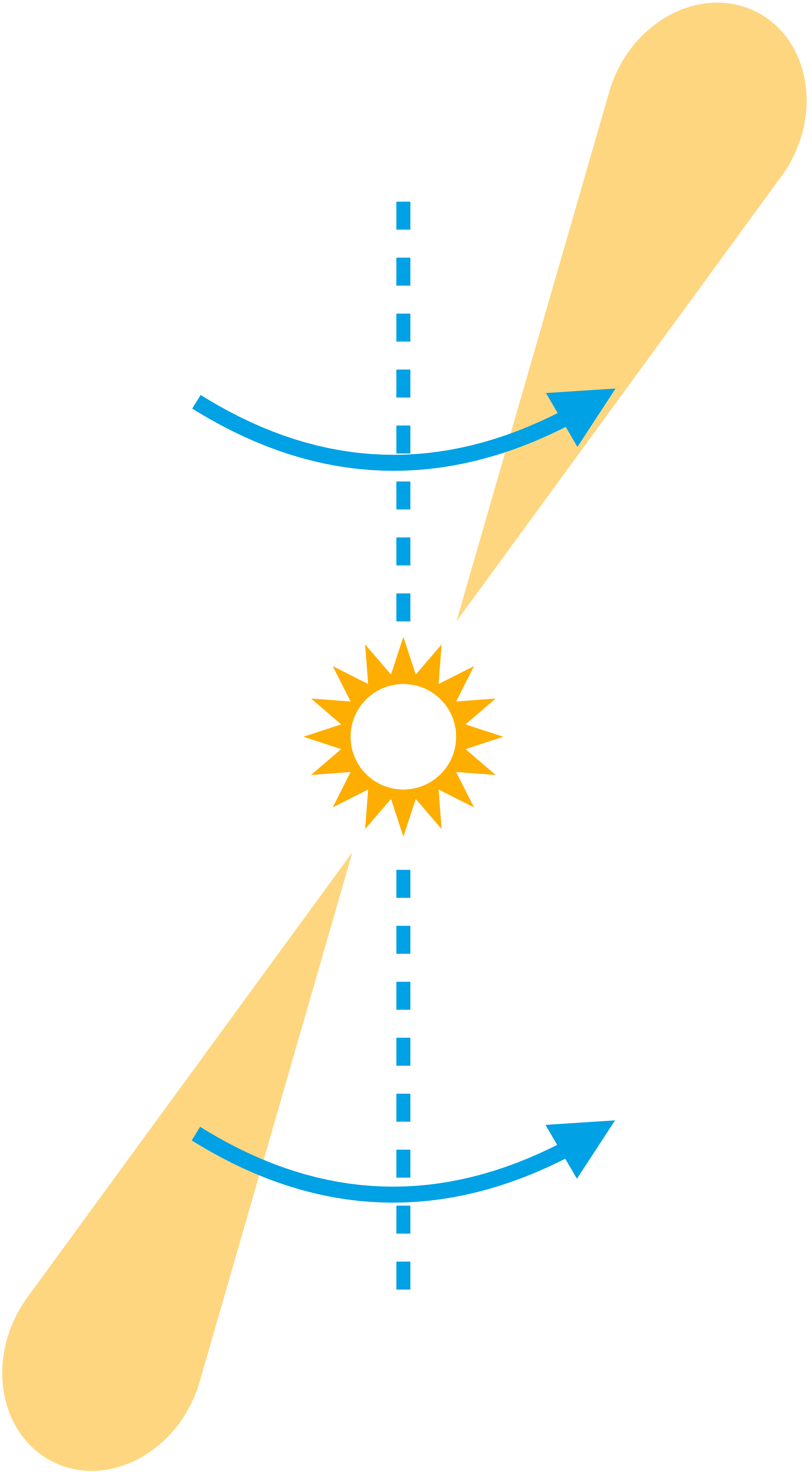

Pulsar timing arrays.

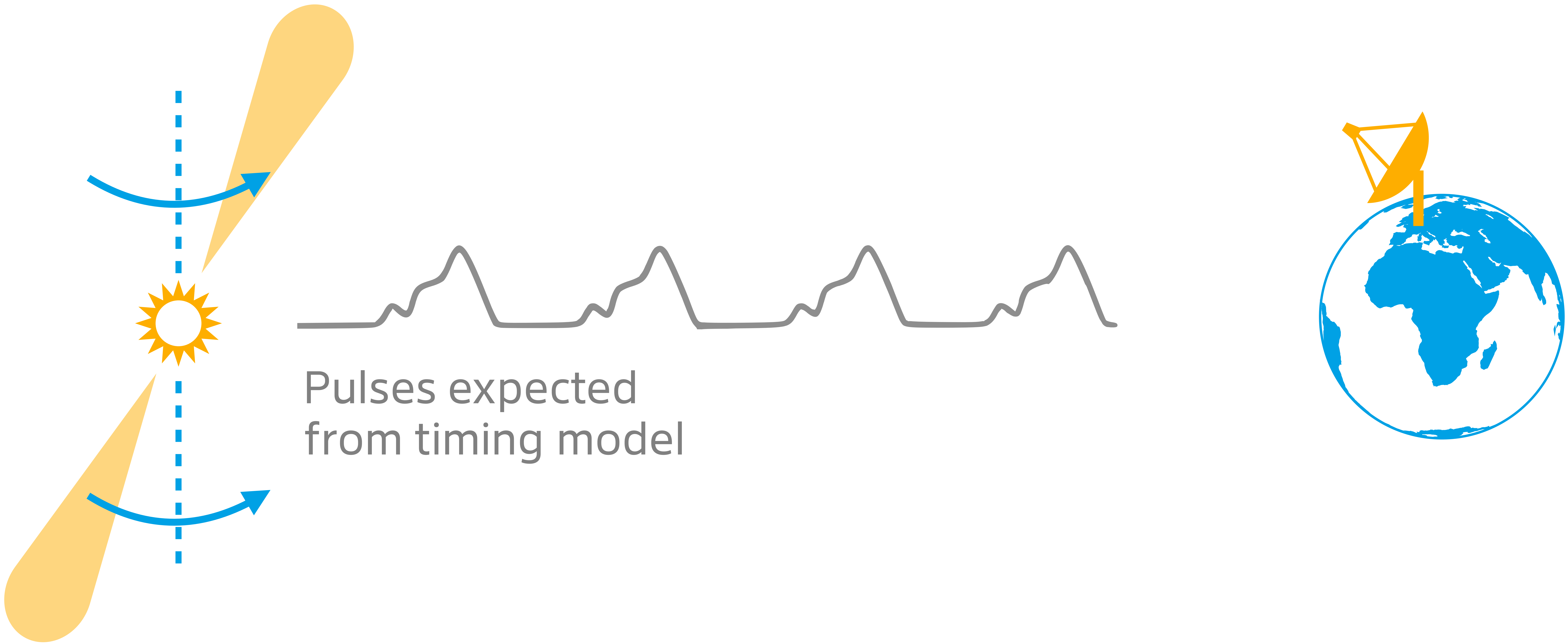

Pulsar timing arrays.

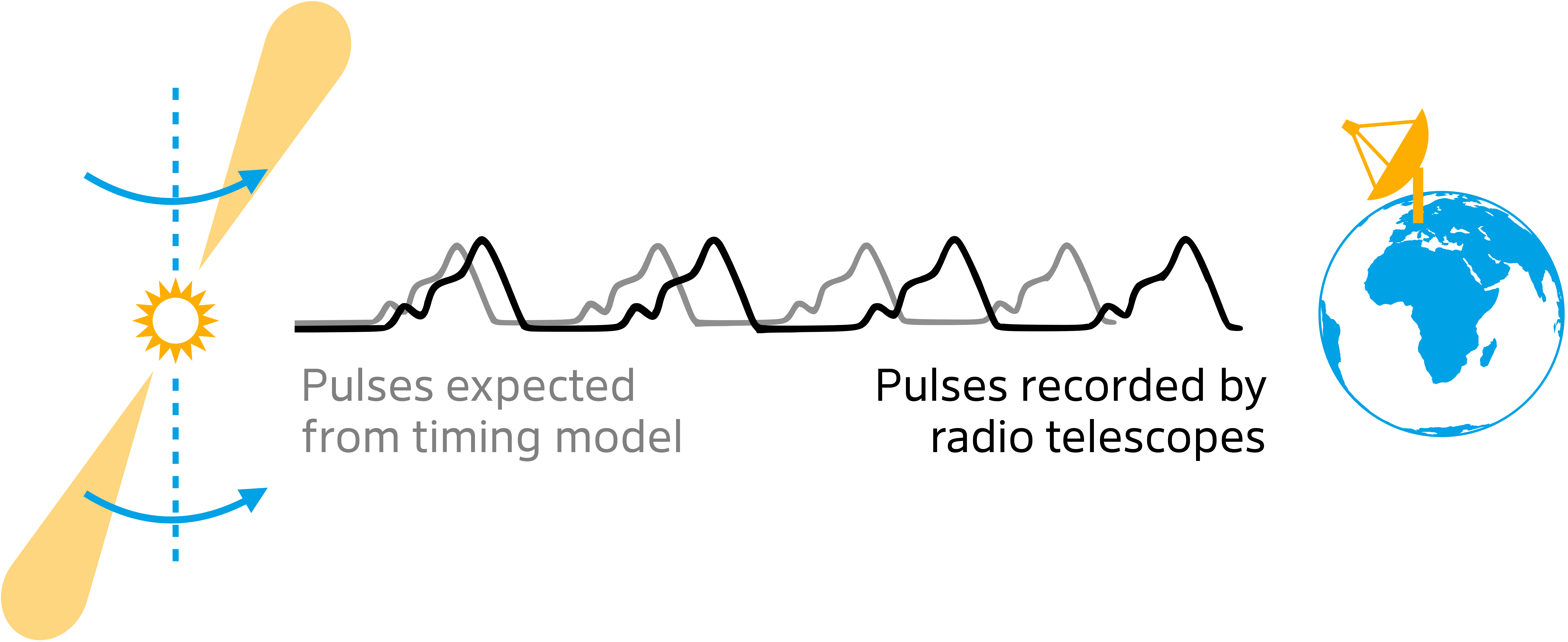

Pulsar timing arrays.

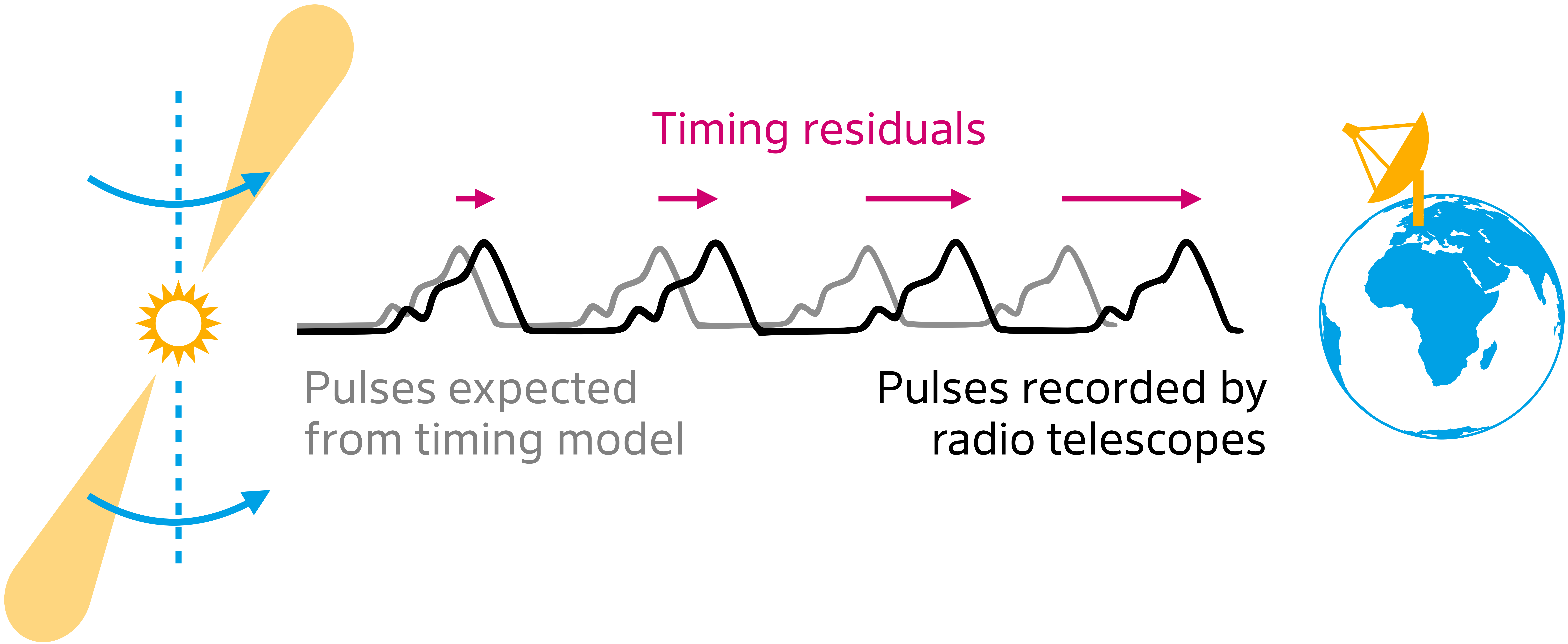

Searching for the Hellings-Downs correlation.

- Fourier analysis of timing residuals in `enterprise`
- PTAs found an underlying „common red process" among $\mathcal{O}(70)$ pulsars
- Signal could have many sources:
  - Pulsars themselves: $\mathcal{B} < 10^{-12}$
  - Clock errors: $\mathcal{B} < 10^{-8}$
  - Ephemeris errors: $\mathcal{B} < 10^{-7}$
  - GWs: $\mathcal{B} = 200 - 1000$ 

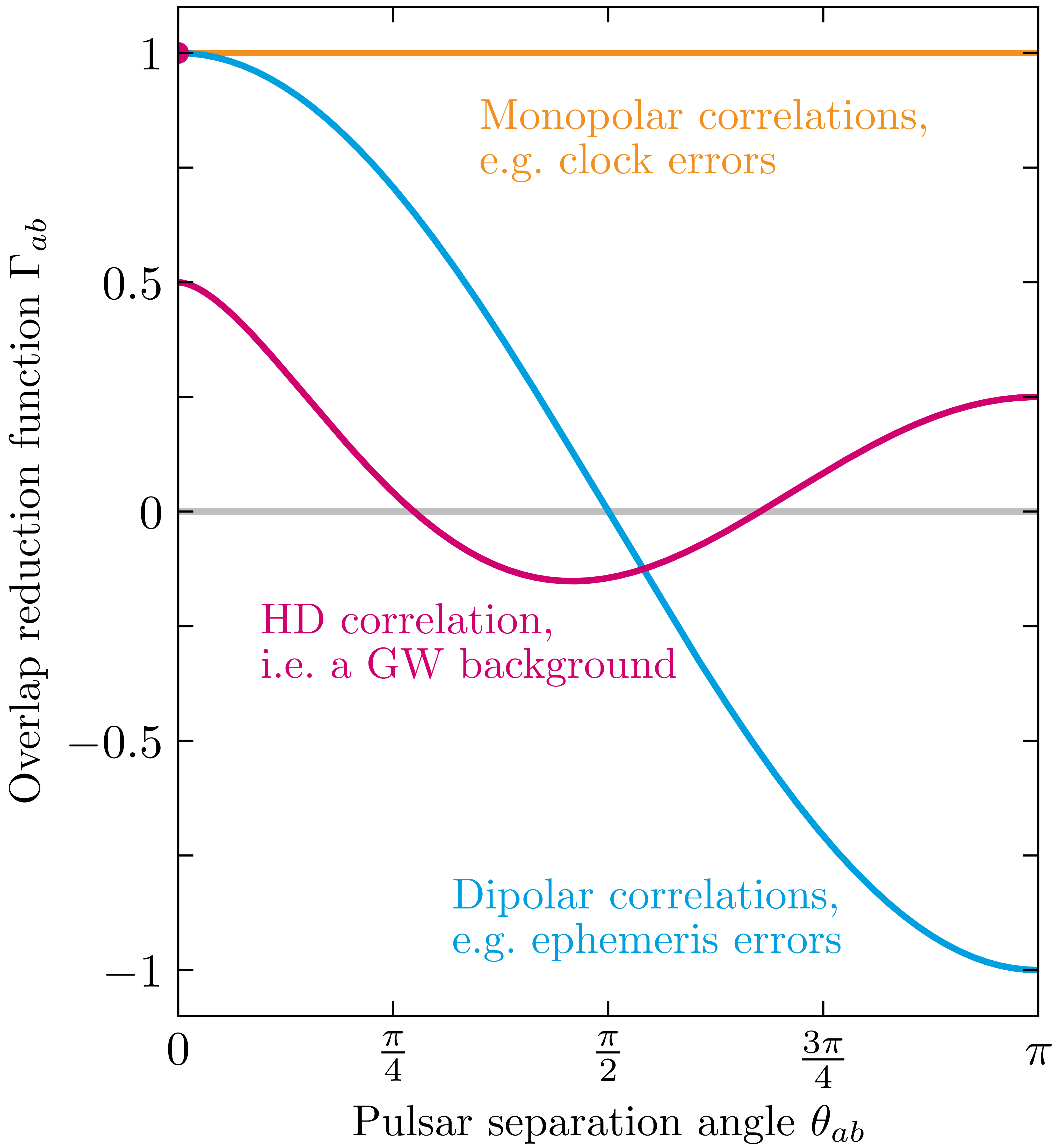

Merging supermassive black holes.

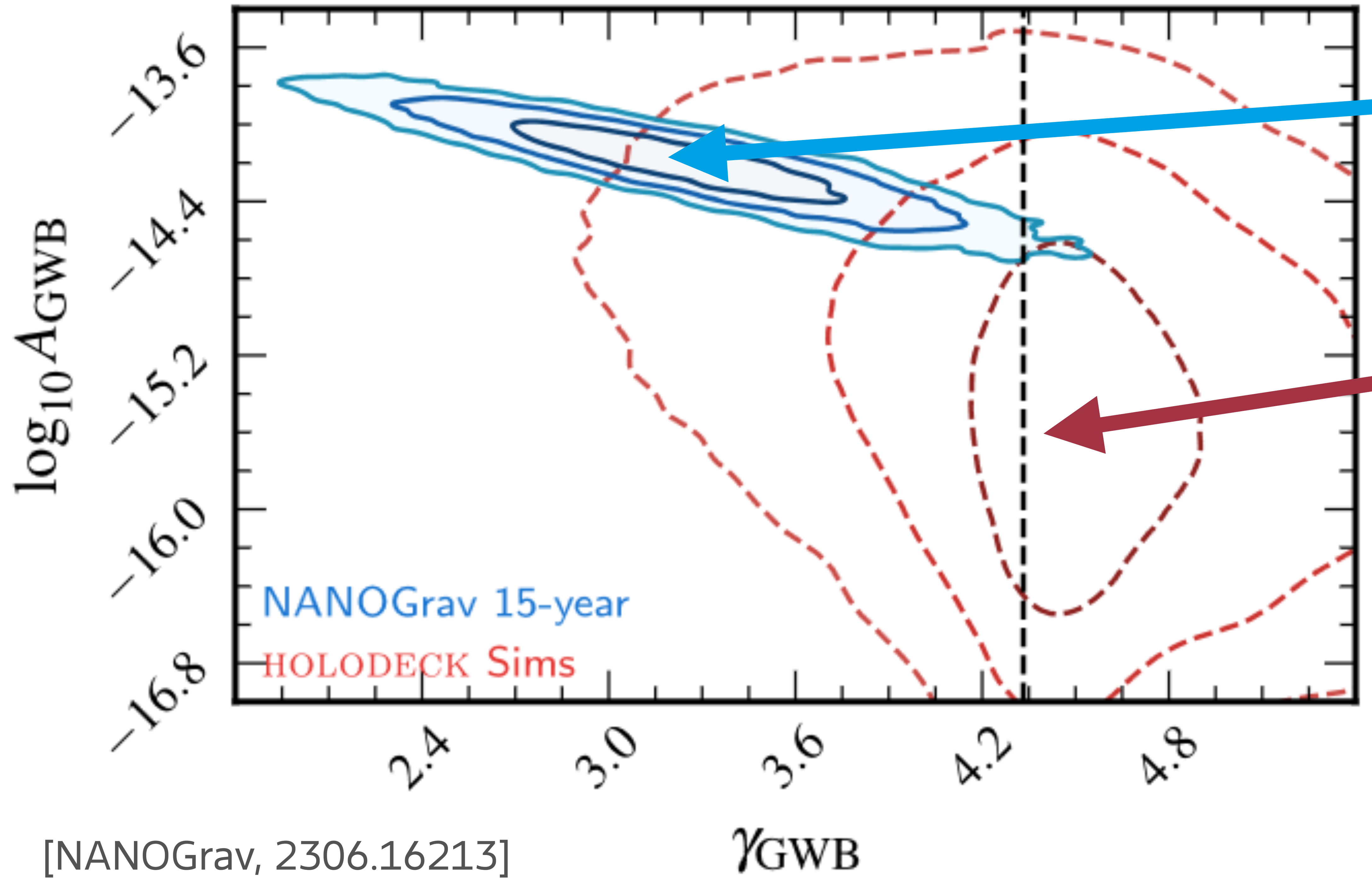

[NANOGrav, 2306.16213]

- Observed signal follows a power-law spectrum with amplitude A and slope γ
- Astrophysical simulations based on realistic BH populations predict much weaker signals with higher γ

Merging supermassive black holes.

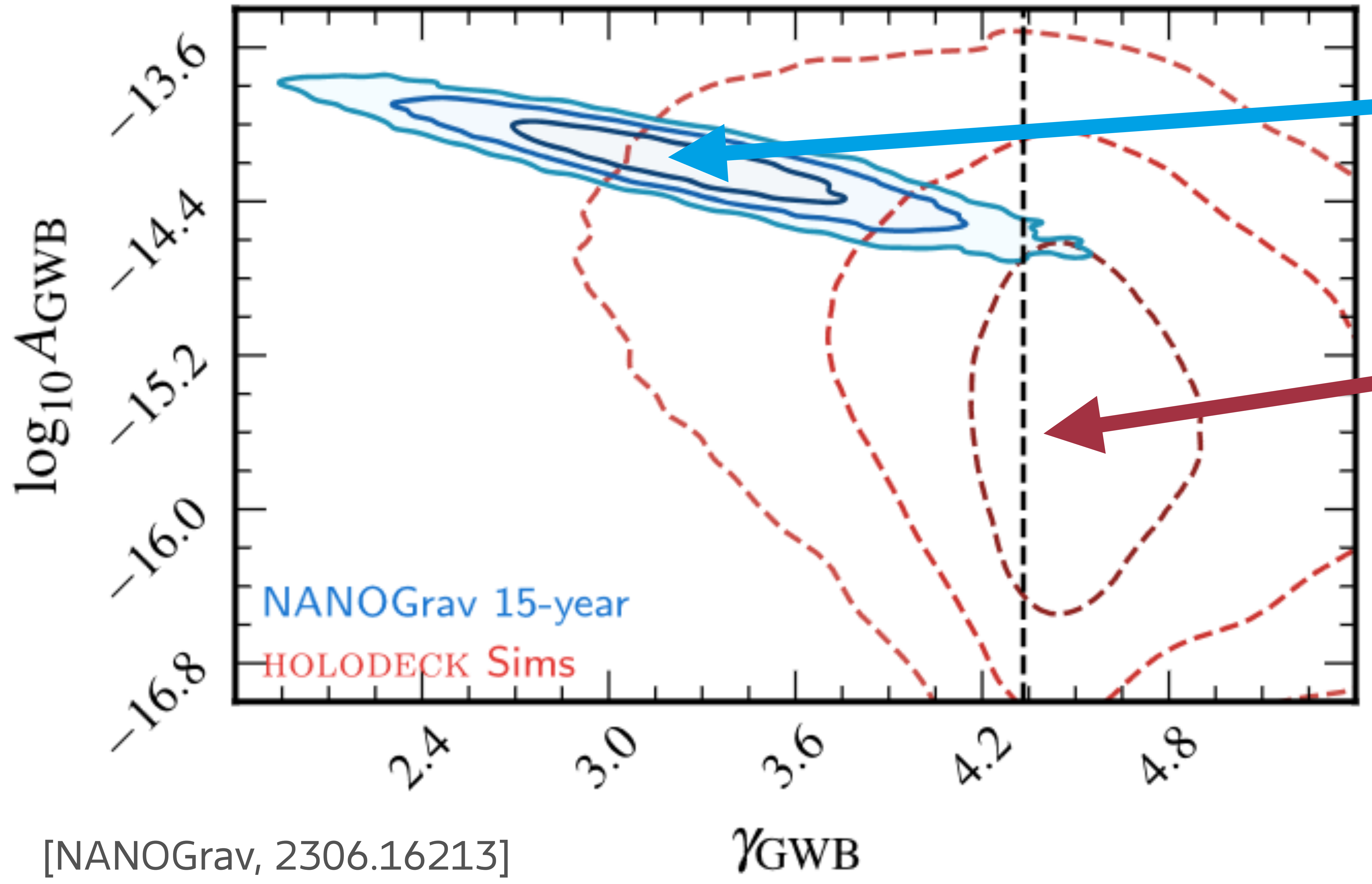

[NANOGrav, 2306.16213]

- Observed signal follows a power-law spectrum with amplitude A and slope γ
- Astrophysical simulations based on realistic BH populations predict much weaker signals with higher γ

Are there other signal sources?

Do PTAs observe a dark sector phase transition?

First-order phase transitions produce GW backgrounds.

Bubbles of the new phase nucleate, collide and perturb the plasma…

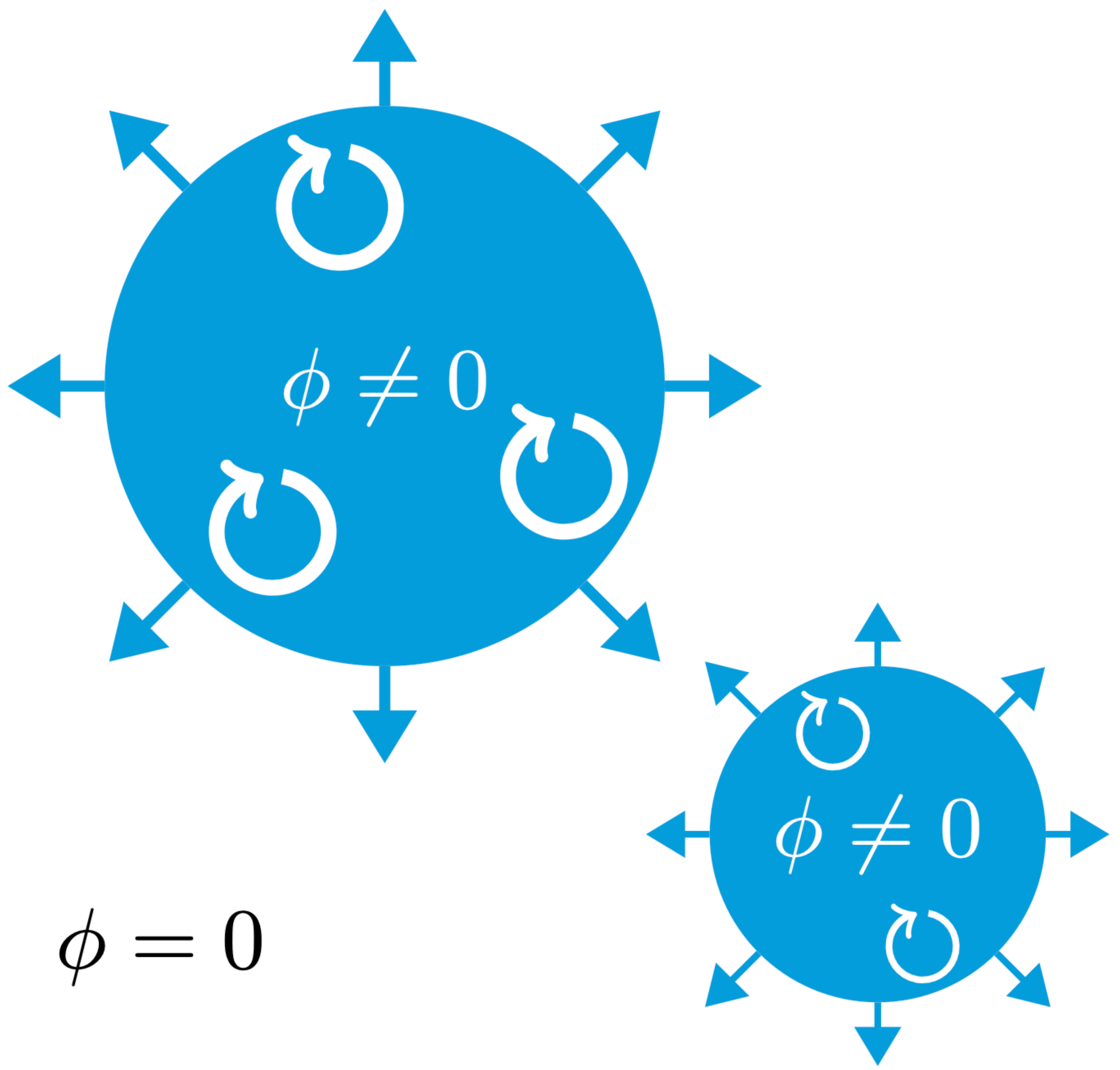

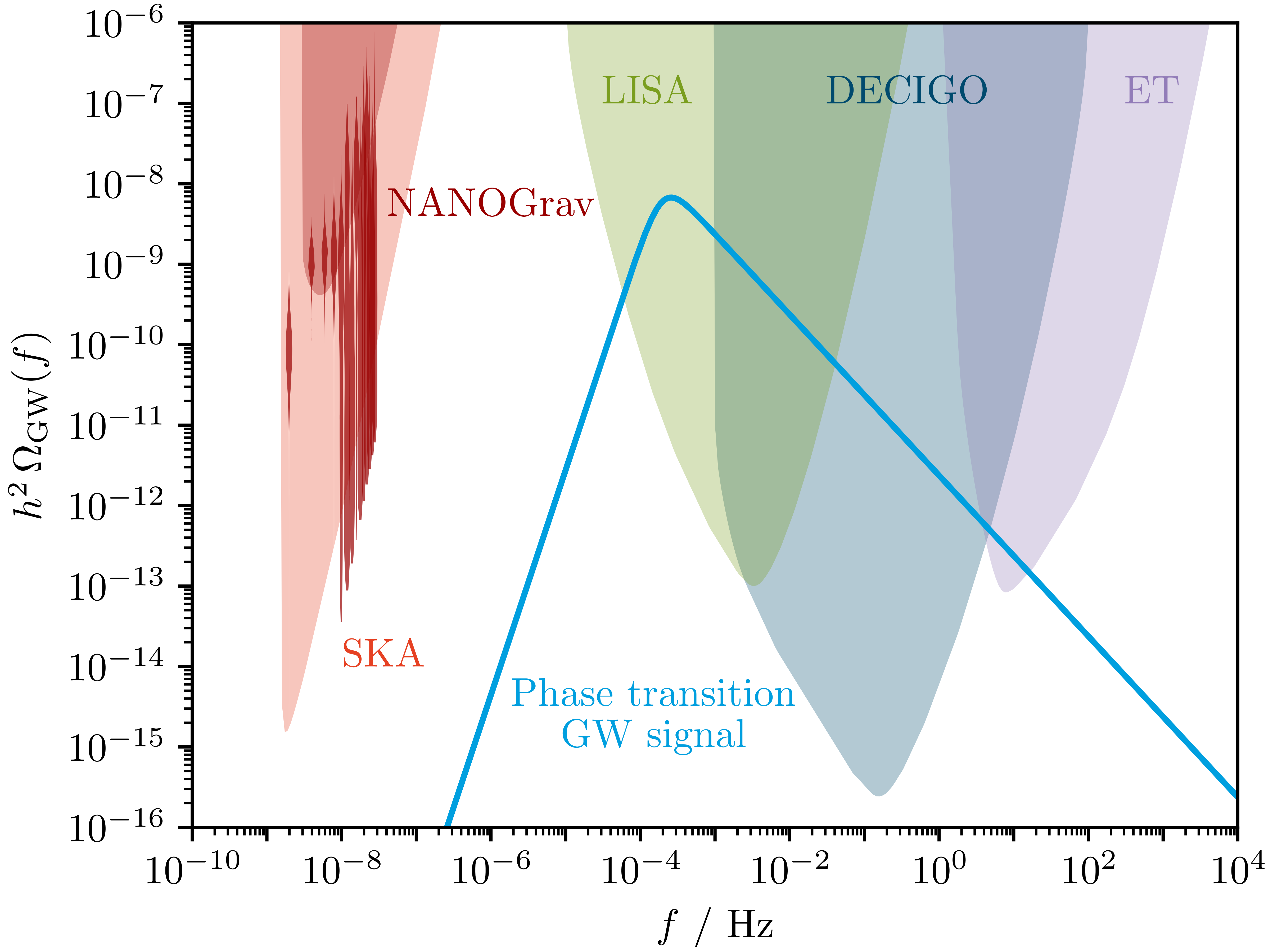

… giving rise to an observable gravitational wave background.

Parametrization of the GW signal.

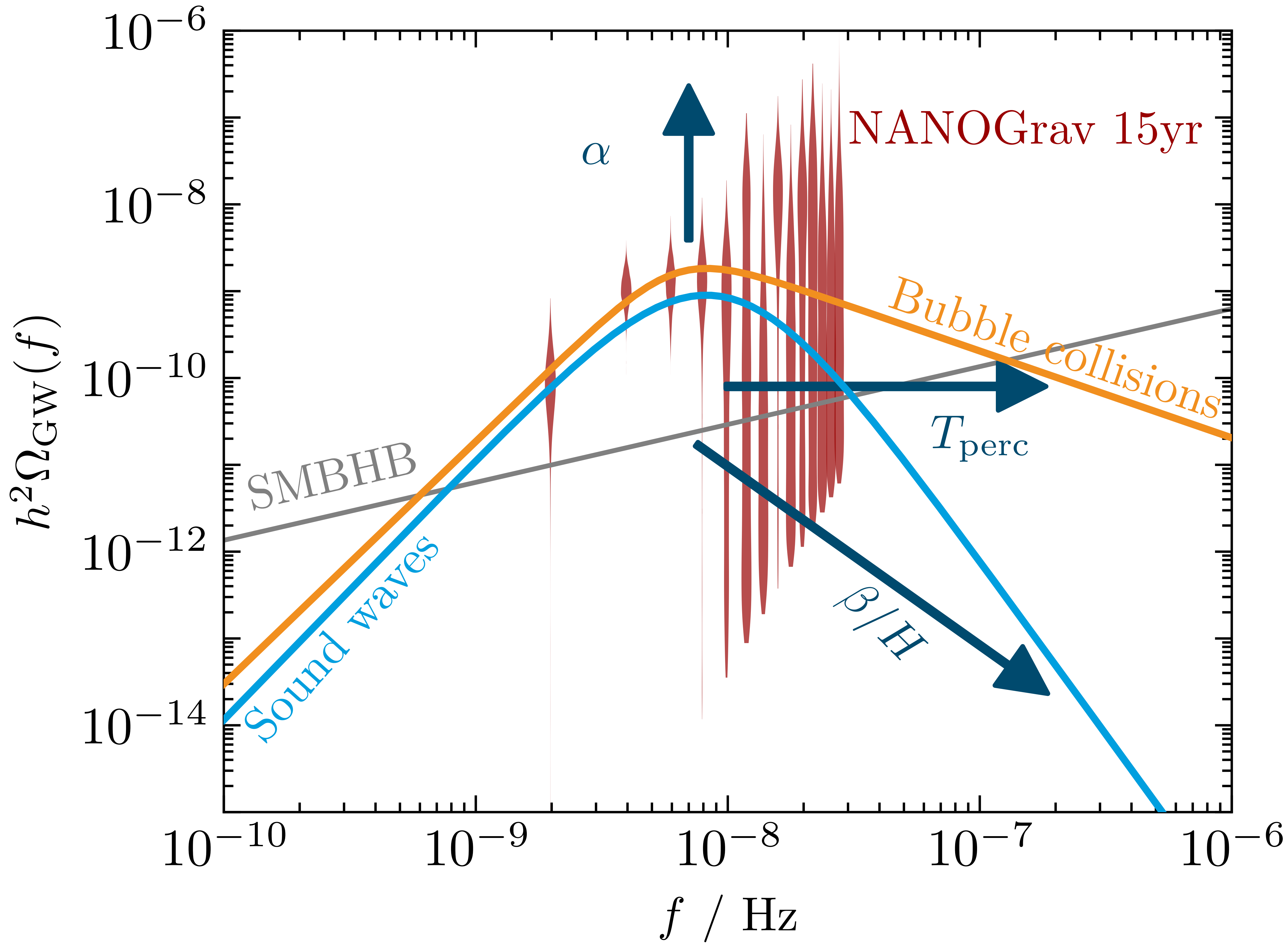

SMBHB: $A = 10^{-15.5}$, $\gamma = 13/3$

$$h^2\Omega_{\rm GW}^{\rm sw,bw}(f) \simeq 10^{-6}\left(\frac{\alpha}{\alpha+1}\right)^2\left(\frac{H}{\beta}\right)^{1,2}\mathcal{S}\left(\frac{f}{f_{\rm peak}}\right)$$

with $\quad f_{\rm peak} \simeq 0.1\,{\rm nHz} \times \dfrac{\beta}{H} \times \dfrac{T}{\rm MeV}$

To fit the new pulsar timing data:

- Strong transitions, $\alpha \approx 1$
- Slow transitions, $\beta/H \approx 10$
- Percolation around $T \approx 10\,{\rm MeV}$

Parametrization of the GW signal.

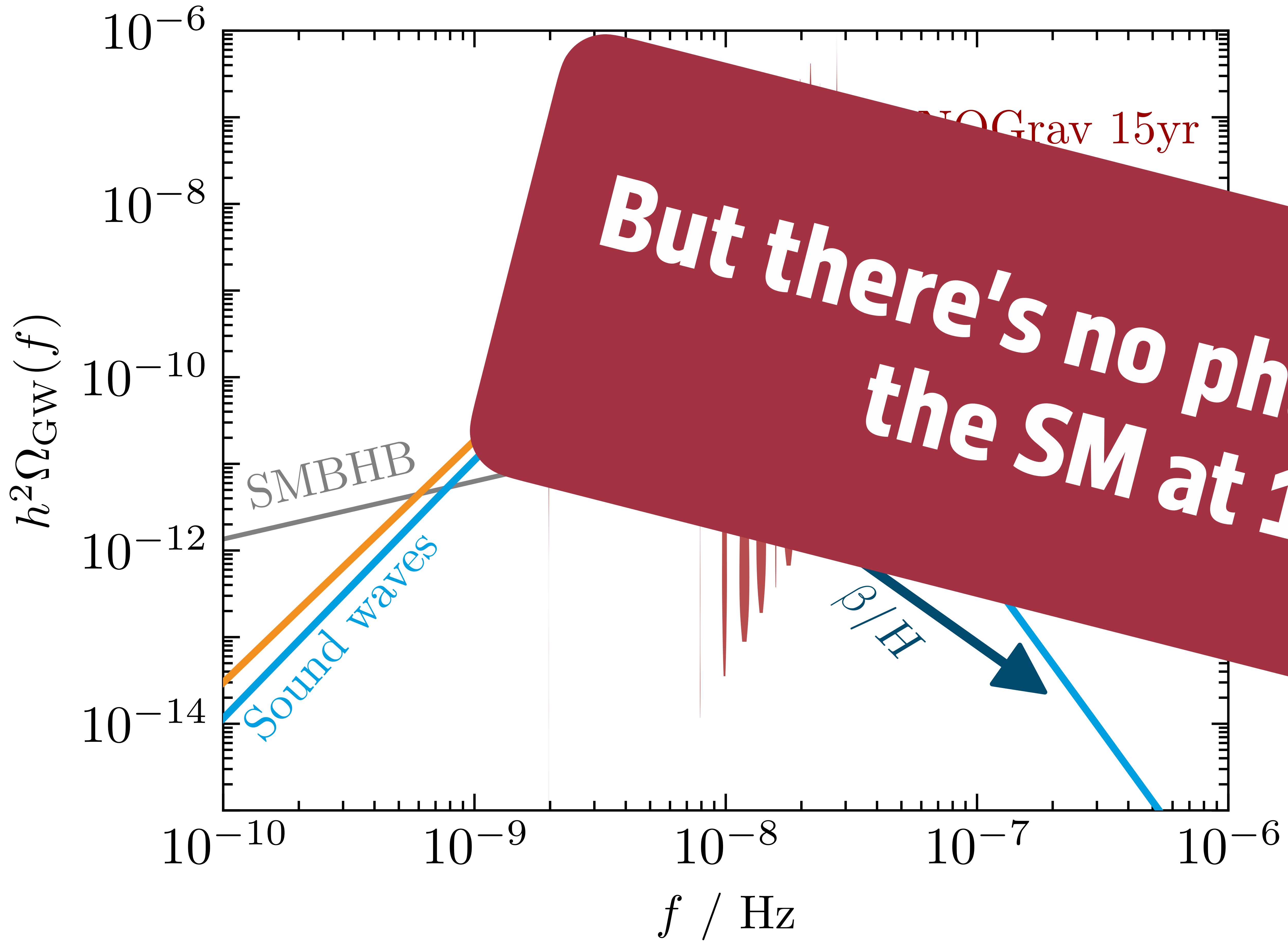

SMBHB: $A = 10^{-15.5}$, $\gamma = 13/3$

$$h^2\Omega_{\mathrm{GW}}^{\mathrm{sw,bw}}(f) \simeq 10^{-6}\left(\frac{\alpha}{\alpha+1}\right)^2\left(\frac{H}{\beta}\right)^{1,2}\mathcal{S}\left(\frac{f}{f_{\mathrm{peak}}}\right)$$

ith $f_{\mathrm{peak}} \simeq 0.1\,\mathrm{nHz} \times \dfrac{\beta}{H} \times \dfrac{T}{\mathrm{MeV}}$

But there's no phase transition in the SM at 10 MeV?!

ing data:

- $\alpha \approx 1$
- $\beta/H \approx 10$
- Percolation around $T \approx 10\,\mathrm{MeV}$

Big Bang Nucleosynthesis and the Cosmic Microwave Background.

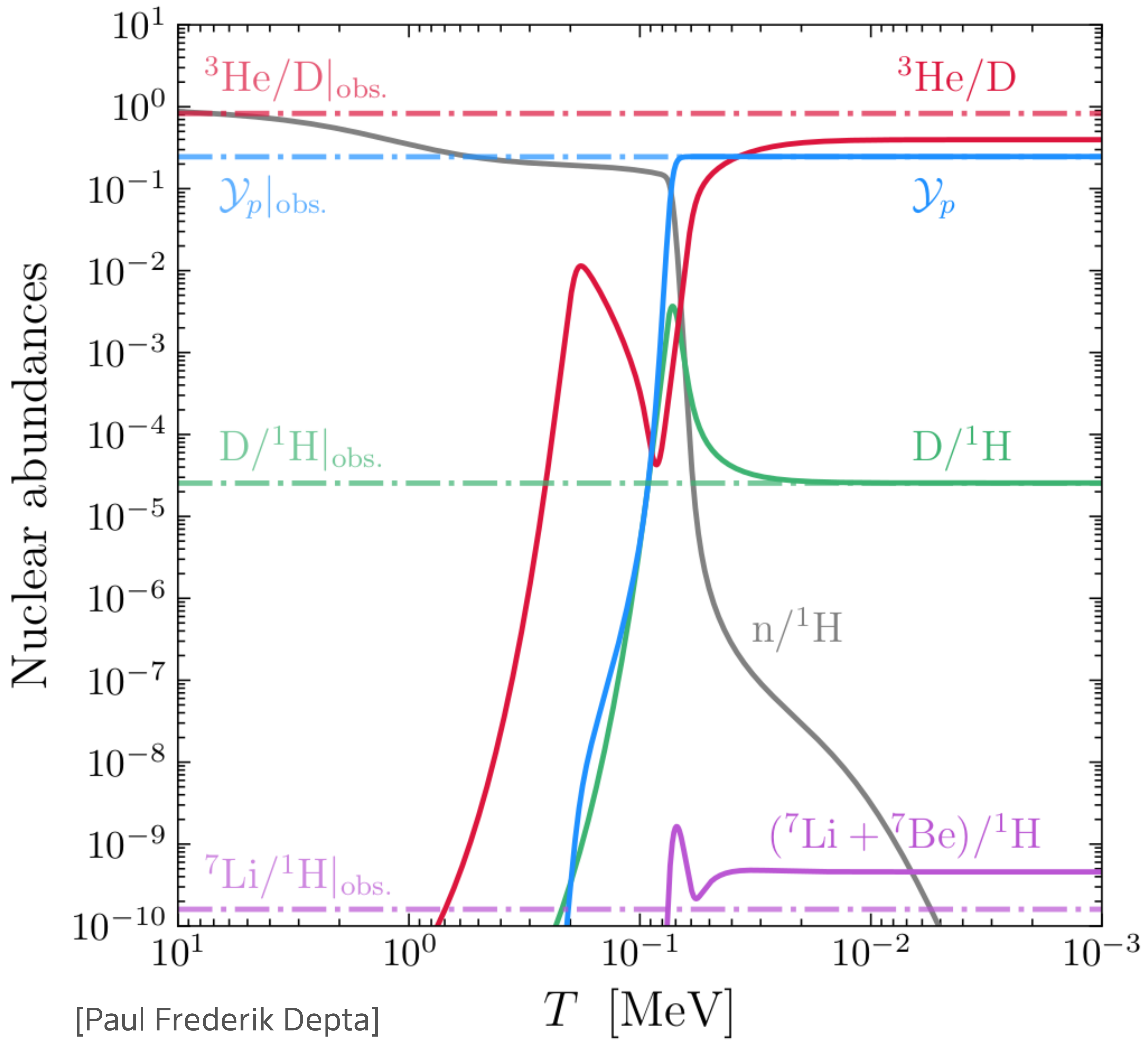

[Paul Frederik Depta]

- Observation of primordial light element abundances in good agreement with standard BBN
- $N_{\text{eff}}^{\text{BBN}} = 2.898 \pm 0.141$

Big Bang Nucleosynthesis and the Cosmic Microwave Background.

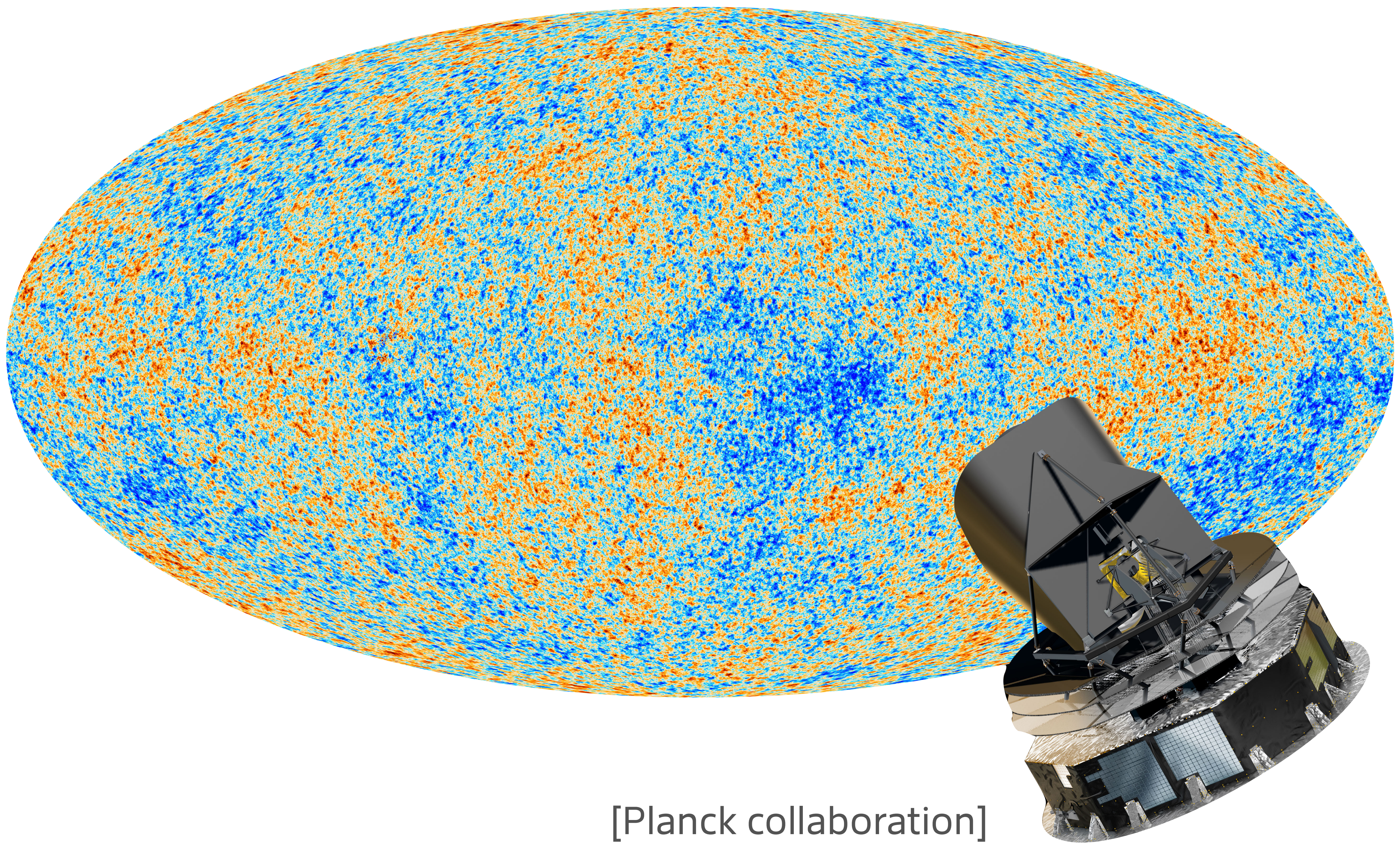

[Planck collaboration]

- Observation of primordial light element abundances in good agreement with standard BBN
- $N_{\text{eff}}^{\text{BBN}} = 2.898 \pm 0.141$
- $N_{\text{eff}}^{\text{CMB}} = 2.99 \pm 0.17$
- Consistent with $N_{\text{eff}}^{\text{SM}} = 3.044$ from 3 ν generations

Big Bang Nucleosynthesis and the Cosmic Microwave Background.

[Planck collaboration]

- Observation of primordial ... dances in ... th

  ... 141

  $N_{\text{eff}} \ldots = 2.99 \pm 0.17$

- Consistent with $N_{\text{eff}}^{\text{SM}} = 3.044$ from 3 ν generations

Thermalized BSM species at T < 1 MeV are ruled out. Before: no constraints.

Adding more Higgs bosons to the Standard model.

There’s no strong first-order phase transition at 10 MeV in the Standard Model. :(

Don’t worry, just put it in a dark sector! :)

Turning on the light in a dark sector.

Stable dark sector

Additional DS energy density accelerates Hubble expansion via

$$\Delta N_{\text{eff}} \gtrsim 6 \times \alpha$$

But we need $\alpha \simeq 1$...

$$\Delta N_{\text{eff}} < 0.22 \,@\, 95\,\%\ \text{C.L.}$$

Decaying dark sector

Can the dark sector decay quickly enough to the SM to get around BBN and CMB constraints?

Stable dark sector phase transition: A naive fit.

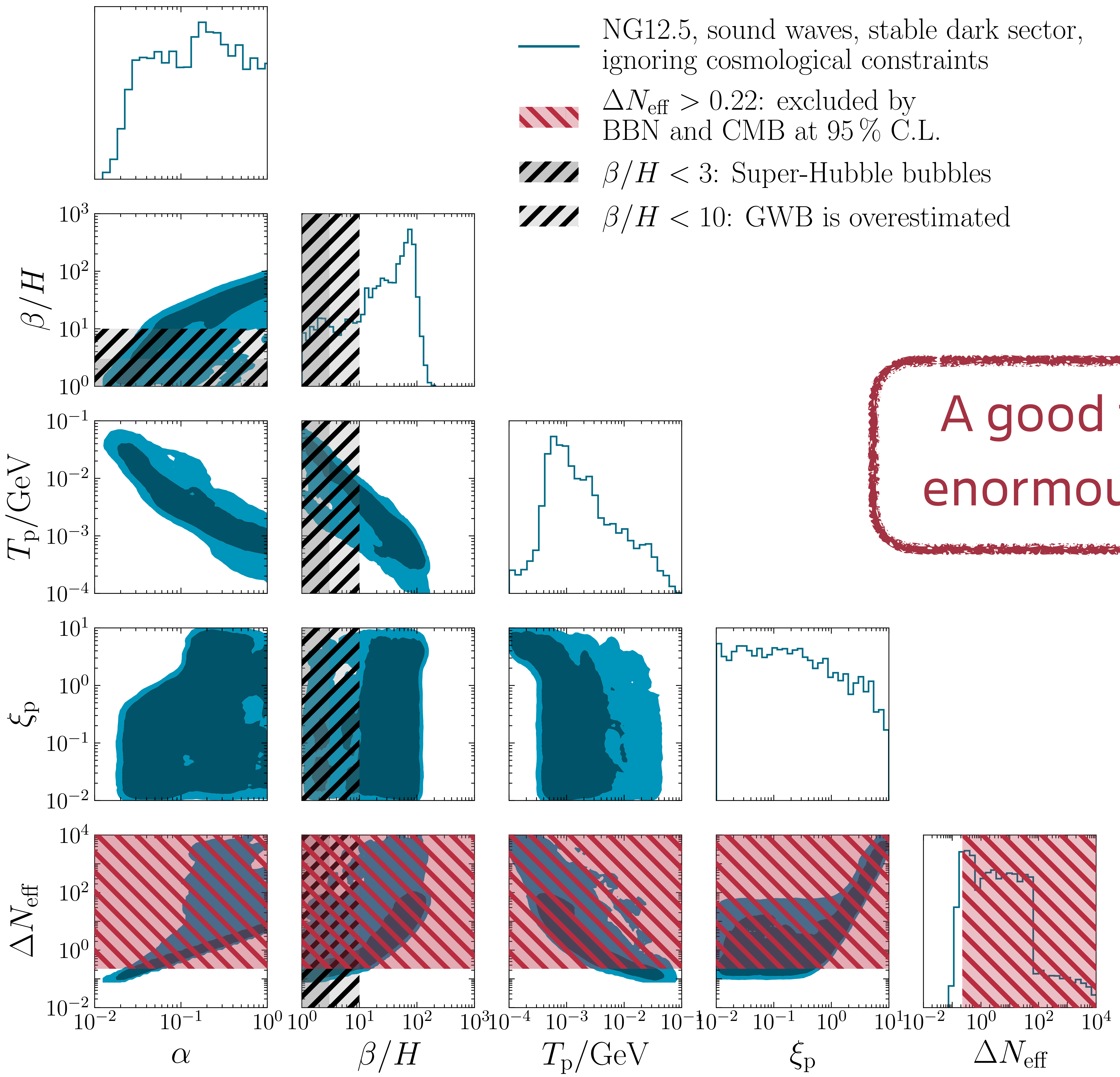

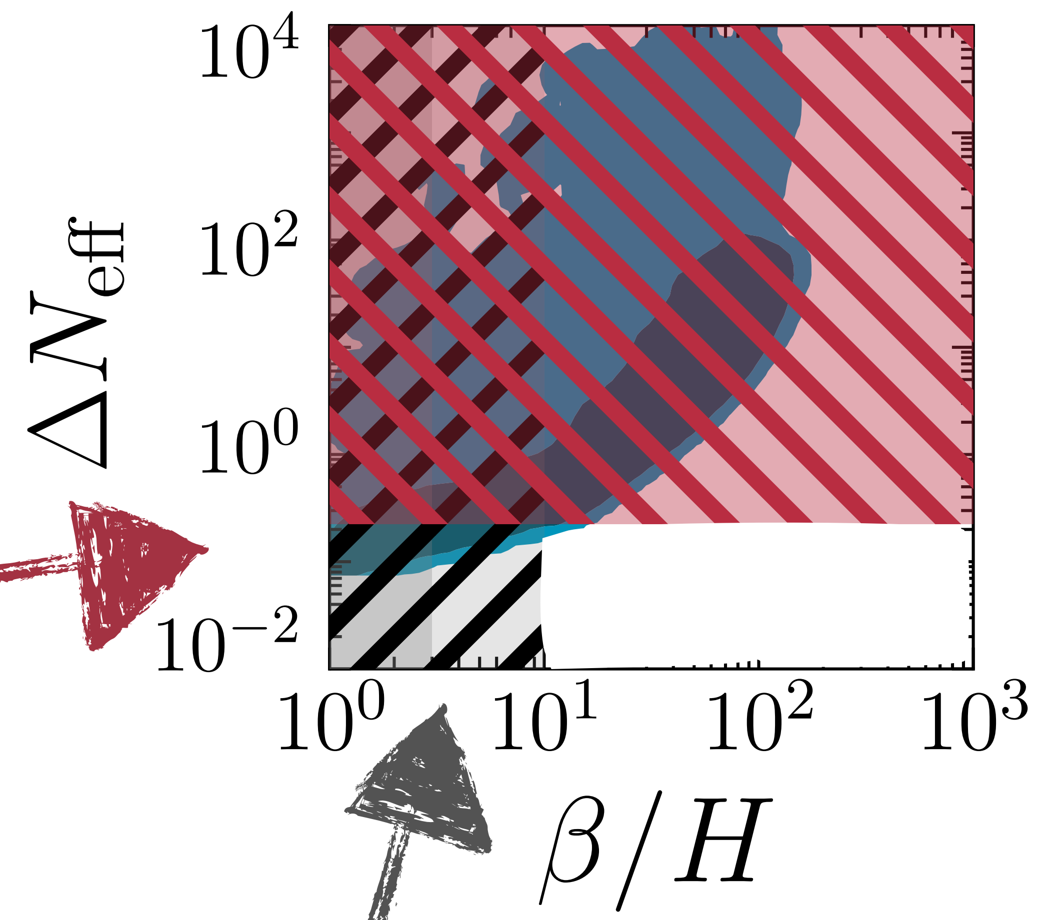

A good fit would require enormous $\Delta N_{\rm eff} \gg 0.22$

Giant bubble sizes would be needed, violating causality & questioning validity of GW predictions

Global fits.

- Combined PTA and BBN/CMB likelihoods in `enterprise`
- $\beta/H > 1$: Would fit the data if GW spectrum were reliable
- $\beta/H > 10$: Shot noise because not explaining PTA data is better than messing up BBN + CMB

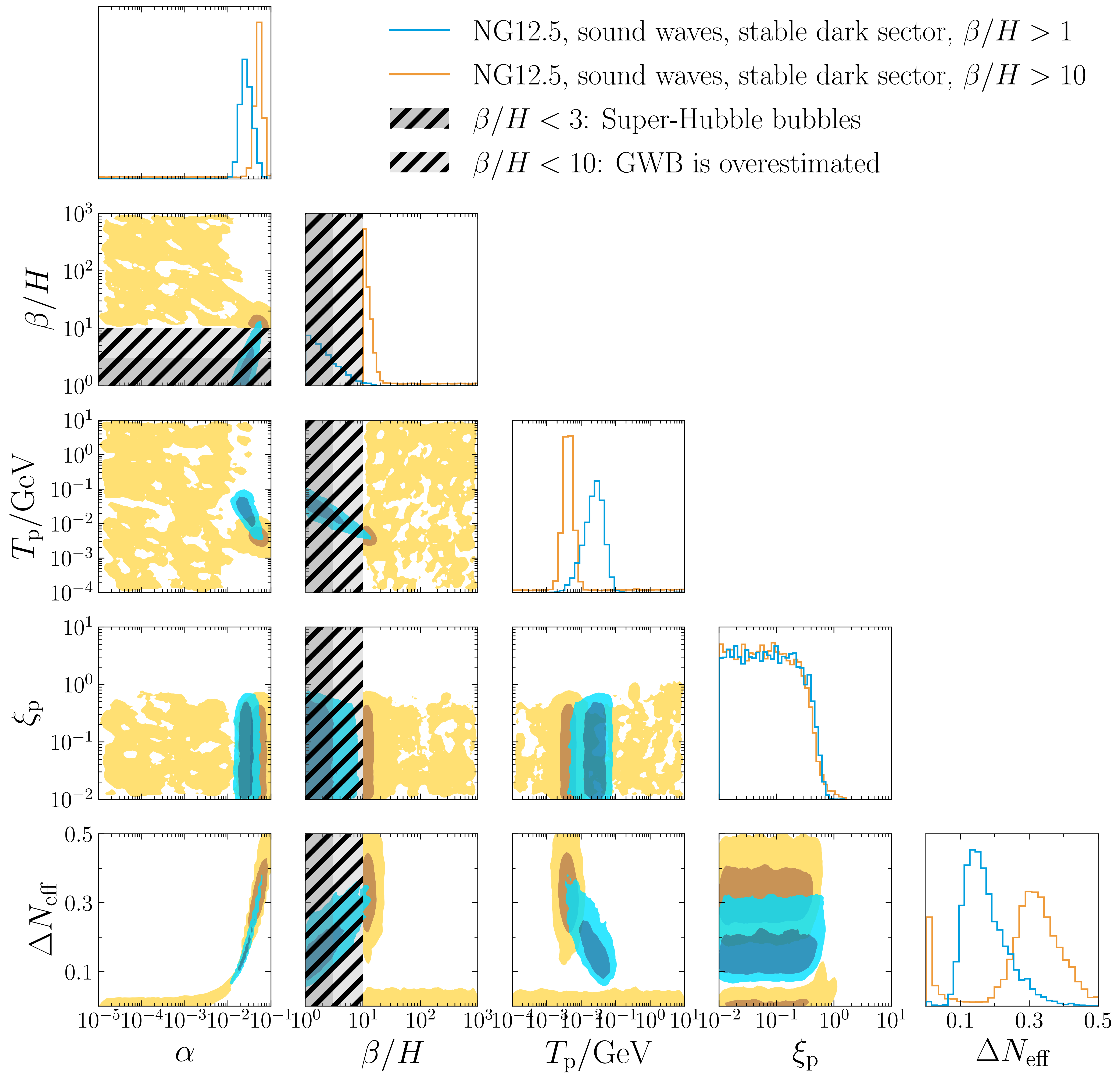

Global fits.

- Combined PTA and BBN/CMB likelihoods in `enterprise`
- $\beta/H > 1$: Would f... GW sp...
- $\beta/H > ...$ ... becaus... data is ... up BBN + CMB

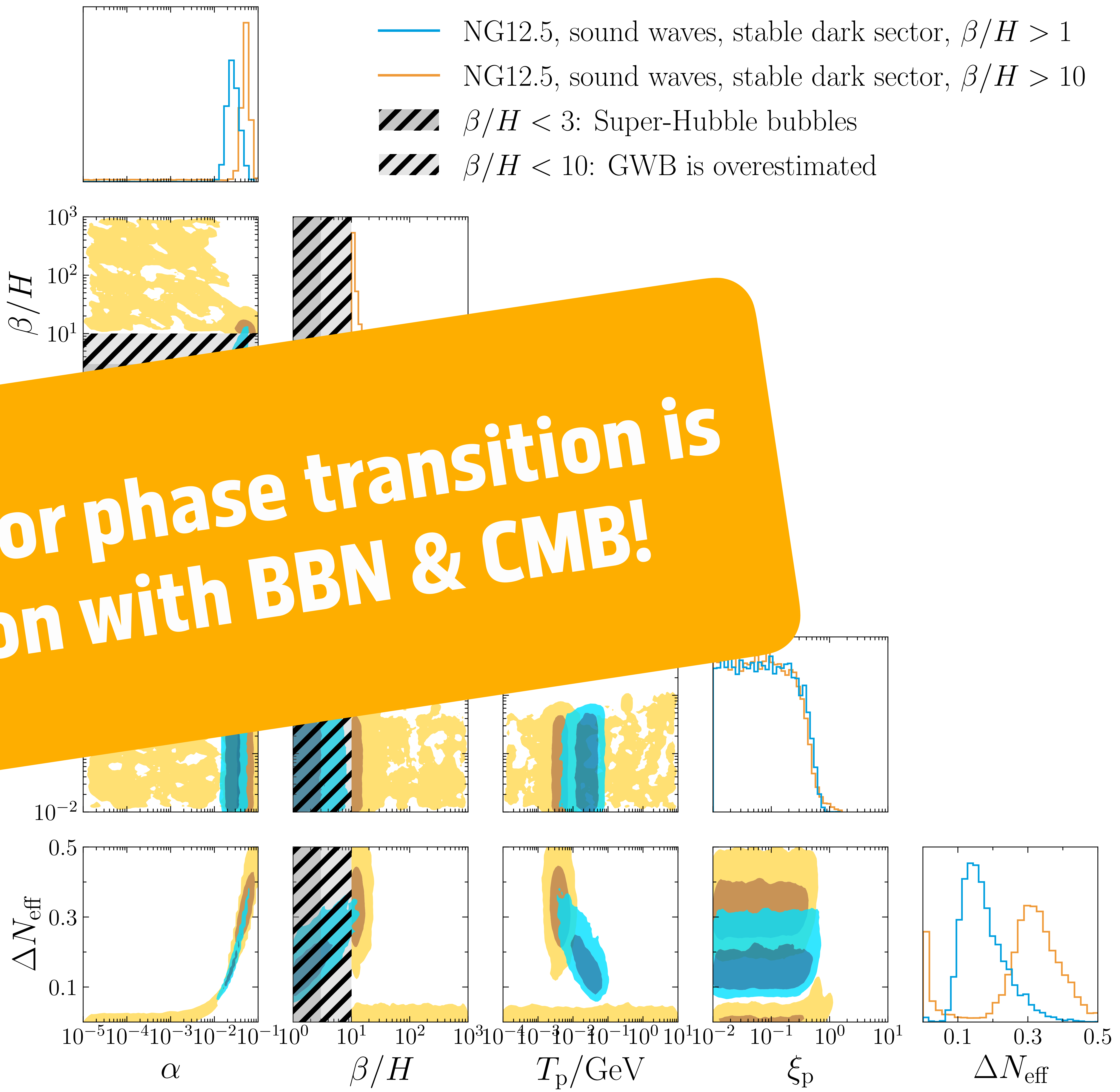

A stable dark sector phase transition is in strong tension with BBN & CMB!

Decays to the rescue.

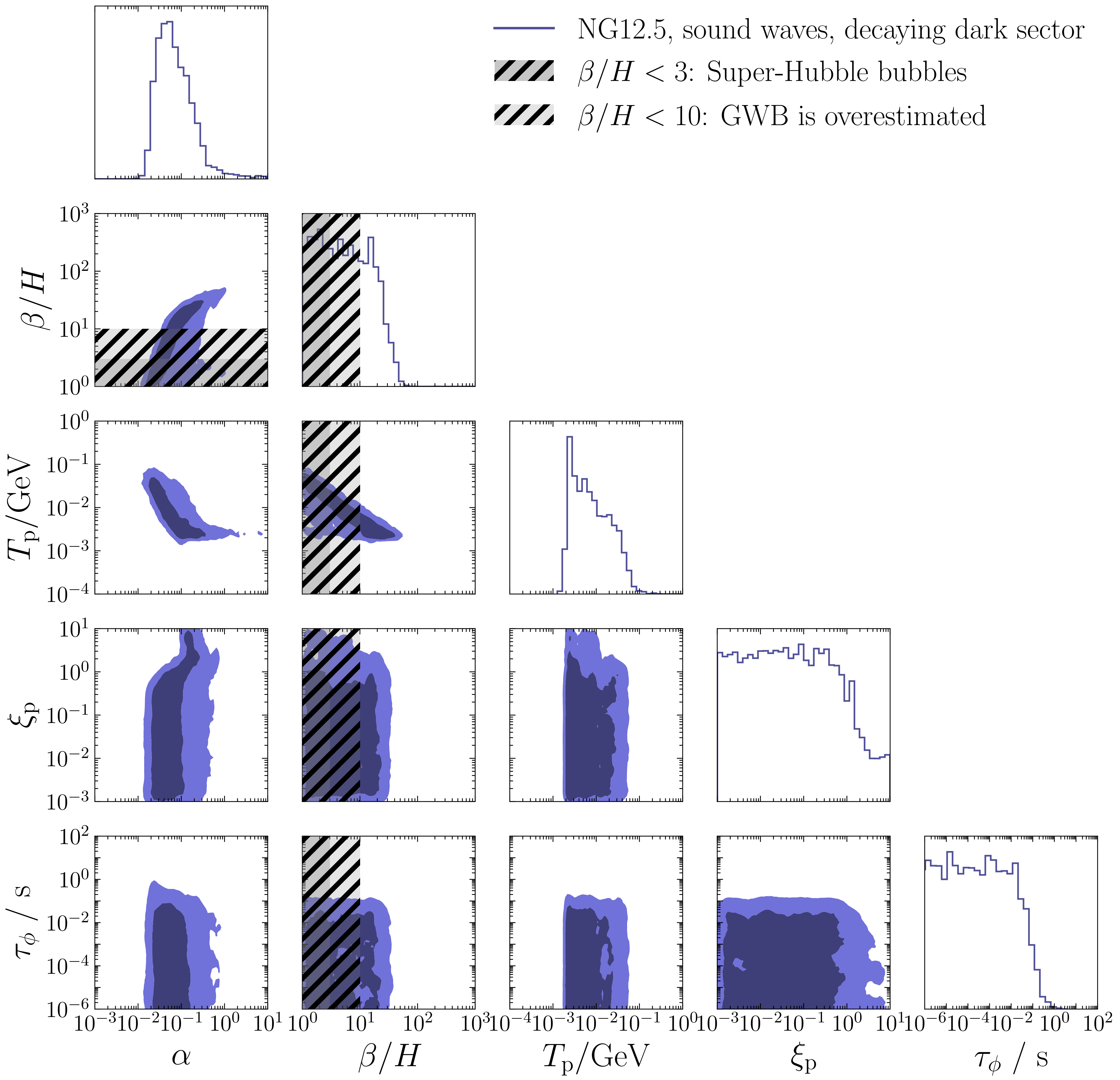

If the dark sector decays quickly ($\tau_\phi \lesssim 0.1$ s) before neutrino decoupling ($T \gtrsim 2$ MeV), a great fit to PTA data can be achieved!

Do PTAs observe primordial black hole mergers?

Supermassive primordial black holes.

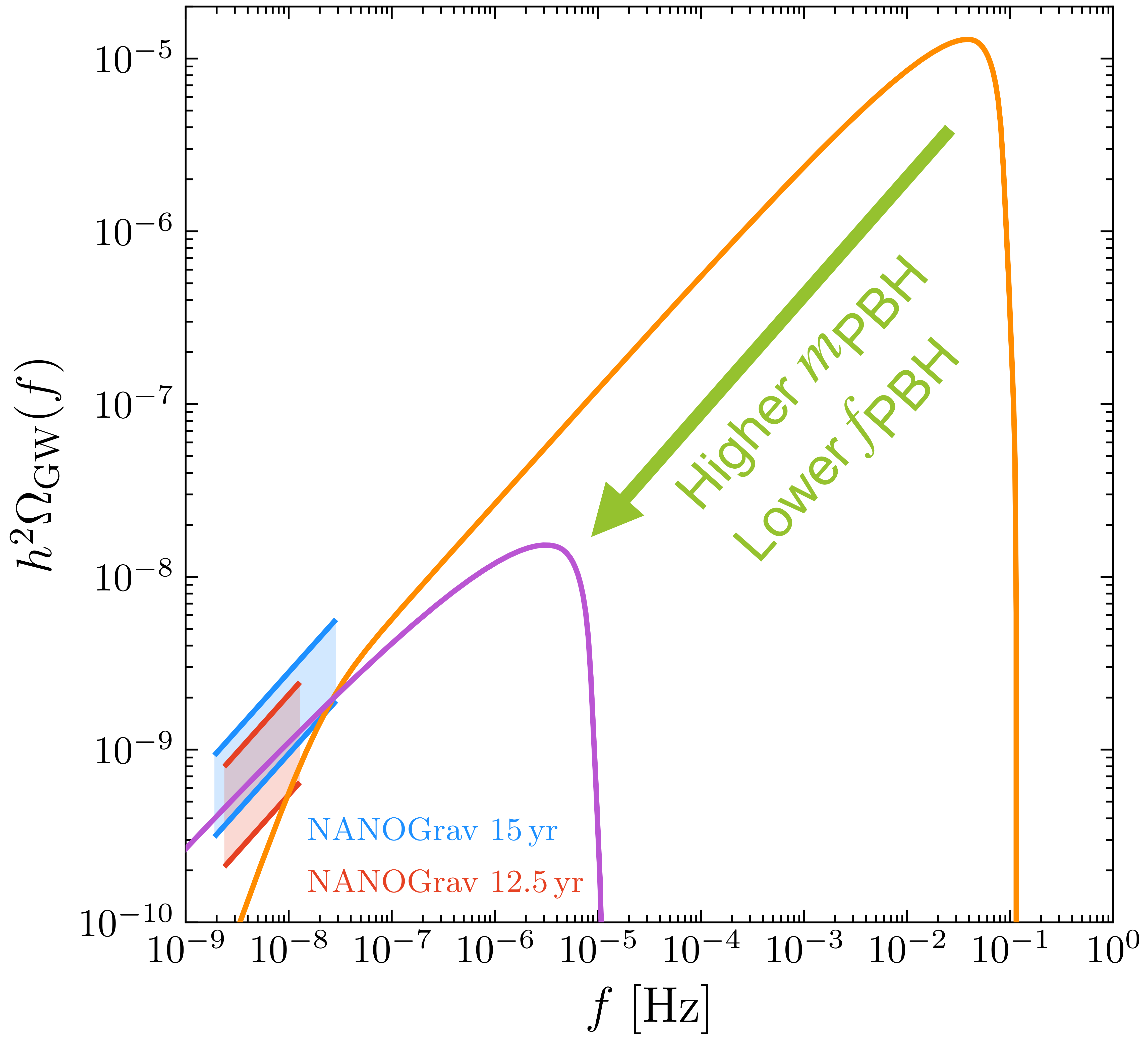

- Inflation leaves large super-Hubble density perturbations
- BHs form when these come into causal contact again, long before first stars form
- Described by mass $m_{\rm PBH}$ and DM fraction $f_{\rm PBH}$

Homogeneously distributed PBHs cannot explain PTA data.

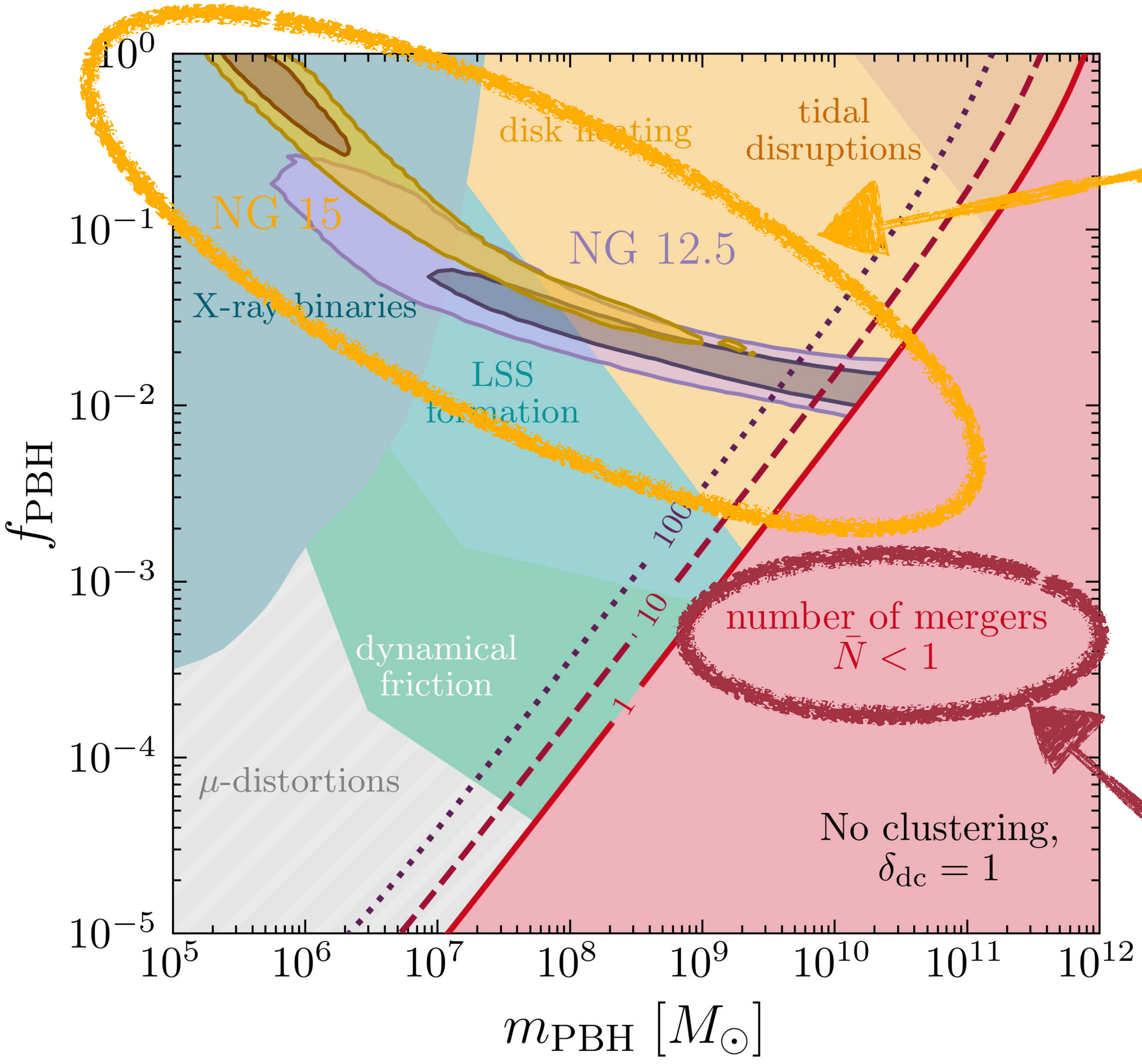

Parameter space favored by PTAs is excluded by astrophysical bounds

Crucial: excluded regions with small merger numbers. Atal et al. came to the wrong conclusion.

PBH clustering.

$$\delta_{\rm dc} = 1$$

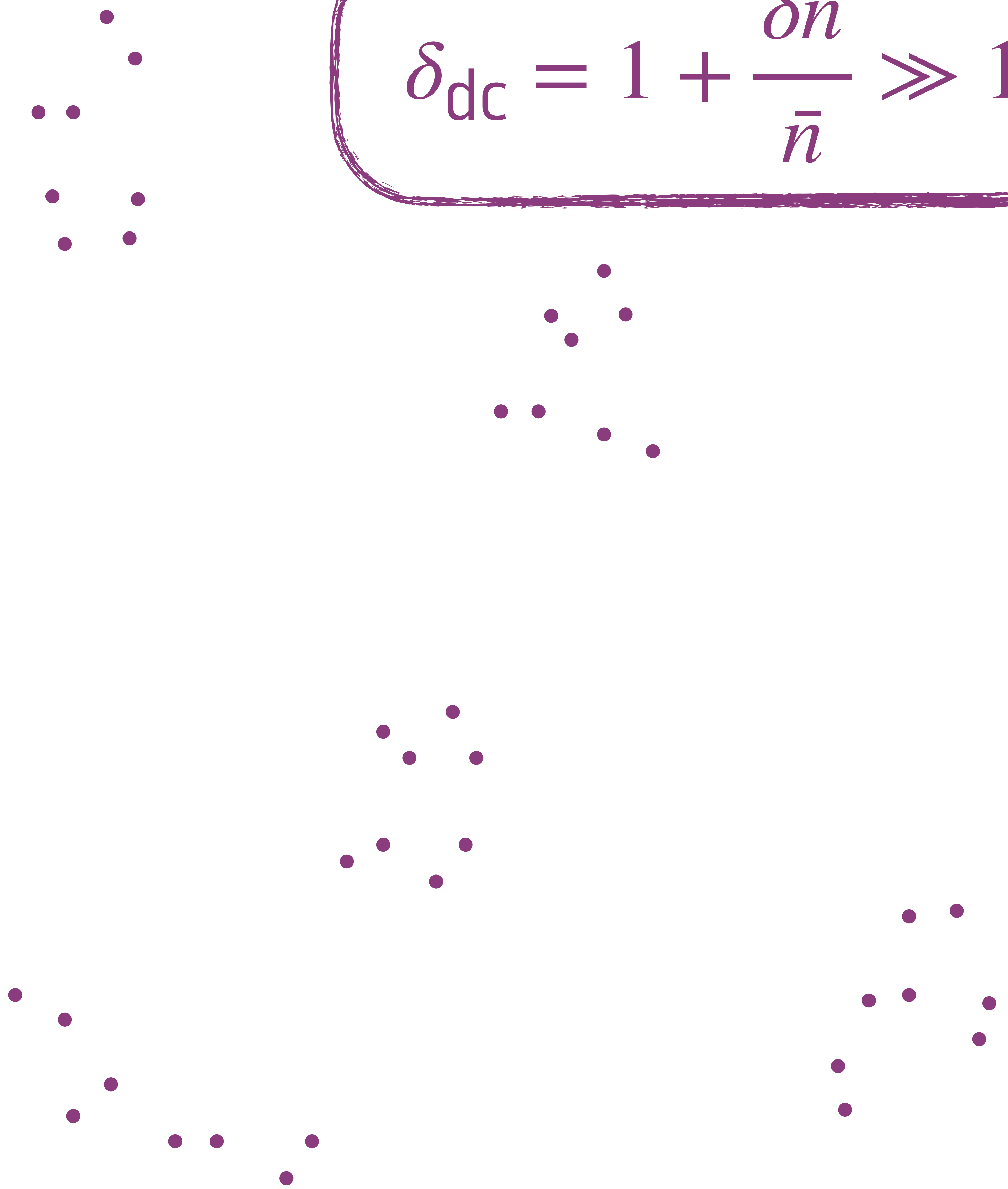

$$\delta_{\rm dc} = 1 + \frac{\delta n}{\bar{n}} \gg 1$$

Clustered PBHs can explain the PTA data.

Clustering increases merger rate and shifts the best fit region below constraints: Good fit is possible! *

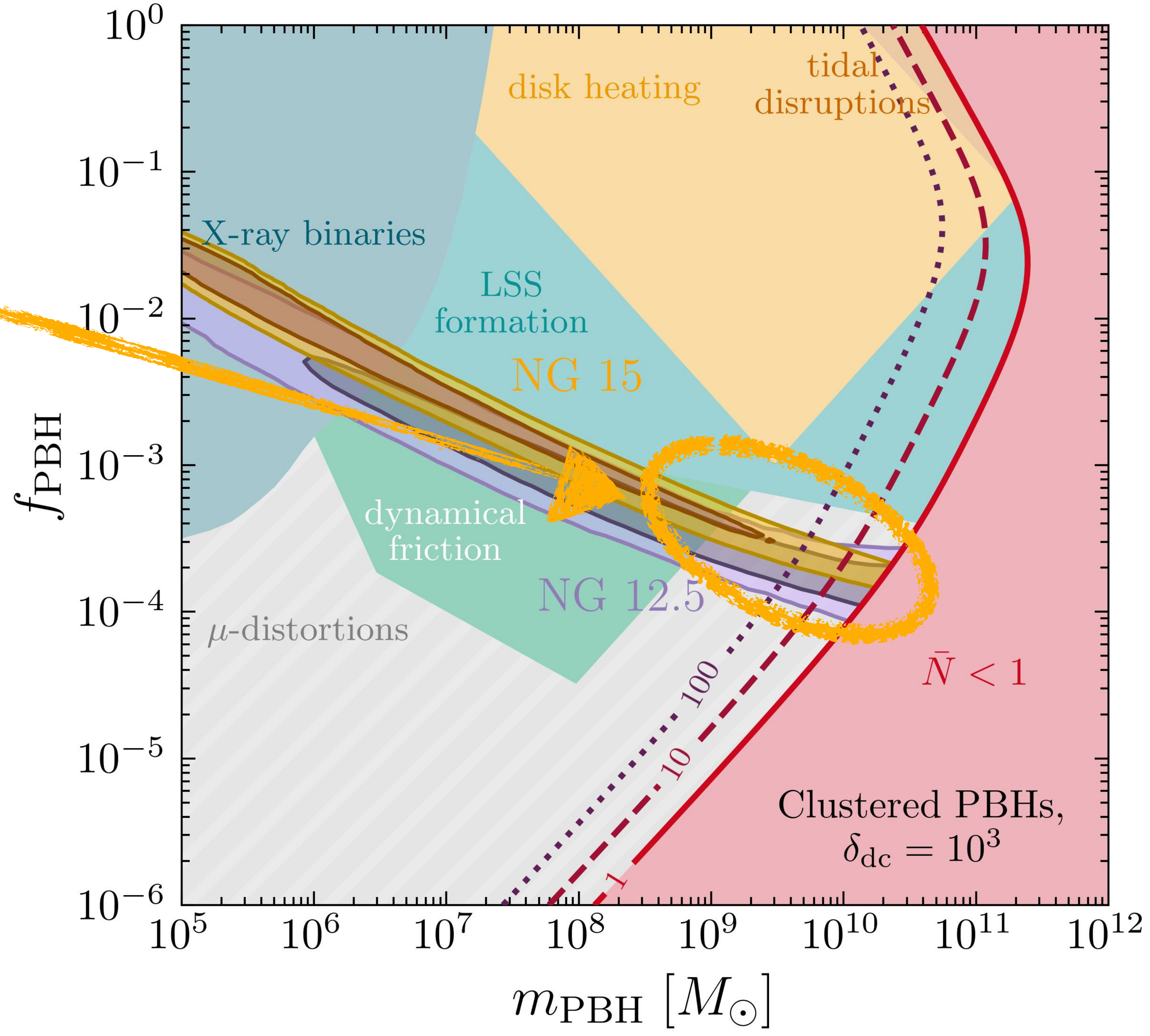

* Caveats: μ-distortion constraints from PBH production need to be circumvented & astrophysical constraints are expected to weaken/shift with clustering

The (first) LISA miracle.

The WIMP miracle.

If DM can annihilate into SM particles with a cross section $\langle \sigma v \rangle$ ...

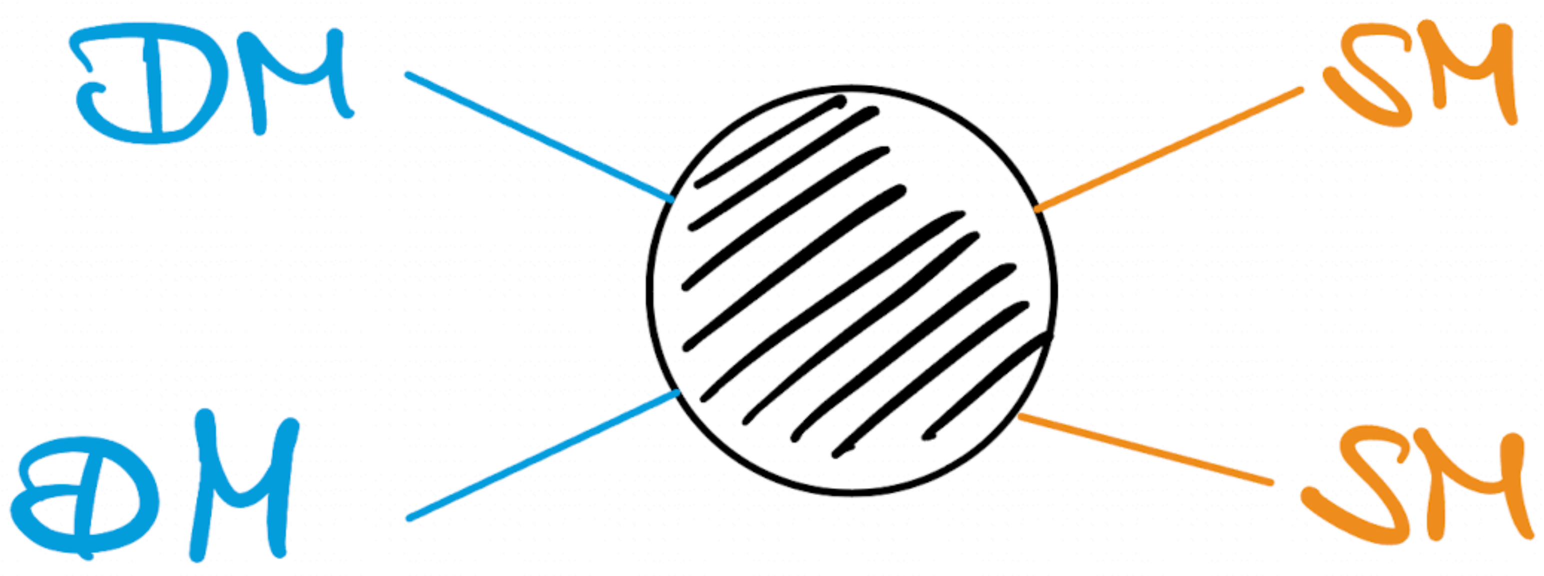

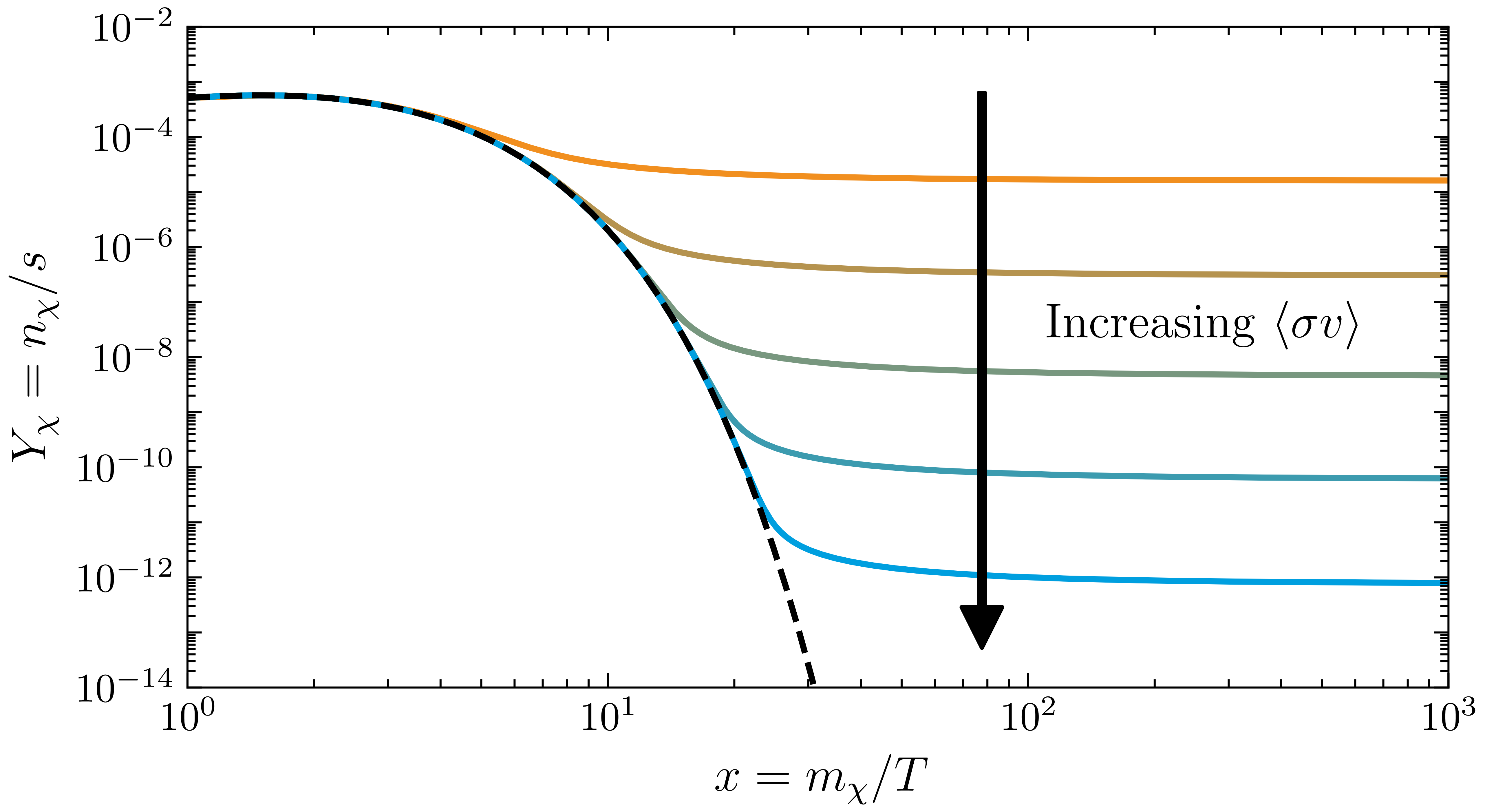

... the DM abundance can freeze out to the observed relic abundance for weak interactions and $m_{\mathrm{DM}} \simeq \mathcal{O}(\mathrm{TeV})$.

Rage, rage against the dying of the WIMP.

Direct detection experiments put this scenario under pressure, excluding „vanilla“ WIMPs.

[Lindner+ 2403.15860]

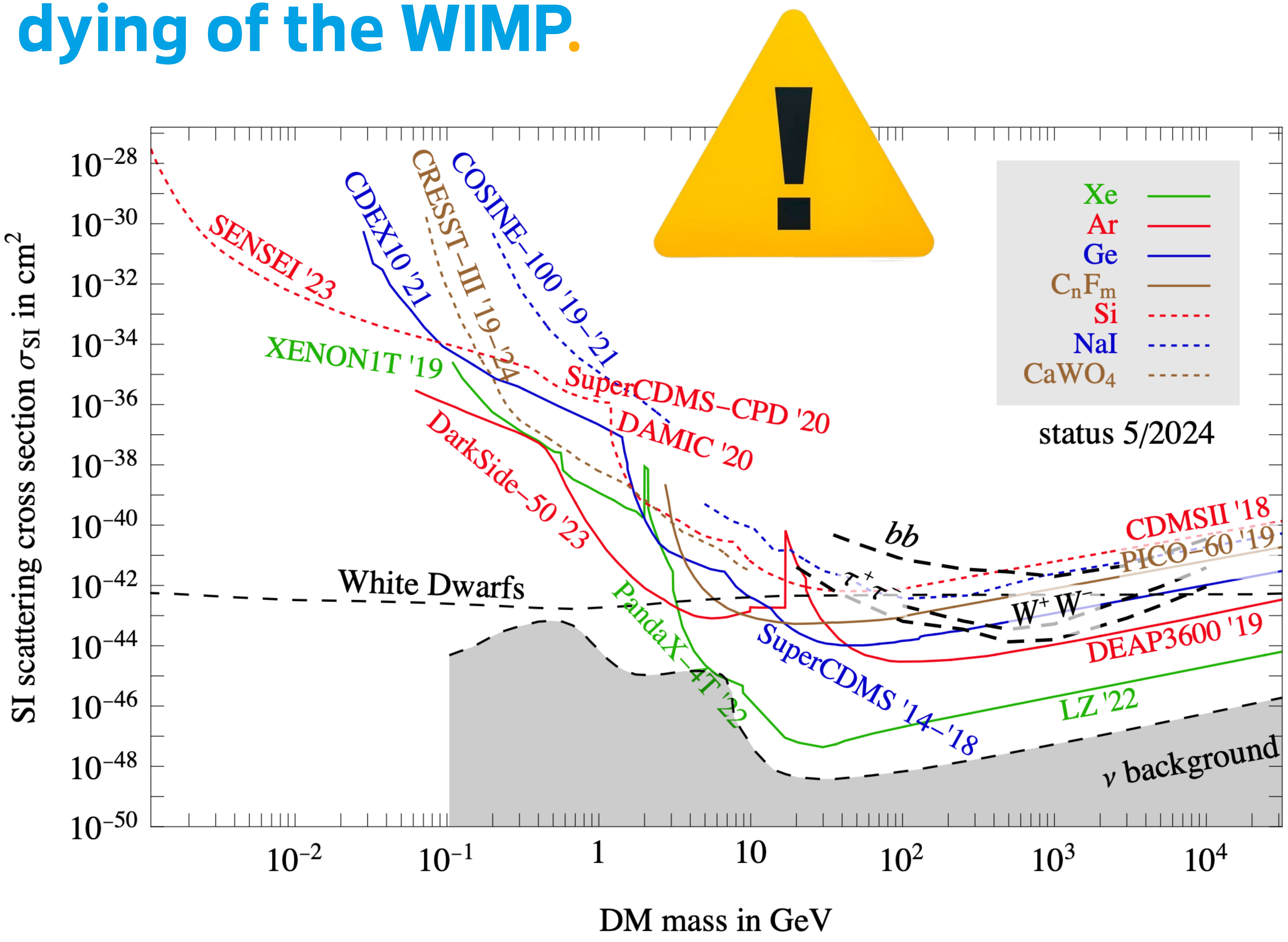

Cirelli+ [2406.01705]

The nightmare scenario.

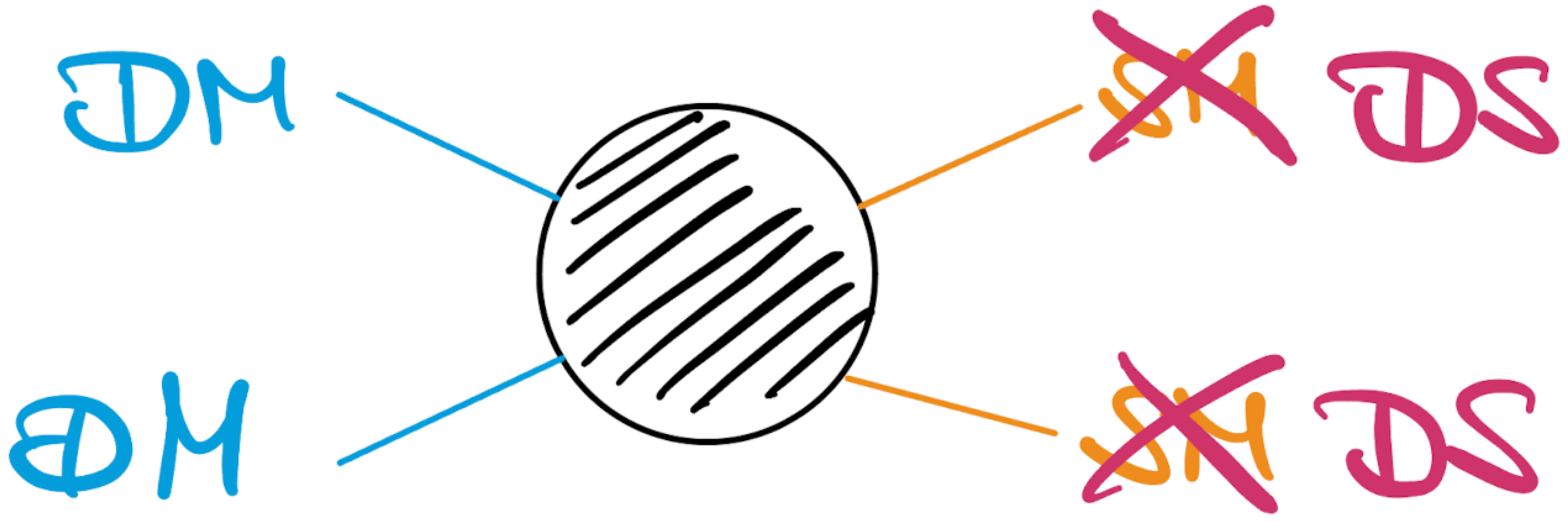

What if WIMPs evade our detection because they never were in contact with the SM and froze out of a secluded dark sector?

Pospelov+ [0711.4866]

The nightmare scenario.

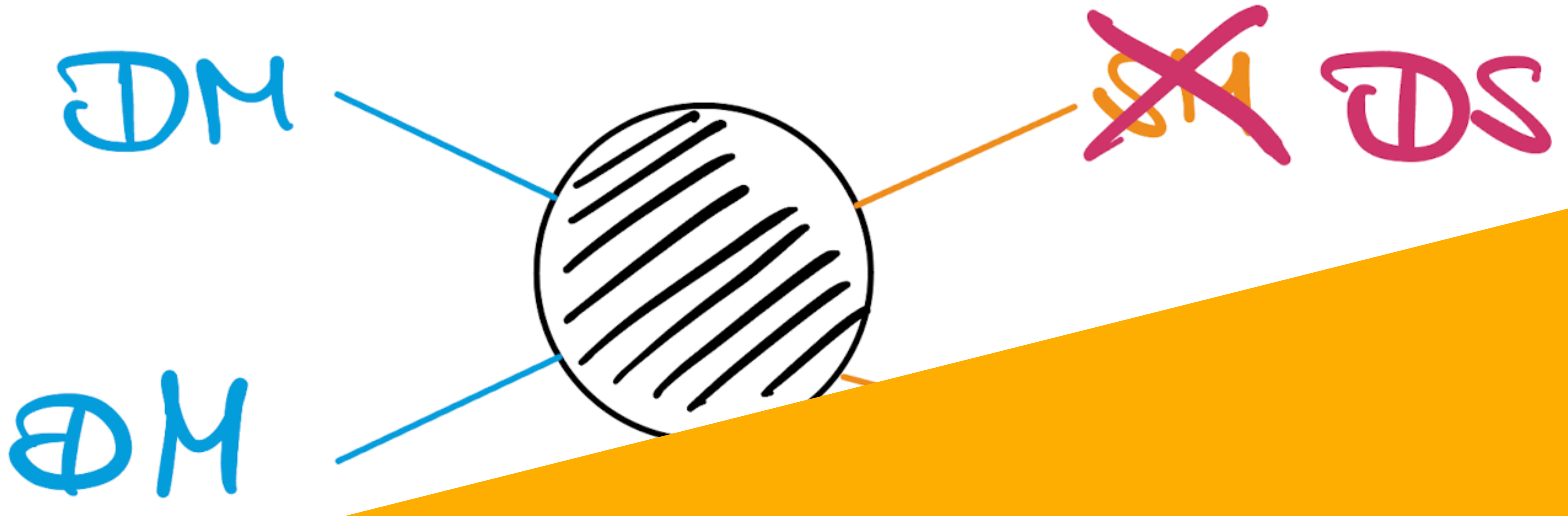

Don't panic! GWs can help.

Our model setup.

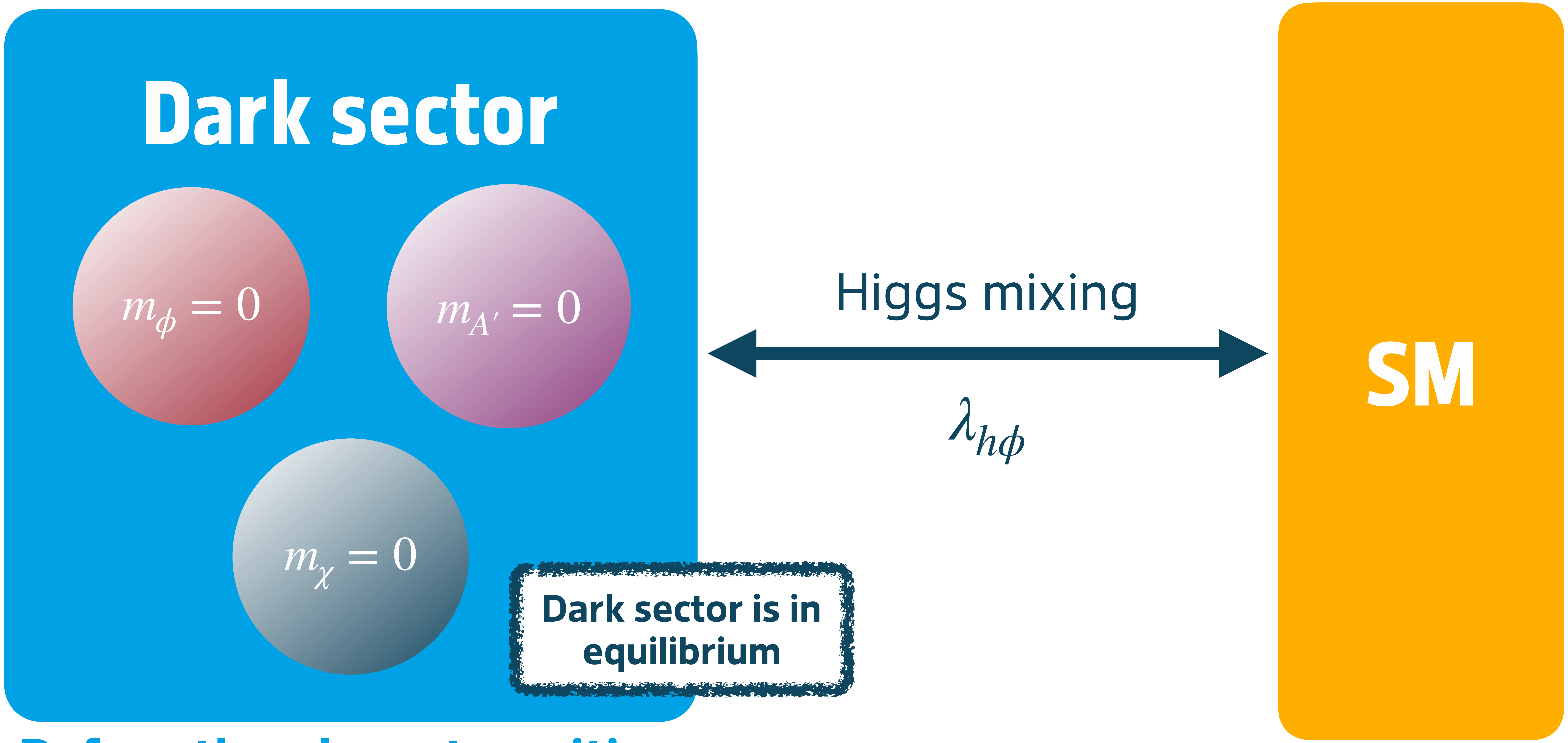

Before the phase transition

Our model setup.

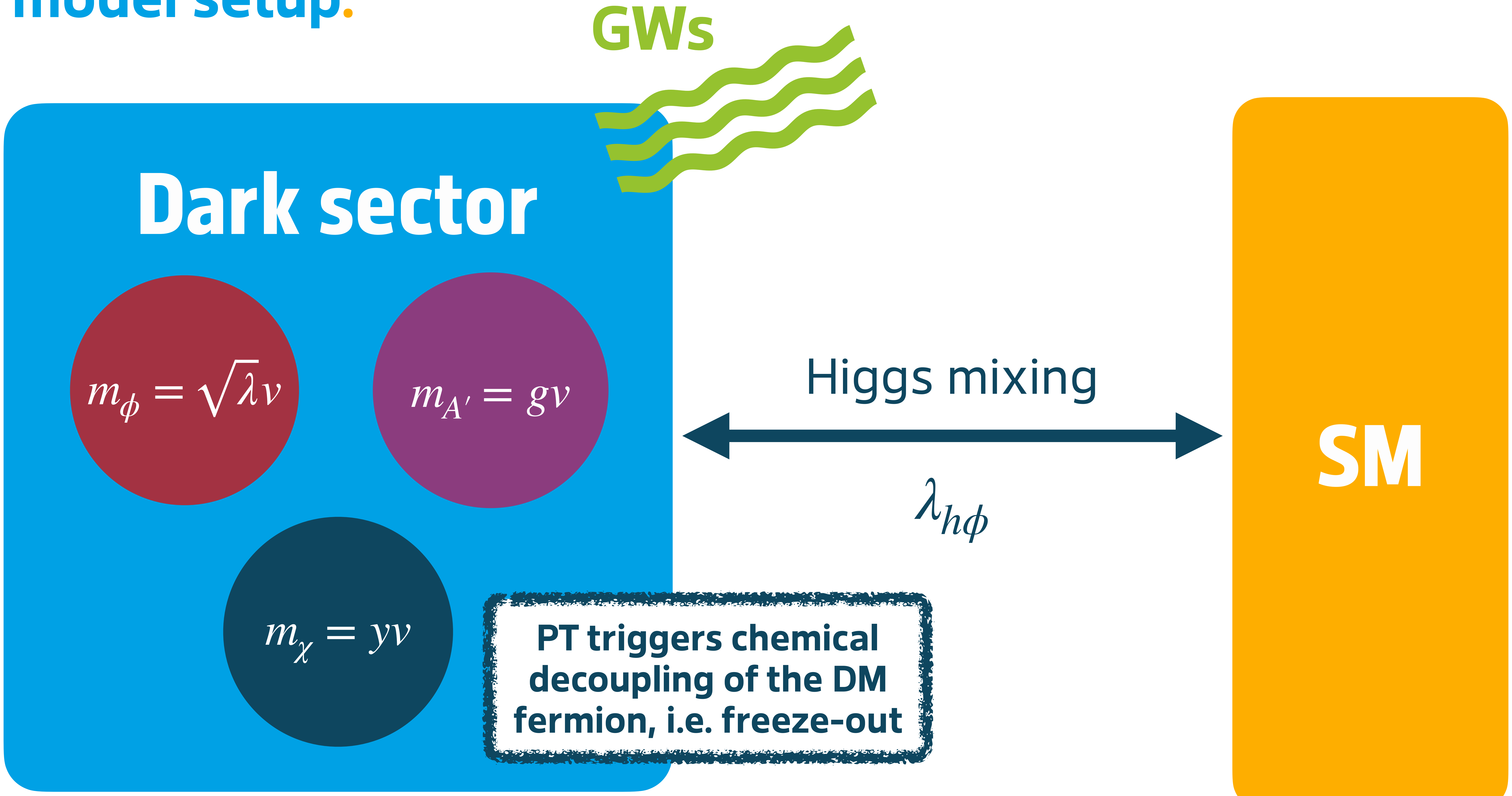

After the phase transition

A first glance at our punchline.

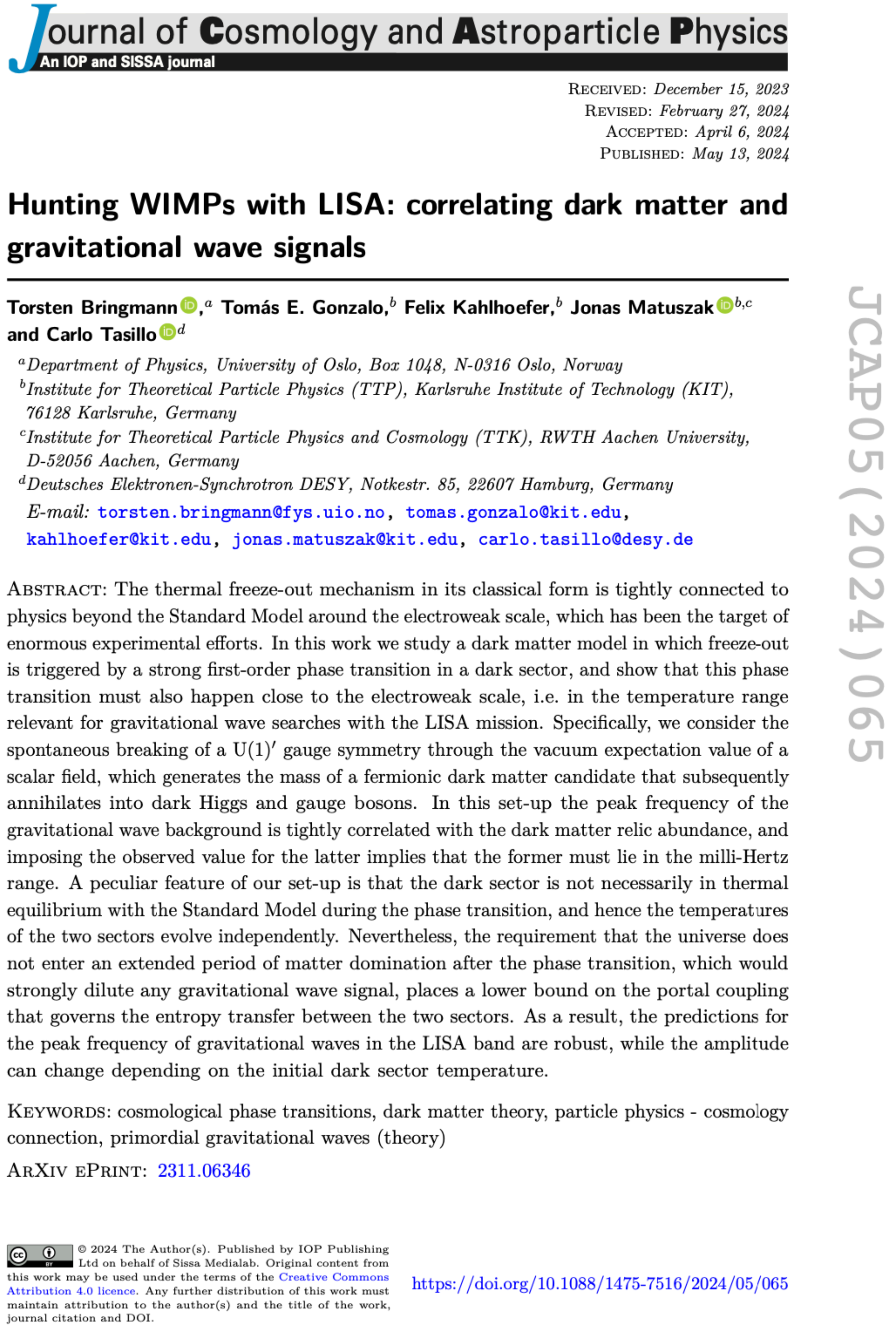
Journal of Cosmology and Astroparticle Physics
An IOP and SISSA journal

Received: December 15, 2023
Revised: February 27, 2024
Accepted: April 6, 2024
Published: May 13, 2024

Hunting WIMPs with LISA: correlating dark matter and gravitational wave signals

Torsten Bringmann,[a] Tomás E. Gonzalo,[b] Felix Kahlhoefer,[b] Jonas Matuszak[b,c] and Carlo Tasillo[d]

[a]Department of Physics, University of Oslo, Box 1048, N-0316 Oslo, Norway
[b]Institute for Theoretical Particle Physics (TTP), Karlsruhe Institute of Technology (KIT), 76128 Karlsruhe, Germany
[c]Institute for Theoretical Particle Physics and Cosmology (TTK), RWTH Aachen University, D-52056 Aachen, Germany
[d]Deutsches Elektronen-Synchrotron DESY, Notkestr. 85, 22607 Hamburg, Germany

E-mail: torsten.bringmann@fys.uio.no, tomas.gonzalo@kit.edu, kahlhoefer@kit.edu, jonas.matuszak@kit.edu, carlo.tasillo@desy.de

Abstract: The thermal freeze-out mechanism in its classical form is tightly connected to physics beyond the Standard Model around the electroweak scale, which has been the target of enormous experimental efforts. In this work we study a dark matter model in which freeze-out is triggered by a strong first-order phase transition in a dark sector, and show that this phase transition must also happen close to the electroweak scale, i.e. in the temperature range relevant for gravitational wave searches with the LISA mission. Specifically, we consider the spontaneous breaking of a U(1)′ gauge symmetry through the vacuum expectation value of a scalar field, which generates the mass of a fermionic dark matter candidate that subsequently annihilates into dark Higgs and gauge bosons. In this set-up the peak frequency of the gravitational wave background is tightly correlated with the dark matter relic abundance, and imposing the observed value for the latter implies that the former must lie in the milli-Hertz range. A peculiar feature of our set-up is that the dark sector is not necessarily in thermal equilibrium with the Standard Model during the phase transition, and hence the temperatures of the two sectors evolve independently. Nevertheless, the requirement that the universe does not enter an extended period of matter domination after the phase transition, which would strongly dilute any gravitational wave signal, places a lower bound on the portal coupling that governs the entropy transfer between the two sectors. As a result, the predictions for the peak frequency of gravitational waves in the LISA band are robust, while the amplitude can change depending on the initial dark sector temperature.

Keywords: cosmological phase transitions, dark matter theory, particle physics - cosmology connection, primordial gravitational waves (theory)

ArXiv ePrint: 2311.06346

https://doi.org/10.1088/1475-7516/2024/05/065

JCAP05(2024)065

Theorem:
There is a correlation between the GW peak frequency and the DM abundance.

Proof:
$f_\text{peak} \propto v$ and $\Omega_\text{DM} \propto v^2$ for a transition with vacuum expectation value v.

Lemma:
$\Omega_\text{DM} h^2 = 0.12 \implies f_\text{peak} \simeq \mathcal{O}(\text{mHz})$. If DM freeze-out is triggered by a strong phase transition, it is observable using LISA.

The miracle at work.

Peak frequency: $f_{\text{peak}} \simeq 10\,\text{mHz} \cancel{\left(\frac{\beta/H}{100}\right)} \left(\frac{\cancel{T}\; v}{1\,\text{TeV}}\right) \simeq 10\,\text{mHz} \left(\frac{v}{1\,\text{TeV}}\right)$

DM abundance: $\Omega_{\text{DM}} h^2 \simeq 0.1 \frac{10^{-8}\,\text{GeV}^{-2}}{\langle \sigma v \rangle} \propto \frac{v^2}{y^2}$

Assuming that dominant annihilation channel is $\chi\chi \to \phi\phi$:

$$\langle \sigma v \rangle \sim \frac{y^4}{m_\chi^2} \sim \frac{y^2}{v^2}$$

Since Yukawa coupling y is **a-priori** arbitrary: **no correlation expected...**

Intermediate Yukawa couplings.

Strong-GW condition:

Sizable couplings and $m_\phi \lesssim m_{A'}$

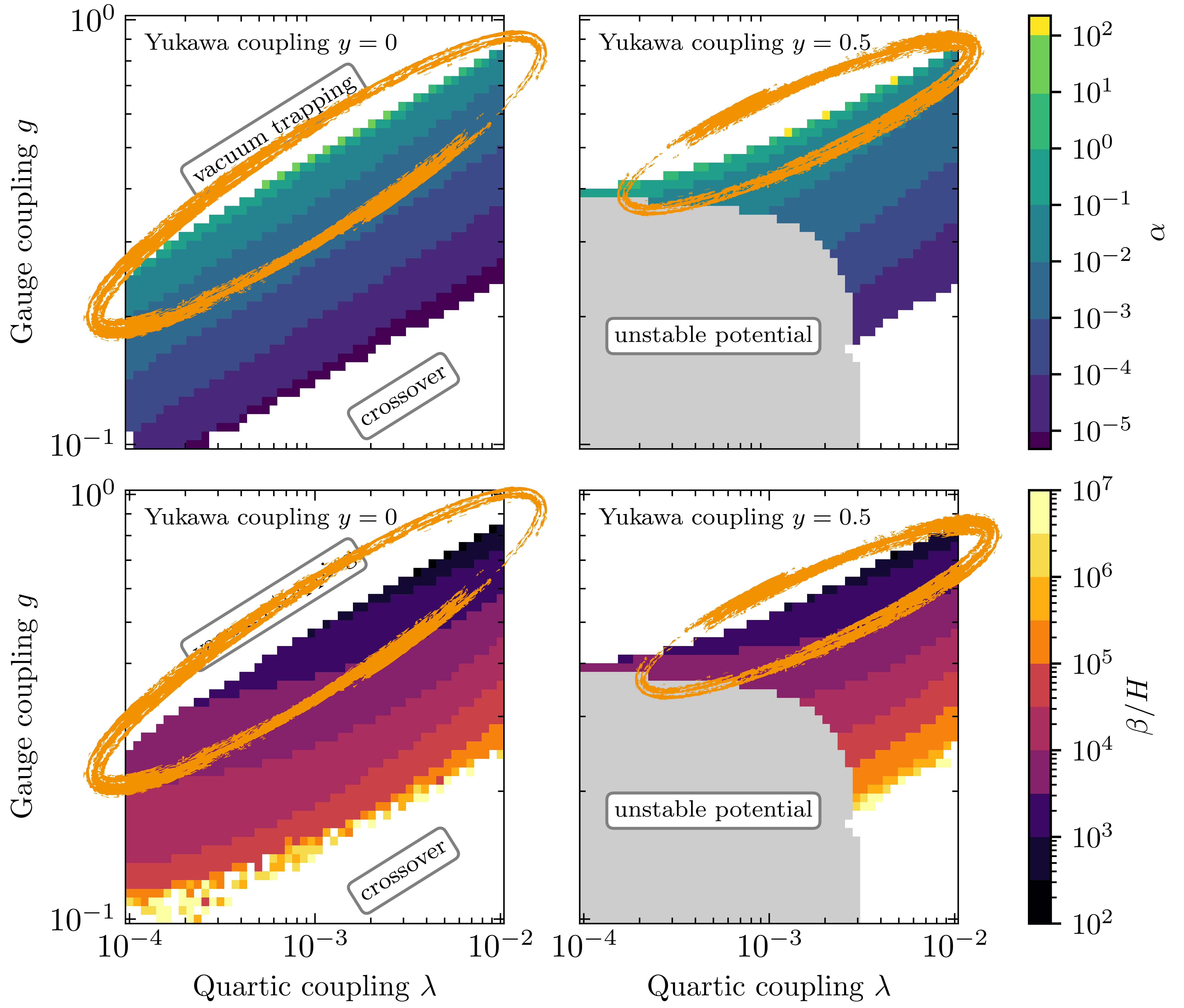

Intermediate Yukawa couplings.

Strong-GW condition:

Sizable couplings and $m_\phi \lesssim m_{A'}$

Freeze-out condition:

DM cannot be lightest dark sector state: $m_\phi < m_\chi$ or $m_{A'} < m_\chi$

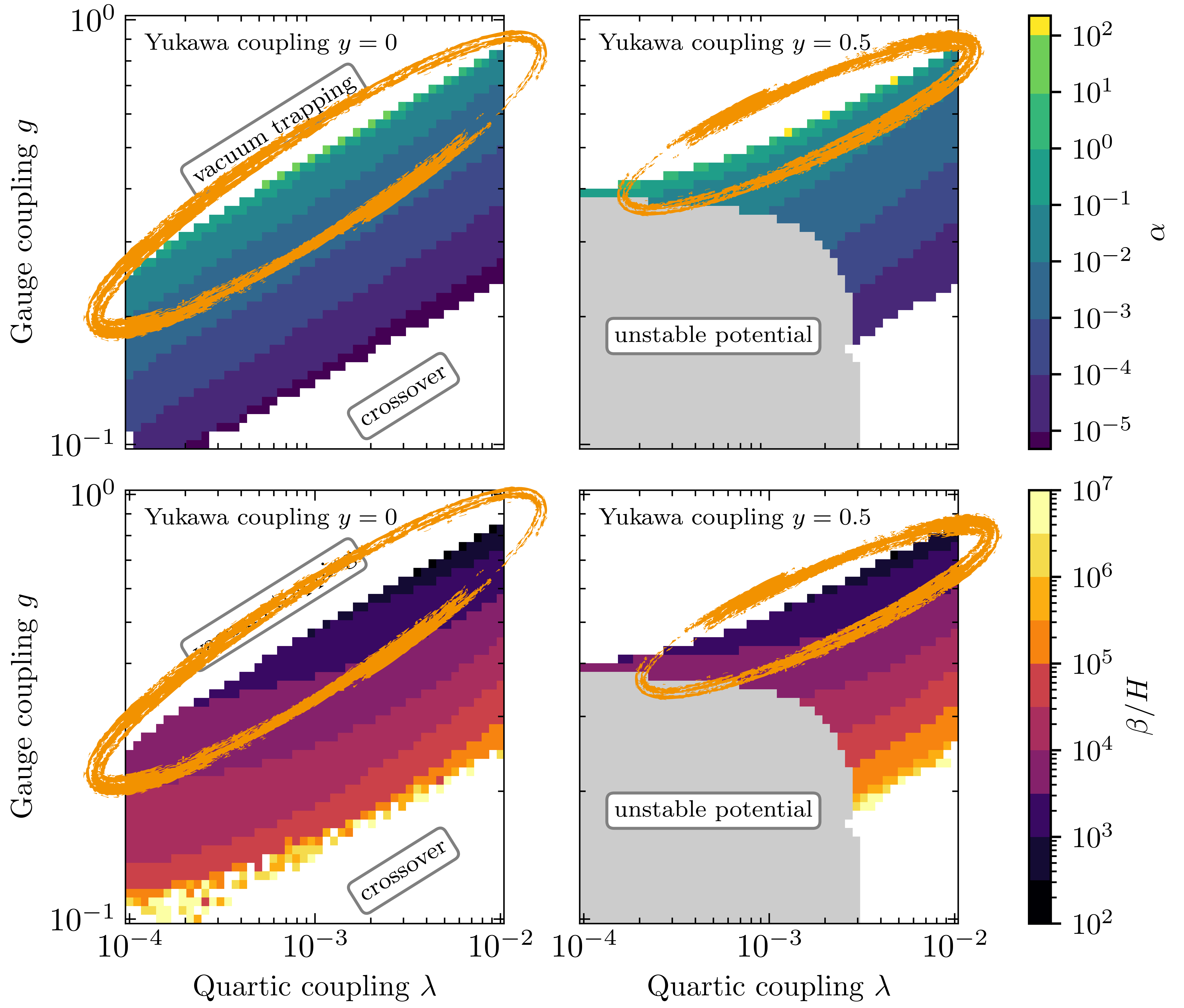

Intermediate Yukawa couplings.

Strong-GW condition:

Sizable couplings and $m_\phi \lesssim m_{A'}$

Freeze-out condition:

DM cannot be lightest dark sector state: $m_\phi < m_\chi$ or $m_{A'} < m_\chi$

Conclusion:

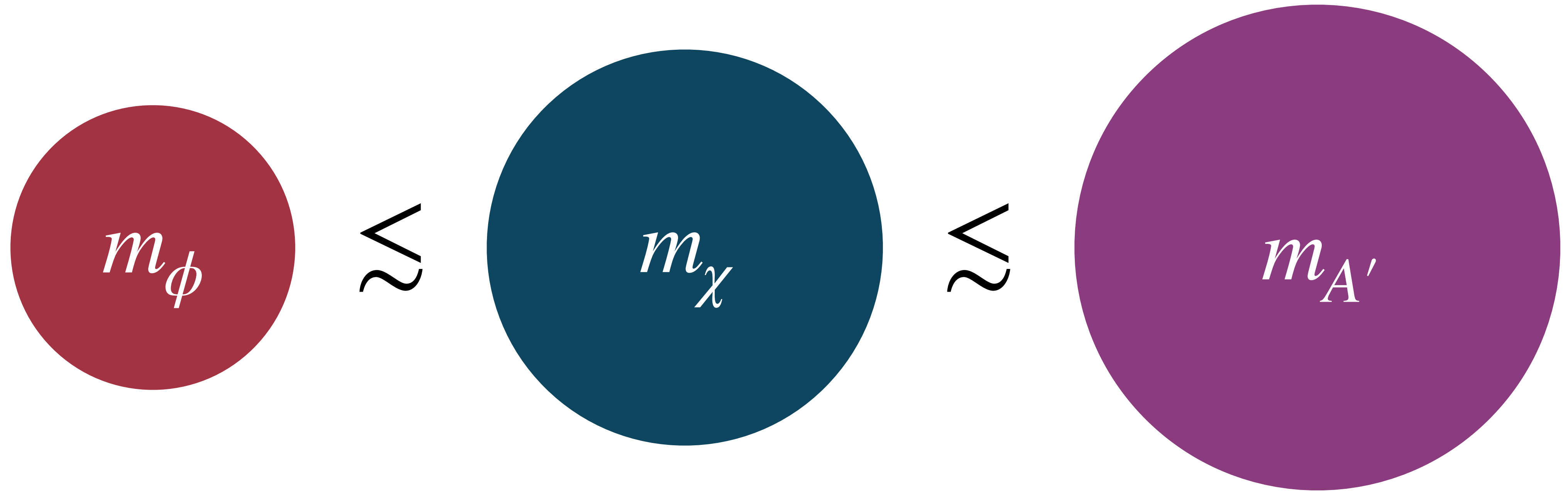

Yukawa couplings are bounded and $\mathcal{O}(0.1)$. Miracles can happen! 🤩

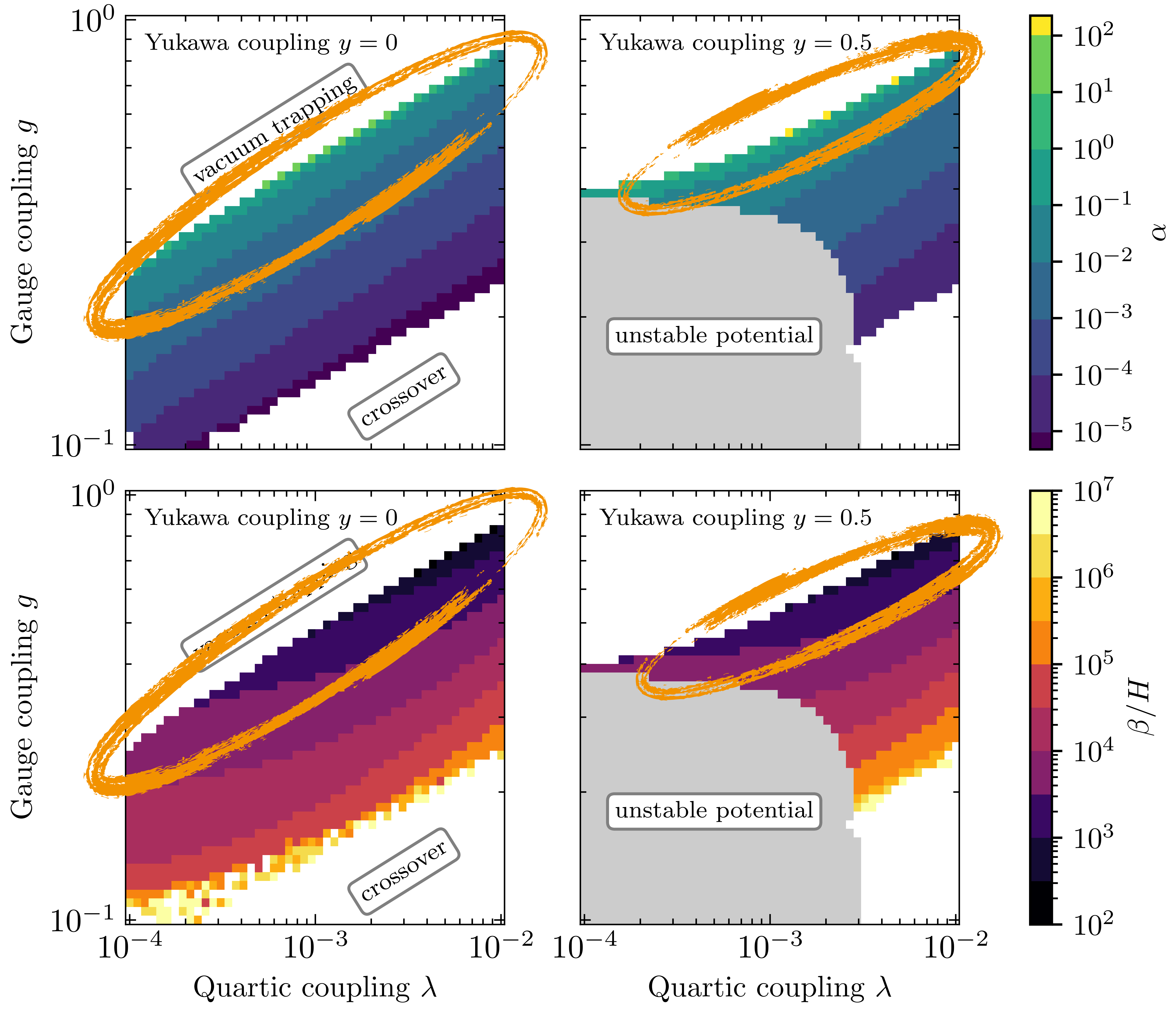

You shouldn't be convinced, yet.

So far we skipped over several potential issues:

- Sizable Yukawa couplings vs. vacuum stability
- What about the $\chi\chi \to A'A'$ and $\chi\chi \to \phi A'$ annihilations?
- Influence of temperature ratio $\xi = T_{\text{DS}}/T_{\text{SM}}$ on $\Omega_{\text{GW}}(f)$ and Ω_{DM}?
- $\lambda_{h\phi}$: Collider bounds? Early matter domination?

You shouldn't be convinced, yet.

So far we skipped over several potential issues:

- Sizable Yukawa couplings vs. vacuum stability
- What about the $\chi\chi \to A'A'$ and $\chi\chi \to \phi A'$ annihilations?
- Influence of temperature ratio $\xi = T_{\rm DS}/T_{\rm SM}$ on $\Omega_{\rm GW}(f)$ and $\Omega_{\rm DM}$?
- $\lambda_{h\phi}$: Collider bounds? Early matter domination?

We performed full model scans* over $\lambda, g, y, v, \xi, \lambda_{h\phi}$ and confirmed the LISA miracle!

* TransitionListener & DarkSUSY [Ertas+ 2109.06208, Bringmann+ 1802.03399]

Results of our scans.

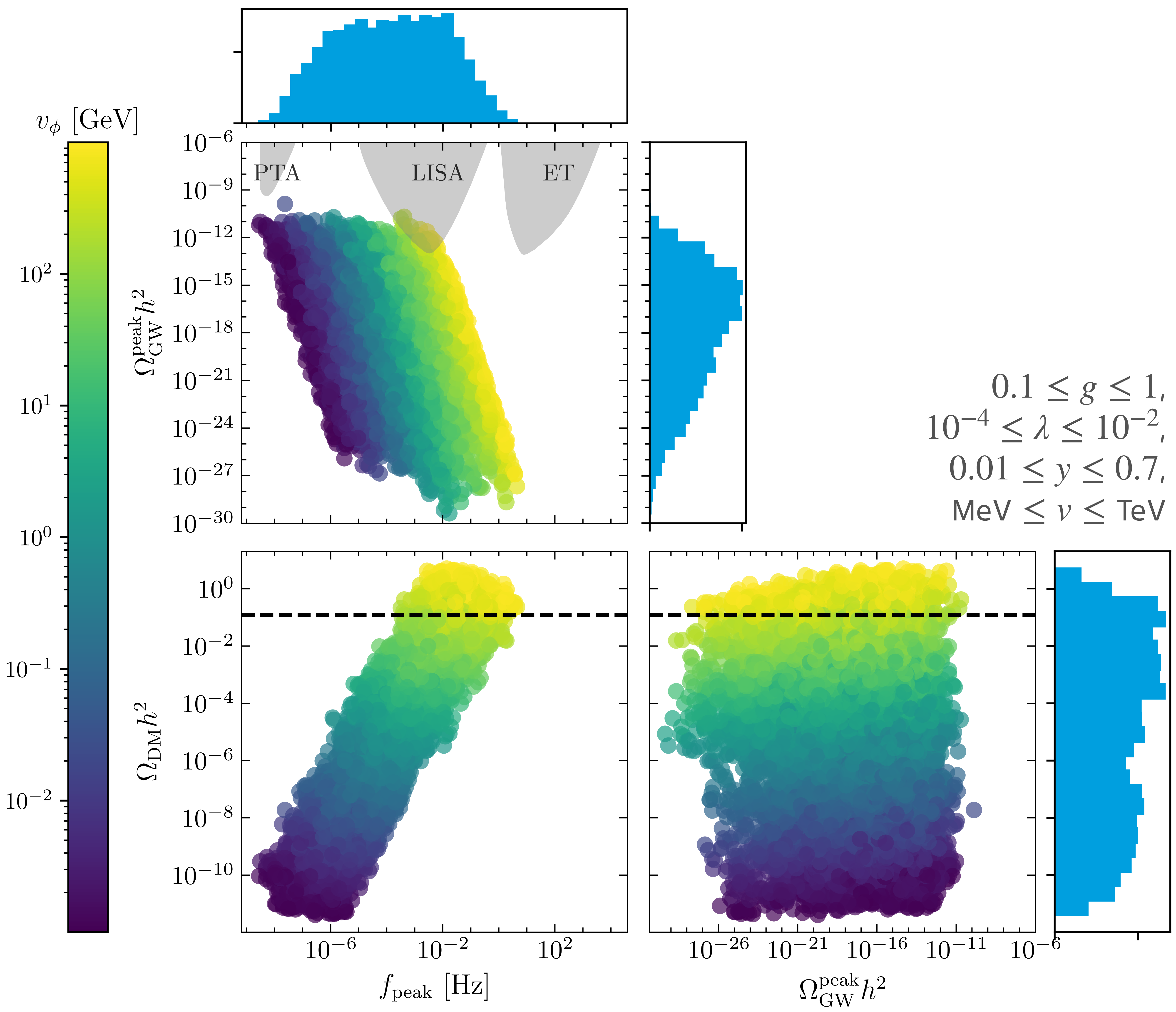

$0.1 \leq g \leq 1,$
$10^{-4} \leq \lambda \leq 10^{-2},$
$0.01 \leq y \leq 0.7,$
$\text{MeV} \leq v \leq \text{TeV}$

Results of our scans.

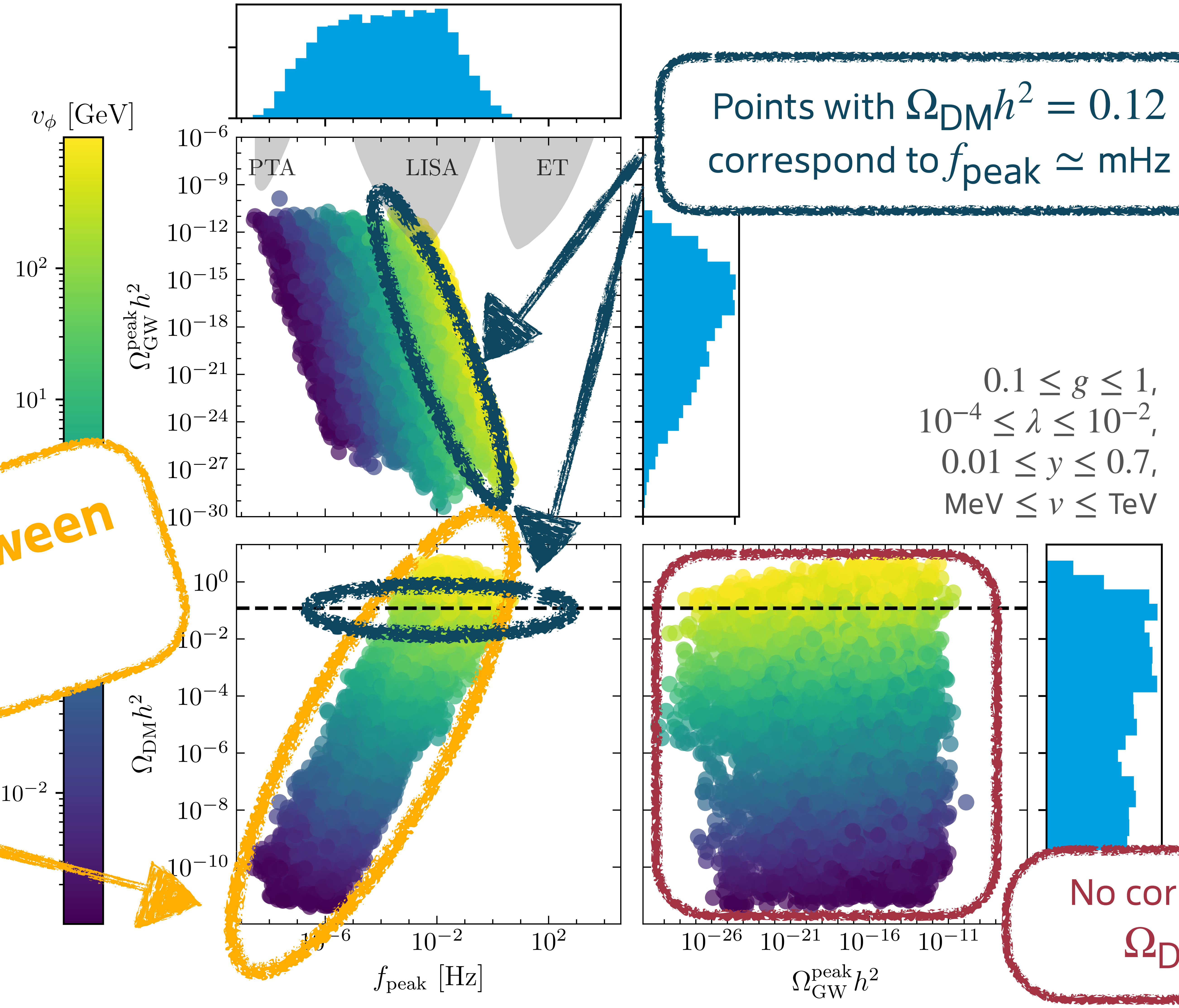

Points with $\Omega_{\rm DM} h^2 = 0.12$ correspond to $f_{\rm peak} \simeq$ mHz

$0.1 \leq g \leq 1$,
$10^{-4} \leq \lambda \leq 10^{-2}$,
$0.01 \leq y \leq 0.7$,
MeV $\leq v \leq$ TeV

Strong correlation between $f_{\rm peak}$ and $\Omega_{\rm DM}$!

No correlation between $\Omega_{\rm DM}$ and $\Omega_{\rm GW}^{\rm peak}$

Now, you should be convinced.

Strong supercooling

35% of points with strong supercooling and correct DM abundance are observable

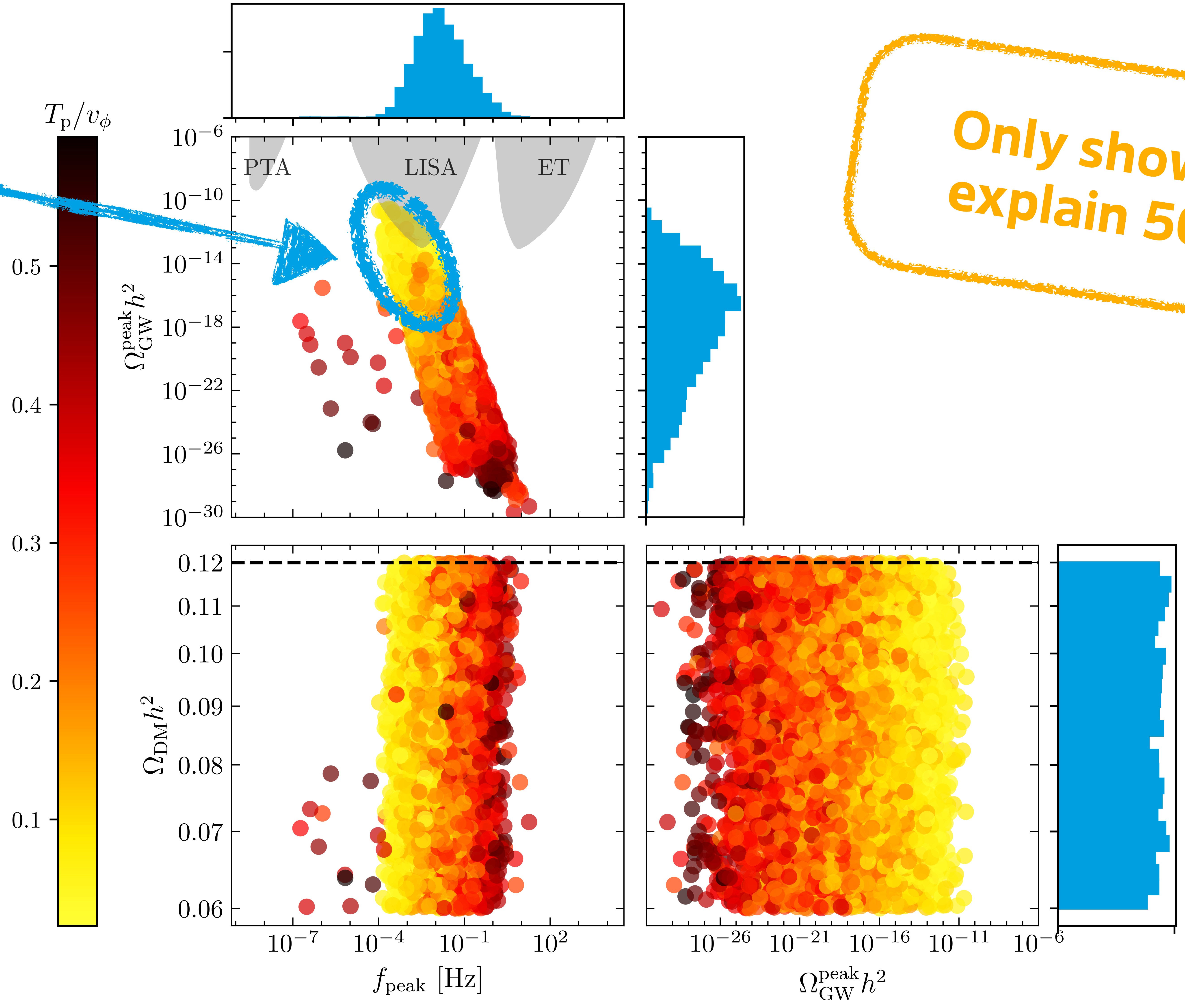

Only show points which explain 50-100% of DM

Conclusions.

- We are only at the dawn of GW cosmology, but can already probe the pre-BBN universe!
- PTAs could have observed a dark sector phase transition or merging supermassive PBHs
  - ➡ Dark sector phase transitions cannot be too strong & quick: Need $\alpha \lesssim 0.1$ and $\beta/H \lesssim 10$ or (better) quick decays ($\tau_\phi \lesssim 0.1$ s)
  - ➡ PBHs need to be clustered, no μ-distortions at production
- A future LISA detection of a GW background would hint towards secluded DS freeze-out


Thank you!

Sensitivity for cosmic GW backgrounds.

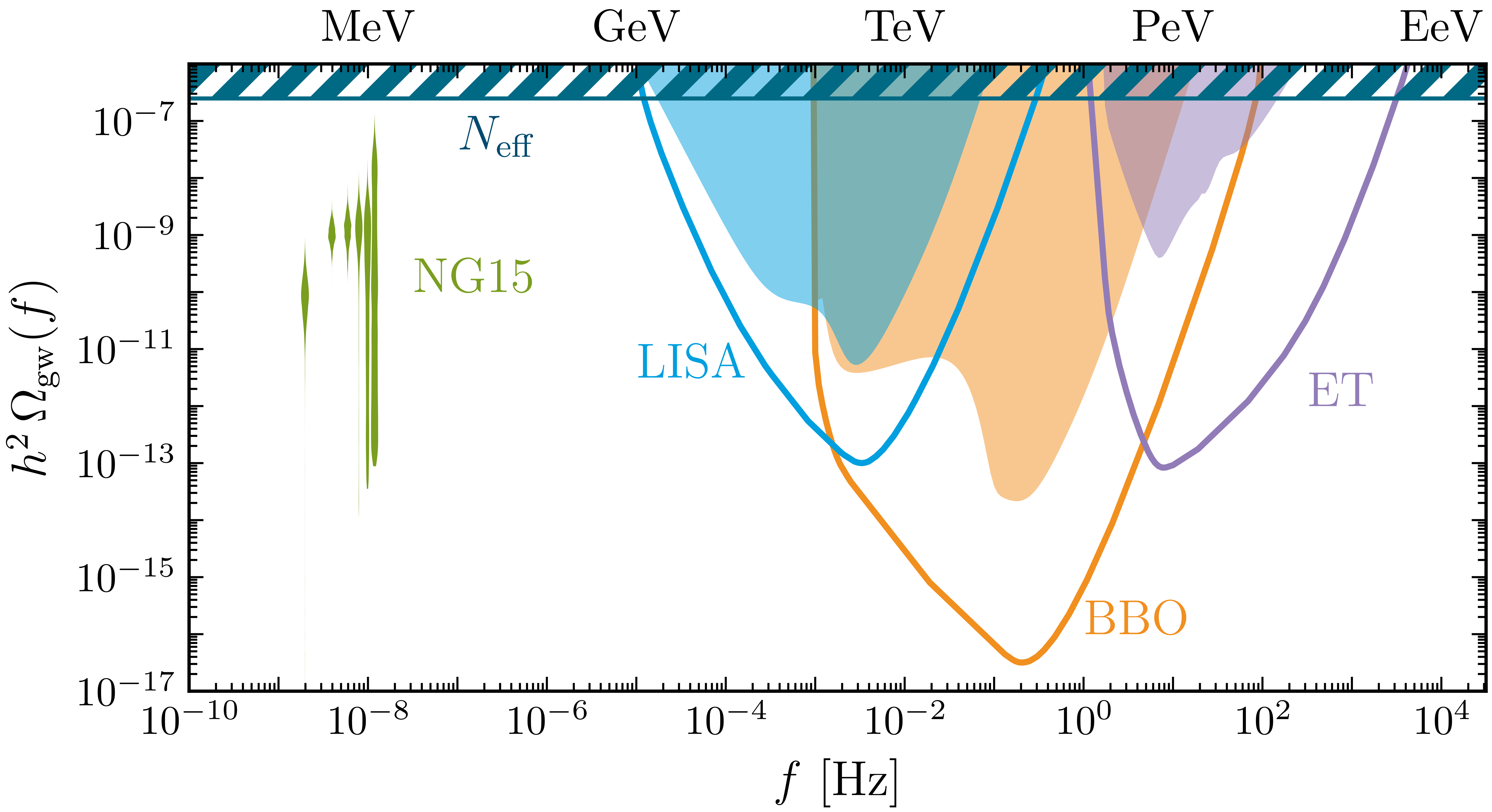

Model details.

$$\mathcal{L} = |D_\mu\Phi|^2 - \frac{1}{4}A'_{\mu\nu}A'^{\mu\nu} + \mu^2\Phi^*\Phi - \lambda(\Phi^*\Phi)^2 + \chi_L^\dagger i\not{D}\chi_L + \chi_R^\dagger i\not{D}\chi_R - y\Phi\chi_L^\dagger\chi_R - y\Phi^*\chi_R^\dagger\chi_L$$

The tree-level scalar potential of our model has a minimum at $v_\phi = \pm\sqrt{\mu^2/\lambda}$. One can hence expand the complex field as $\Phi = (v_\phi + \phi + i\varphi)/\sqrt{2}$, where ϕ and φ are real scalar fields. In addition, the chiral fermions χ_L and χ_R can be written as a Dirac fermion χ. The Lagragian in eq. (2.1) can thus be re-written as

$$\begin{aligned}\mathcal{L} =& \frac{1}{2}\partial_\mu\phi\partial^\mu\phi + \frac{1}{2}\partial_\mu\varphi\partial^\mu\varphi - \frac{1}{4}A'_{\mu\nu}A'^{\mu\nu} - \frac{1}{2}m_\phi^2\phi^2 + \frac{1}{2}m_{A'}^2A'^2_\mu \\ & - gA'_\mu[\varphi\partial^\mu\phi - \phi\partial^\mu\varphi - v_\phi\partial^\mu\varphi] + \frac{g^2}{2}\phi^2A'^2_\mu + \frac{g^2}{2}\varphi^2A'^2_\mu + g^2v_\phi\phi A'^2_\mu \\ & - \lambda v_\phi\phi^3 - \lambda v_\phi\varphi^2\phi - \frac{\lambda}{4}\phi^2\varphi^2 - \frac{\lambda}{4}\phi^4 - \frac{\lambda}{4}\varphi^4 \\ & + i\bar{\chi}\not{\partial}\chi - m_\chi\bar{\chi}\chi + \frac{g}{2}\bar{\chi}\not{A}'\gamma^5\chi - \frac{y}{\sqrt{2}}\phi\bar{\chi}\chi + i\frac{y}{\sqrt{2}}\varphi\bar{\chi}\gamma^5\chi\,,\end{aligned}$$

$$m_\phi^2 = -\mu^2 + 3\lambda v_\phi^2 = 2\lambda v_\phi^2, \quad m_\varphi^2 = 0, \quad m_{A'}^2 = g^2v_\phi^2, \quad m_\chi^2 = \frac{y^2}{2}v_\phi^2.$$

In any case: Novel PBH bounds.

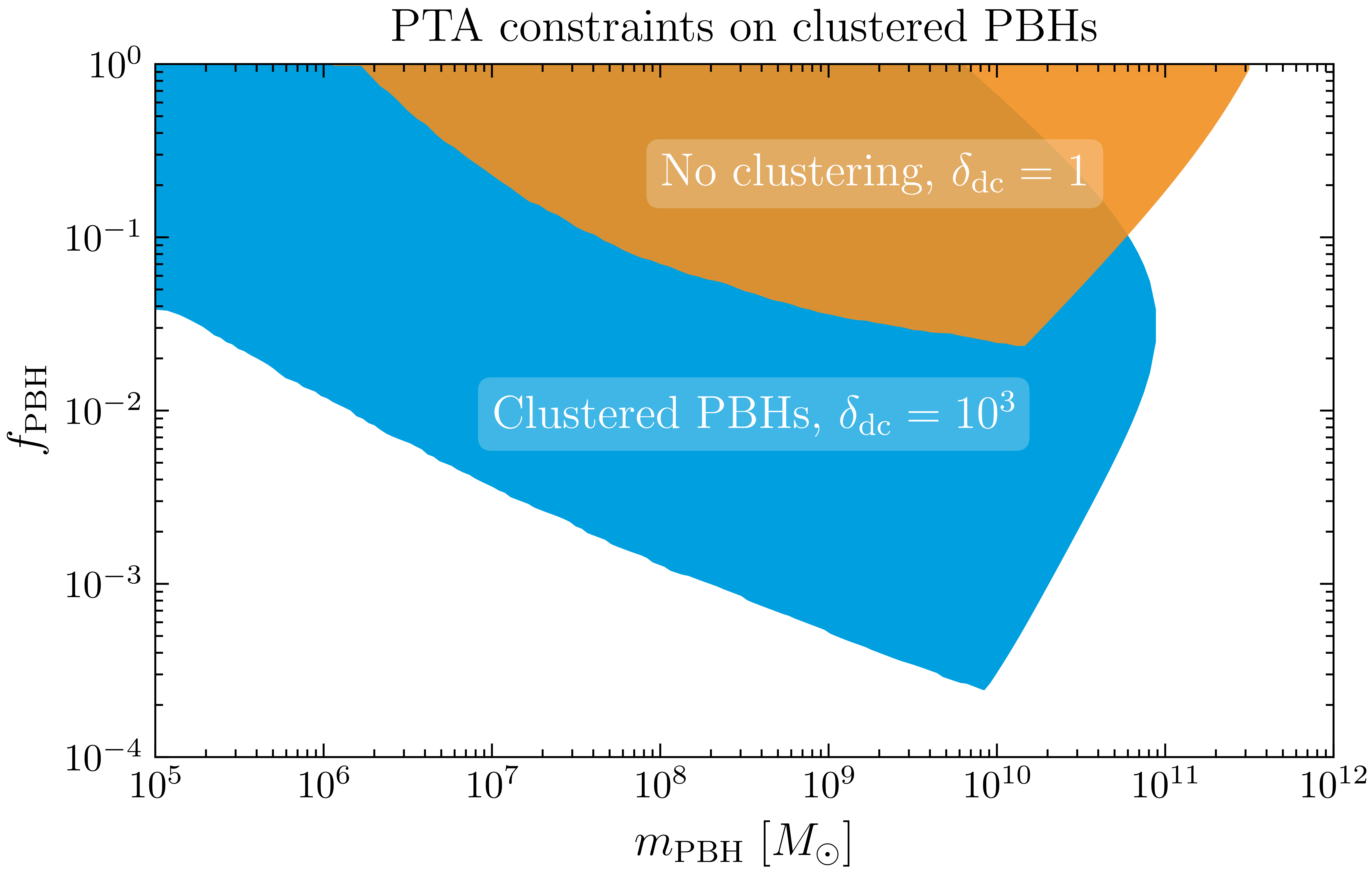

In the shaded regions, the GW signal exceeds the measured PTA signal.

GWB details.

$$h^2\Omega_{\rm GW}(f) = \mathcal{R}h^2\,\tilde{\Omega}\left(\frac{\kappa_{\rm sw}\,\alpha}{\alpha+1}\right)^2\left(\frac{\beta}{H}\right)^{-1}\mathcal{Y}\,S(f)$$

$$\mathcal{R}h^2 = \Omega_\gamma h^2\left(\frac{h_{\rm SM,0}}{h_{\rm tot,p}}\right)^{4/3}\left(\frac{g_{\rm tot,p}}{g_{\gamma,0}}\right) = 1.653\cdot 10^{-5}\left(\frac{100}{h_{\rm tot,p}}\right)^{4/3}\left(\frac{g_{\rm tot,p}}{100}\right)$$

$$\mathcal{Y} = \min\left[1,\tau_{\rm sh}H\right] \simeq \min\left[1,\frac{3.38}{\beta/H}\sqrt{\frac{1+\alpha}{\kappa_{\rm sw}\,\alpha}}\right]$$

$$S(f) = \left(\frac{f}{f_{\rm peak}}\right)^3\left(\frac{7}{4+3\,(f/f_{\rm peak})^2}\right)^{7/2}$$

$$f_{\rm peak} = 8.9\,{\rm mHz}\left(\frac{T_{\rm p}}{100\ {\rm GeV}}\right)\left(\frac{\beta/H}{1000}\right)\left(\frac{g_{\rm tot,p}}{100}\right)^{1/2}\left(\frac{100}{h_{\rm tot,p}}\right)^{1/3}$$

Effect of Yukawa coupling on effective potential.

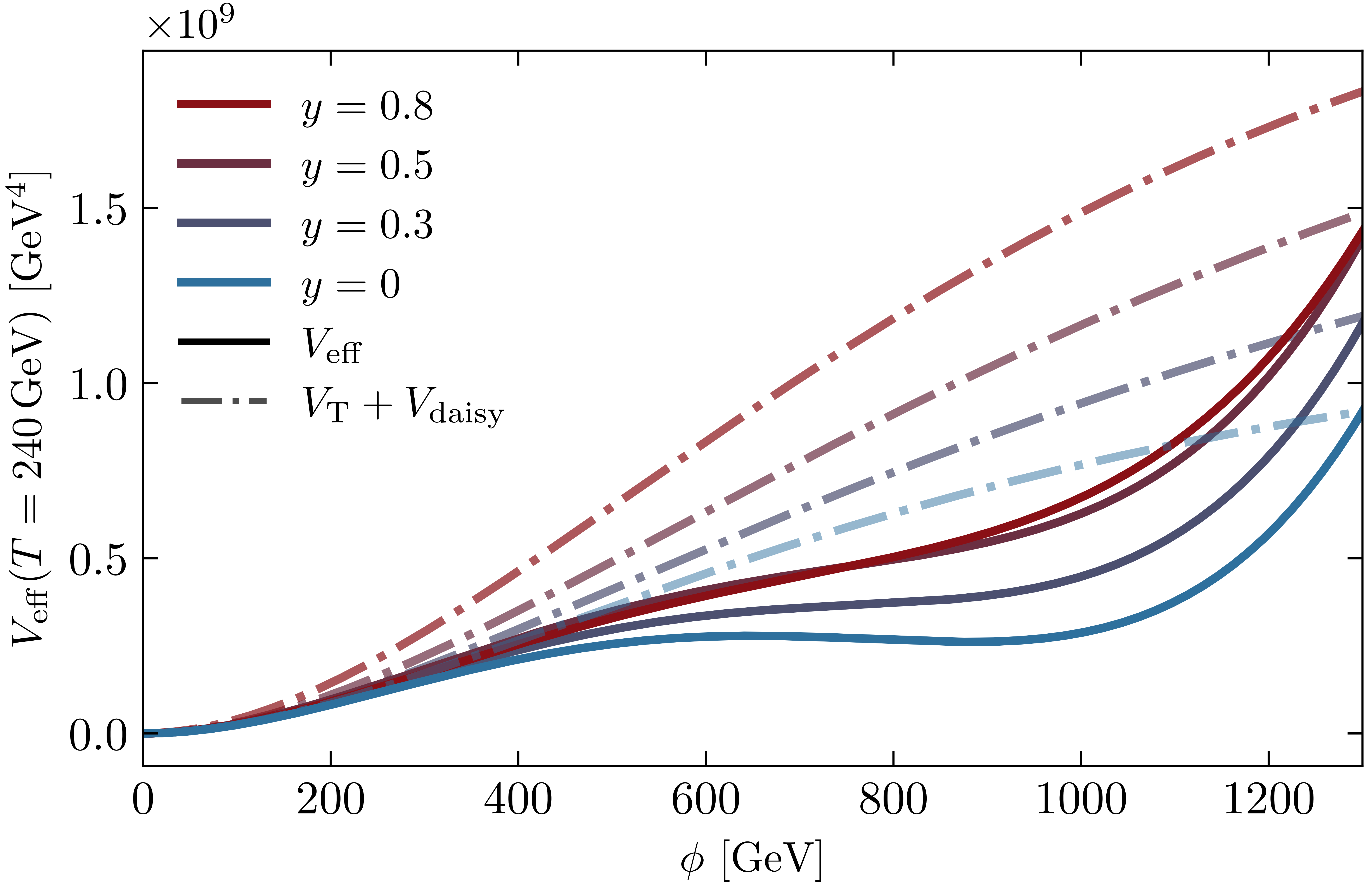

Grid scans over couplings.

Comparison with hot dark sector phase transition.

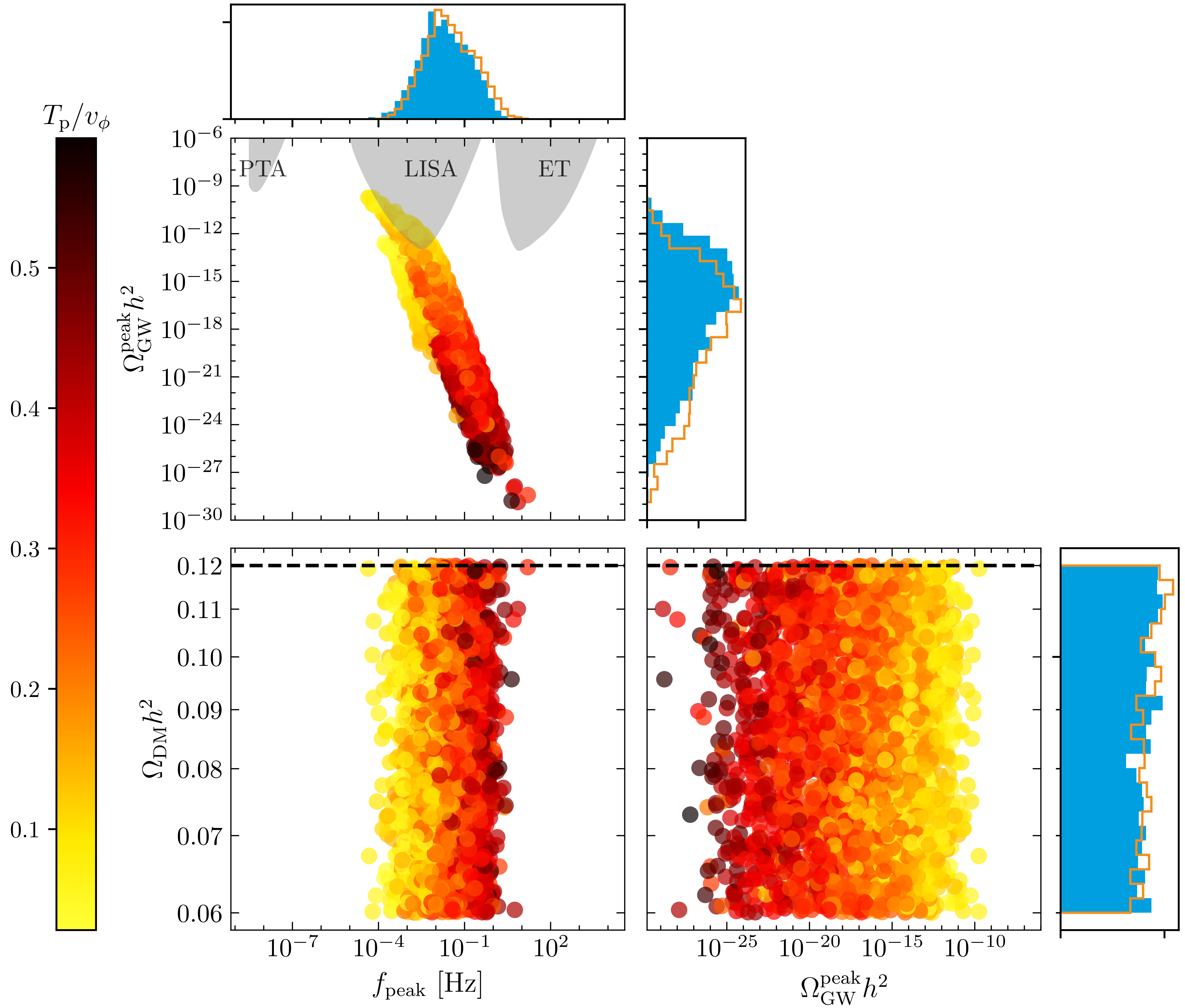

Evolution of energy densities.

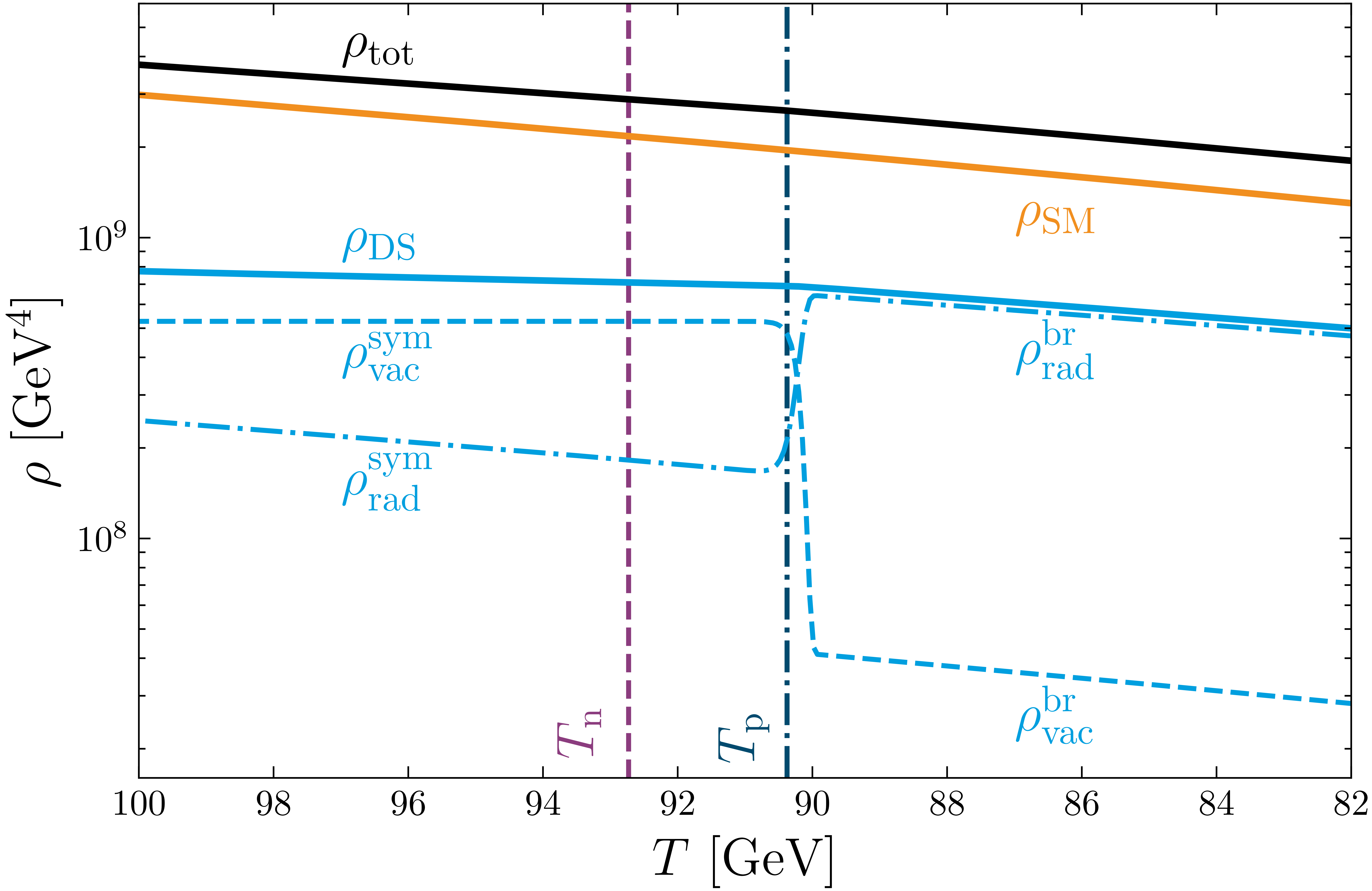

Out-of-equilibrium fraction of the dark sector.

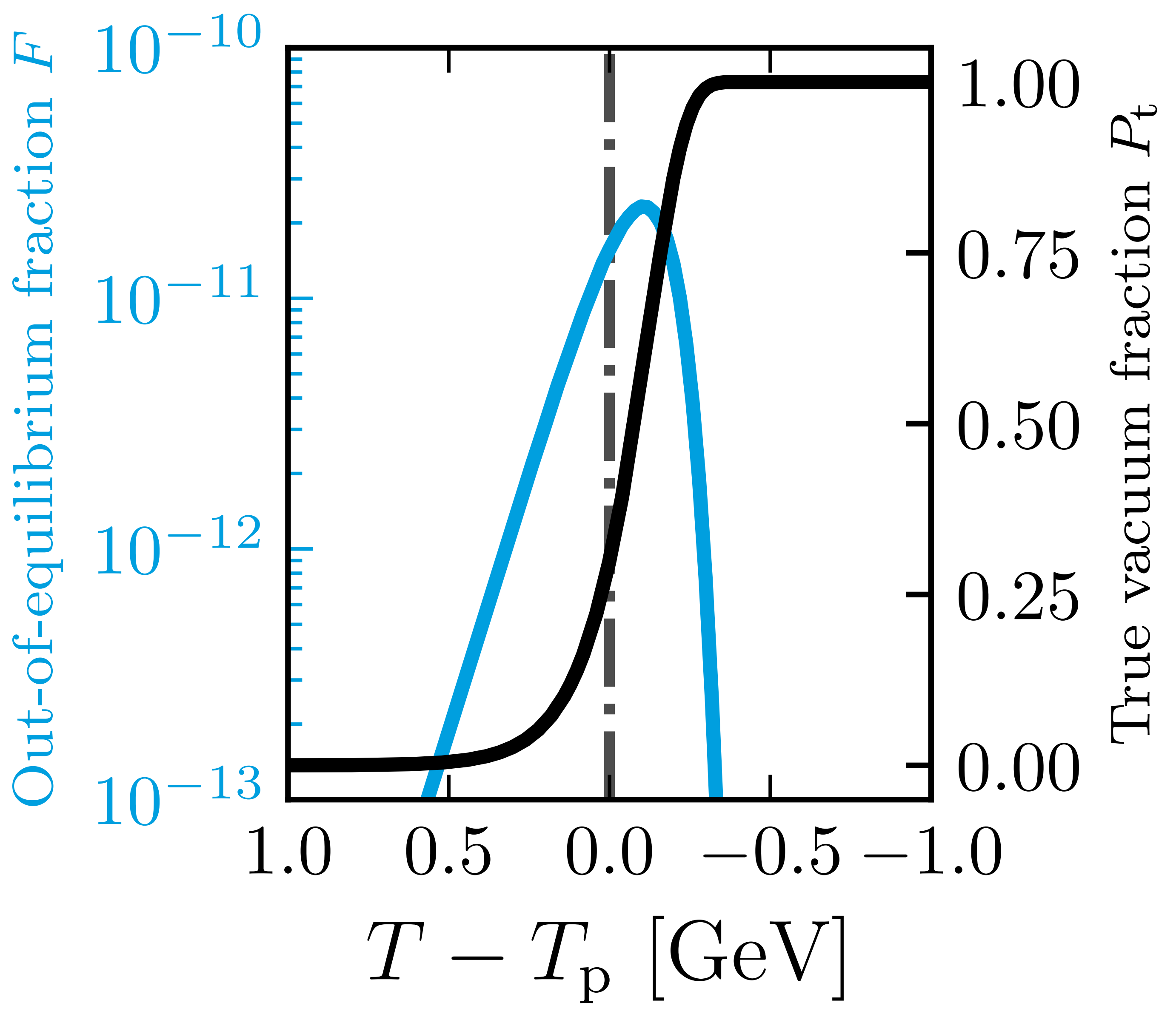

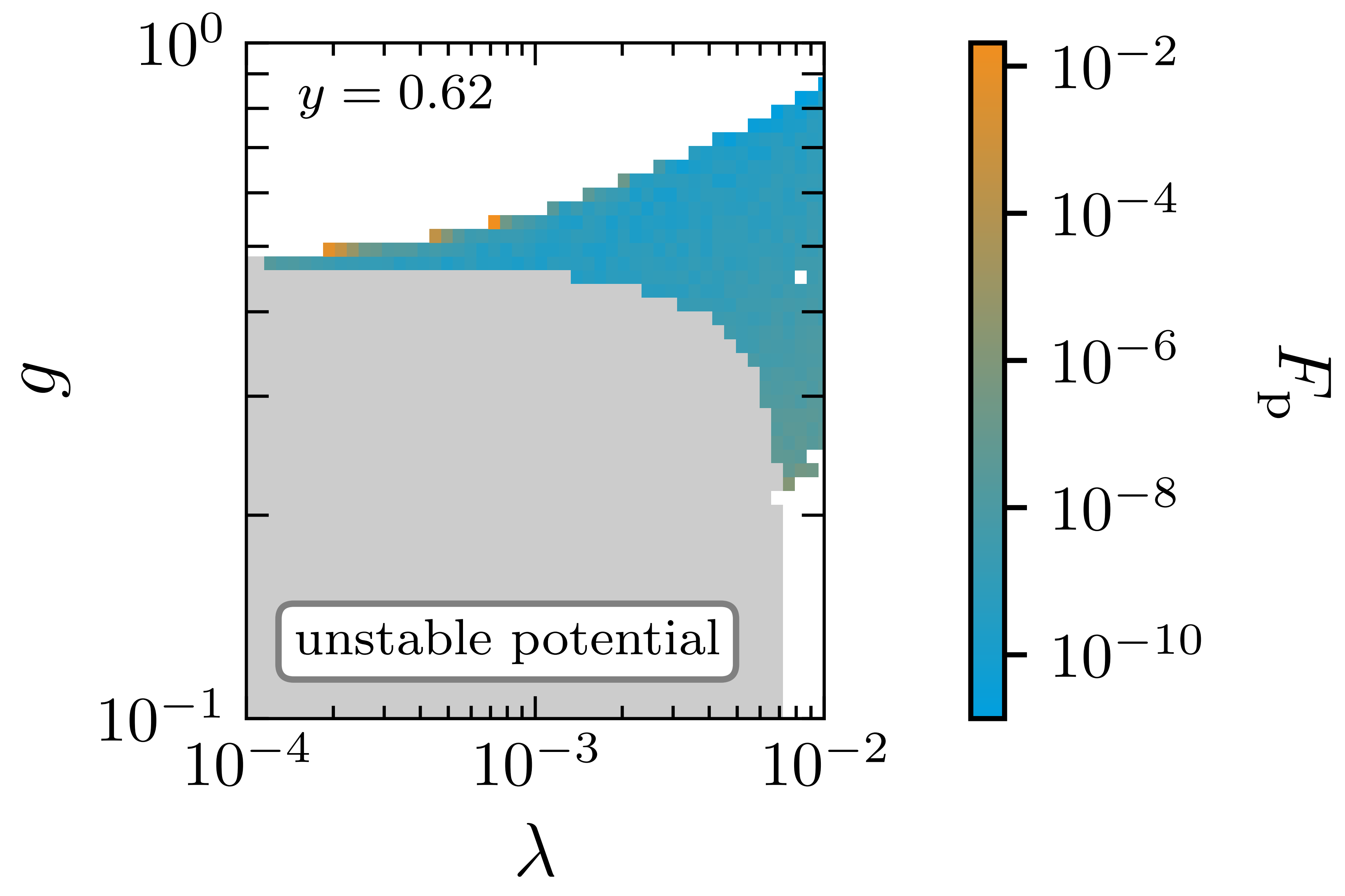

$$F(t) \equiv P(t-\tau) - P(t) > 0$$

$$\begin{aligned} F(t) &\approx \exp\left(-0.34 e^{\beta(t-t_p-\tau)}\right) - \exp\left(-0.34 e^{\beta(t-t_p)}\right) \\ &\approx \beta\tau e^{\beta(t-t_p)} \exp\left(-0.34 e^{\beta(t-t_p)}\right) \leq 0.37\beta\tau\,. \end{aligned} \tag{4.6}$$

Here, the last term follows by inserting the time at which $F(t)$ peaks, which is found to be $t \approx t_p - 1.08/\beta$. Alternatively, one can interpret F as the volume fraction of a shell around the bubbles with the width of the mean free path of the particles that just entered the bubbles.

Dilution effect.

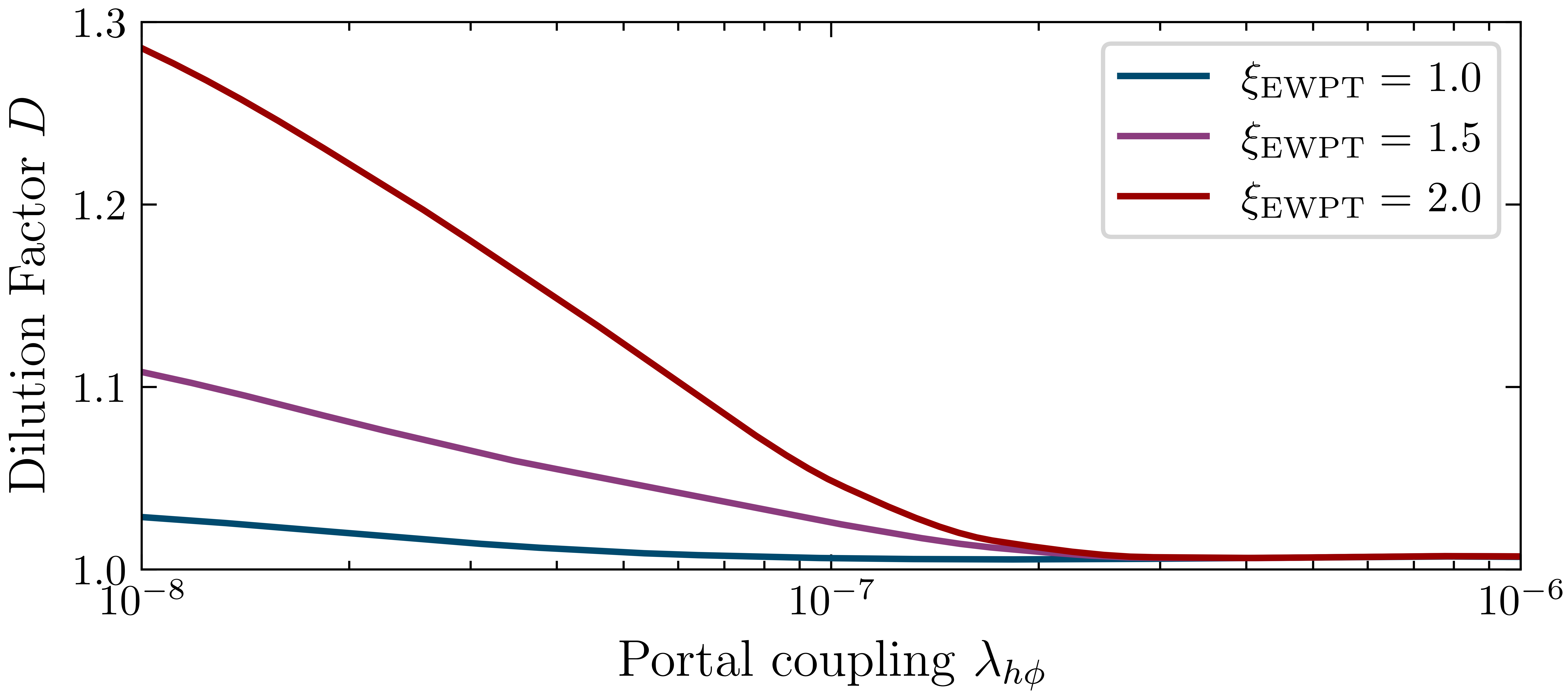

Effect of $\lambda_{h\phi}$ and ξ.

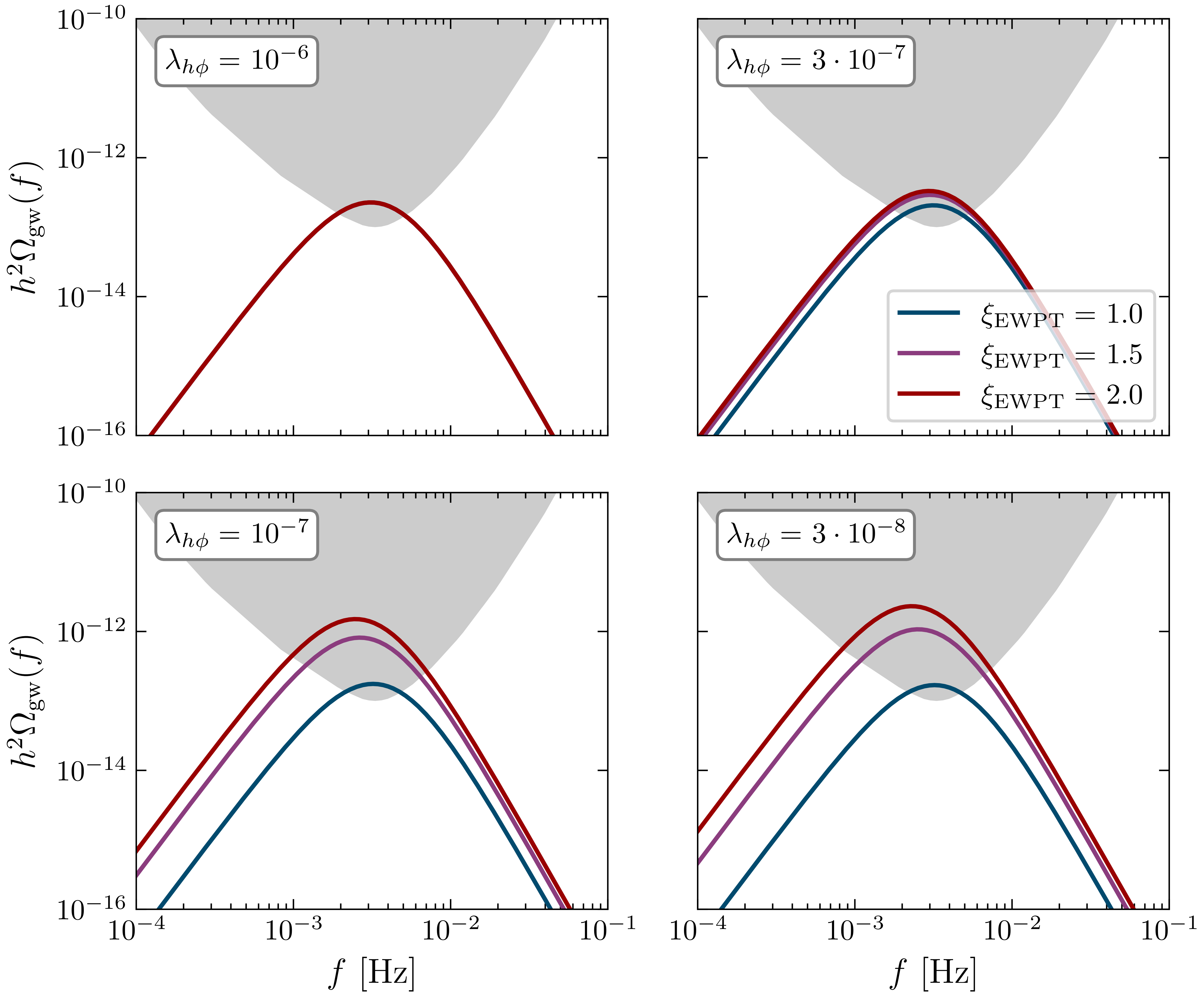

Temperature evolution in the dark sector.

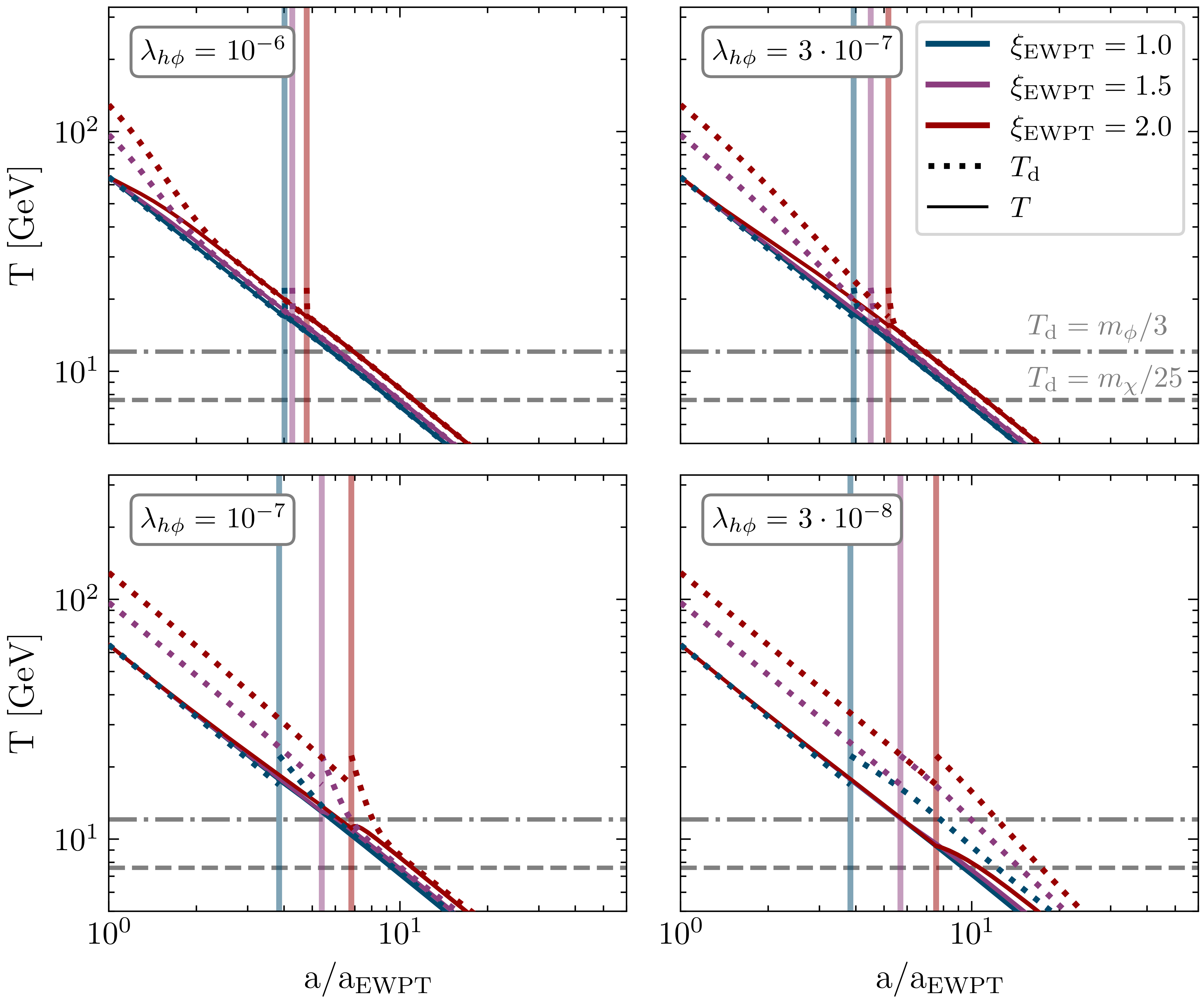

Detection probabilities.

	Fraction of parameter points observable by LISA	
	$\xi_{\rm EWPT}=1,\ \lambda_{h\phi}=10^{-6}$	$\xi_{\rm EWPT}=2,\ \lambda_{h\phi}=10^{-7}$
Full sample	0.1%	0.5%
First-order PT	0.8%	3%
First-order PT + relic density	3%	8%
Strong supercooling	10%	21%
Strong supercooling + relic density	35%	69%

Table 2. Fraction of parameter points that predict an observable GW signal for LISA after imposing various selection requirements on the sample of points drawn from the parameter ranges discussed in section 2.5.

Bödeker-Moore criterion.

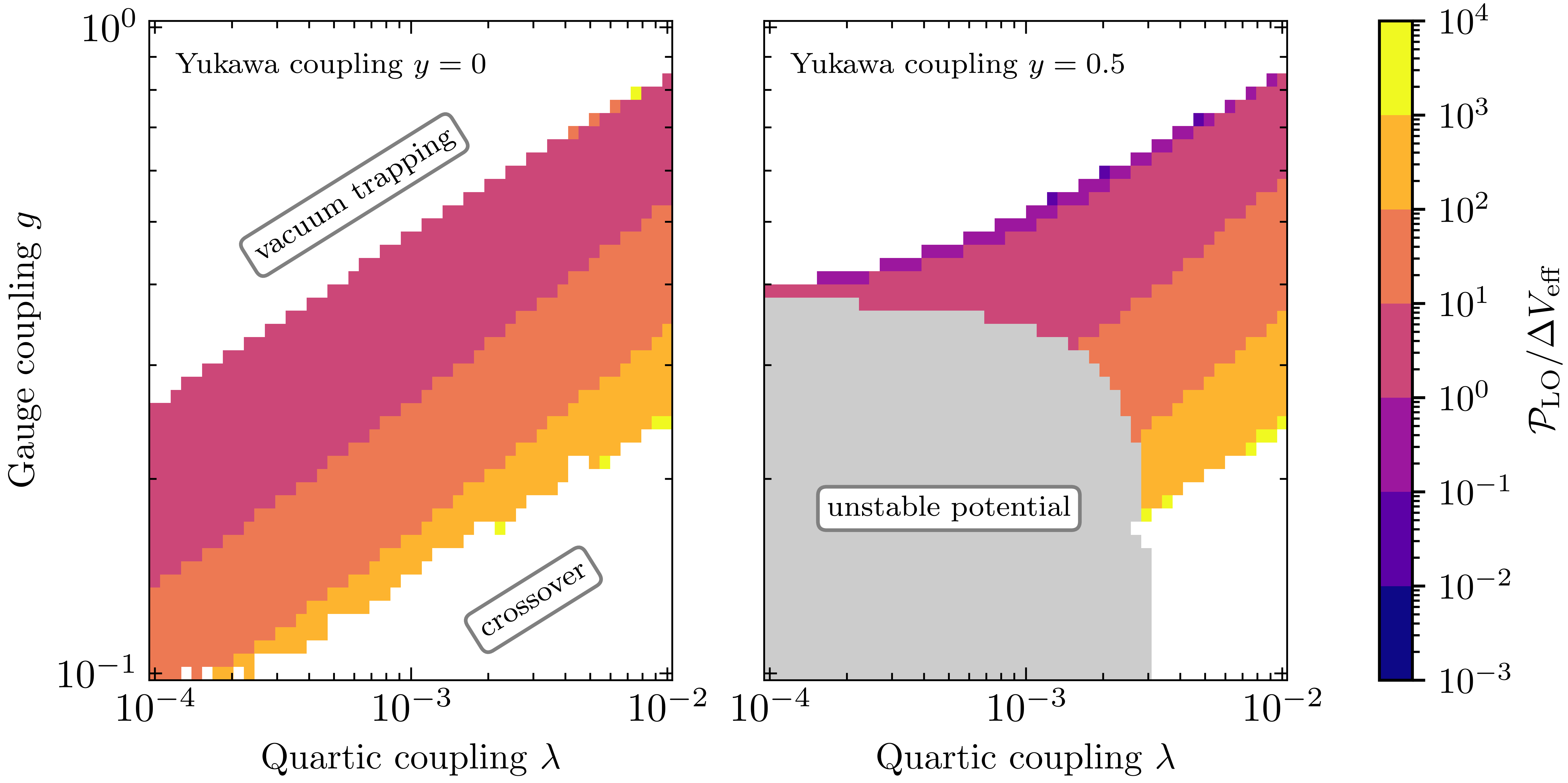

$$\text{Bödeker-Moore criterion:} \quad \begin{cases} \Delta V_{\rm eff} > \mathcal{P}_{\rm LO} & \text{Relativistic bubble walls} \\ \Delta V_{\rm eff} < \mathcal{P}_{\rm LO} & \text{Non-relativistic bubble walls} \end{cases}$$

A brief history of time.

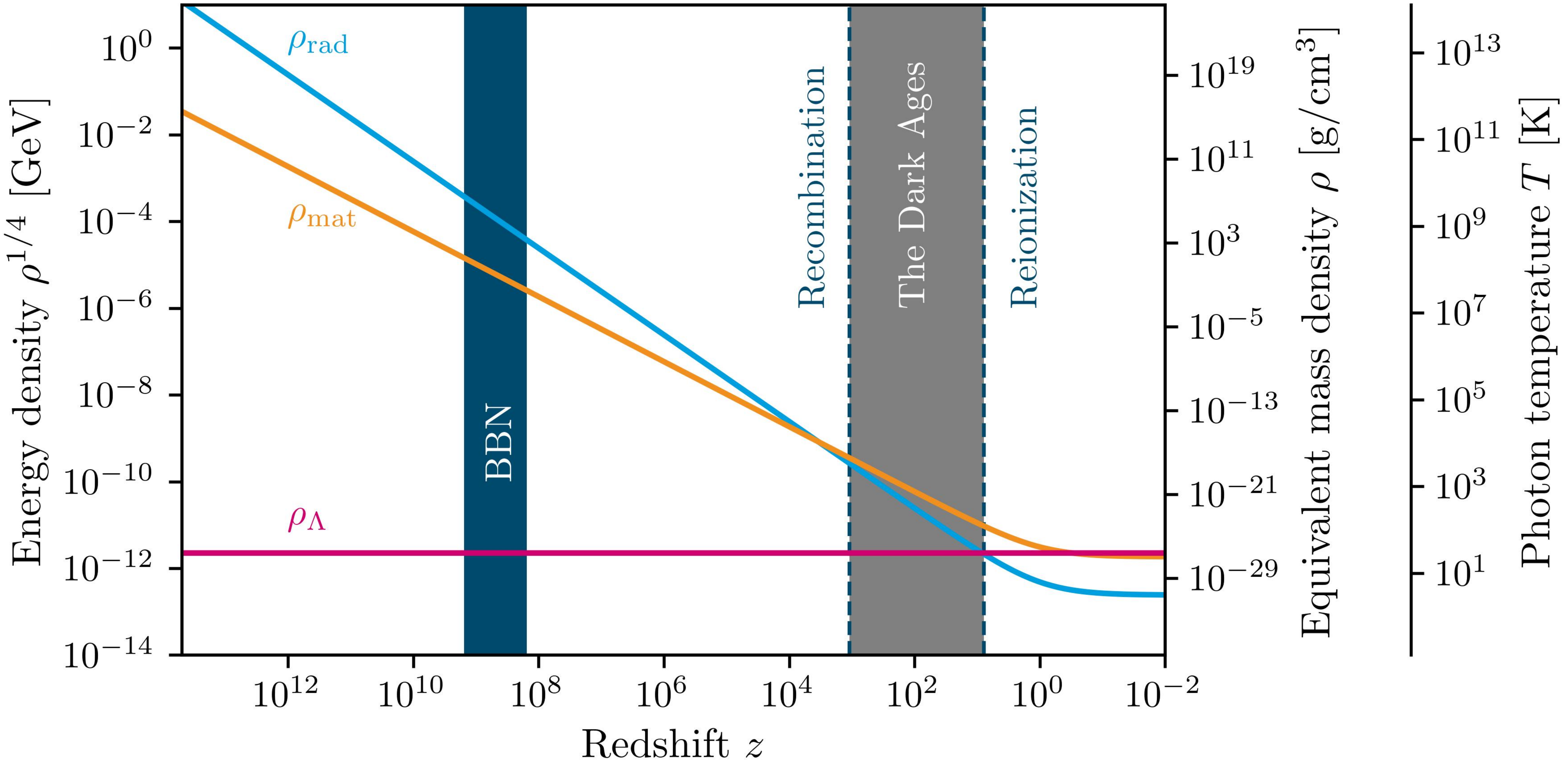

A brief history of time.

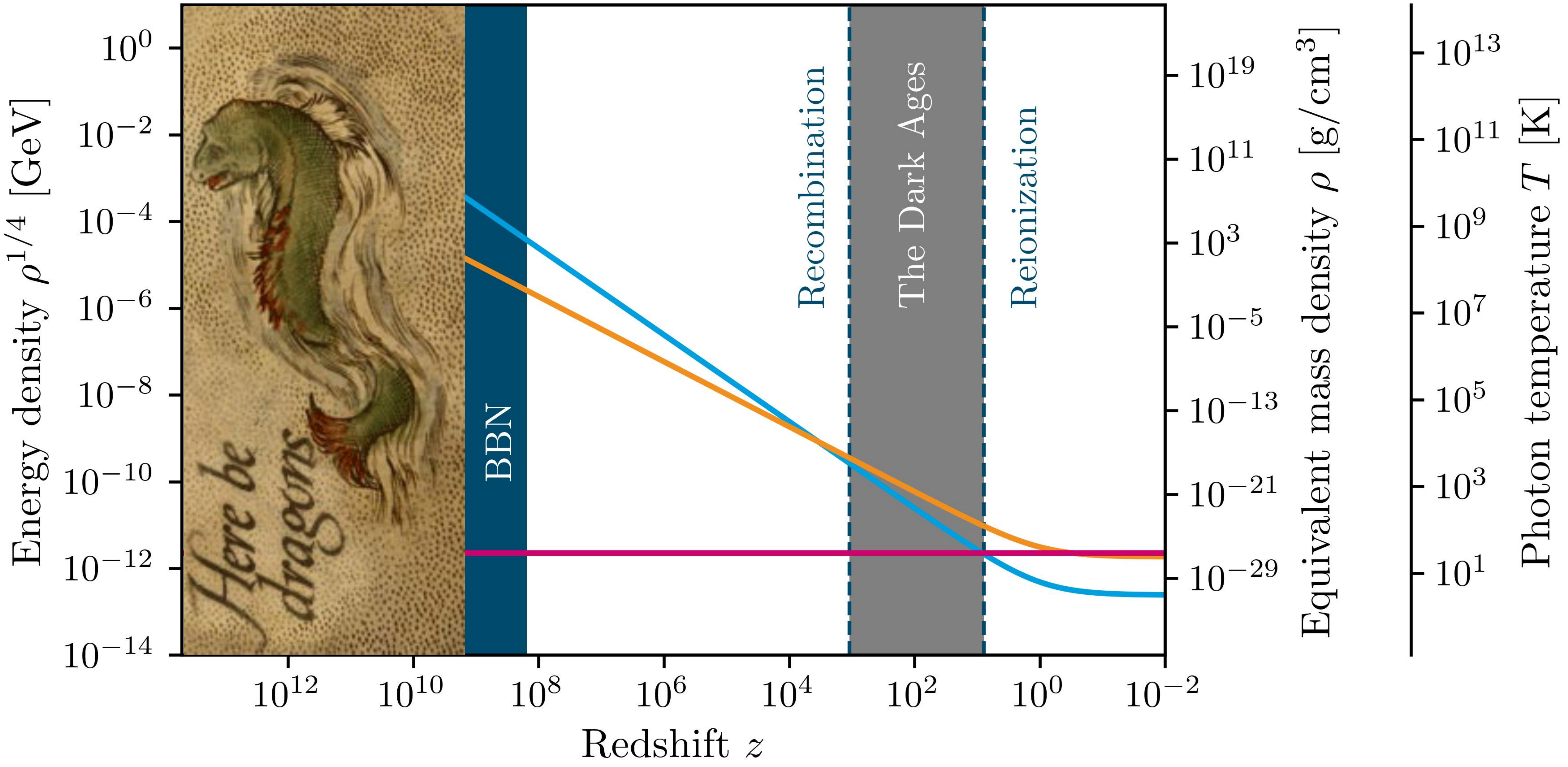

Possible cosmological sources of the PTA signal.

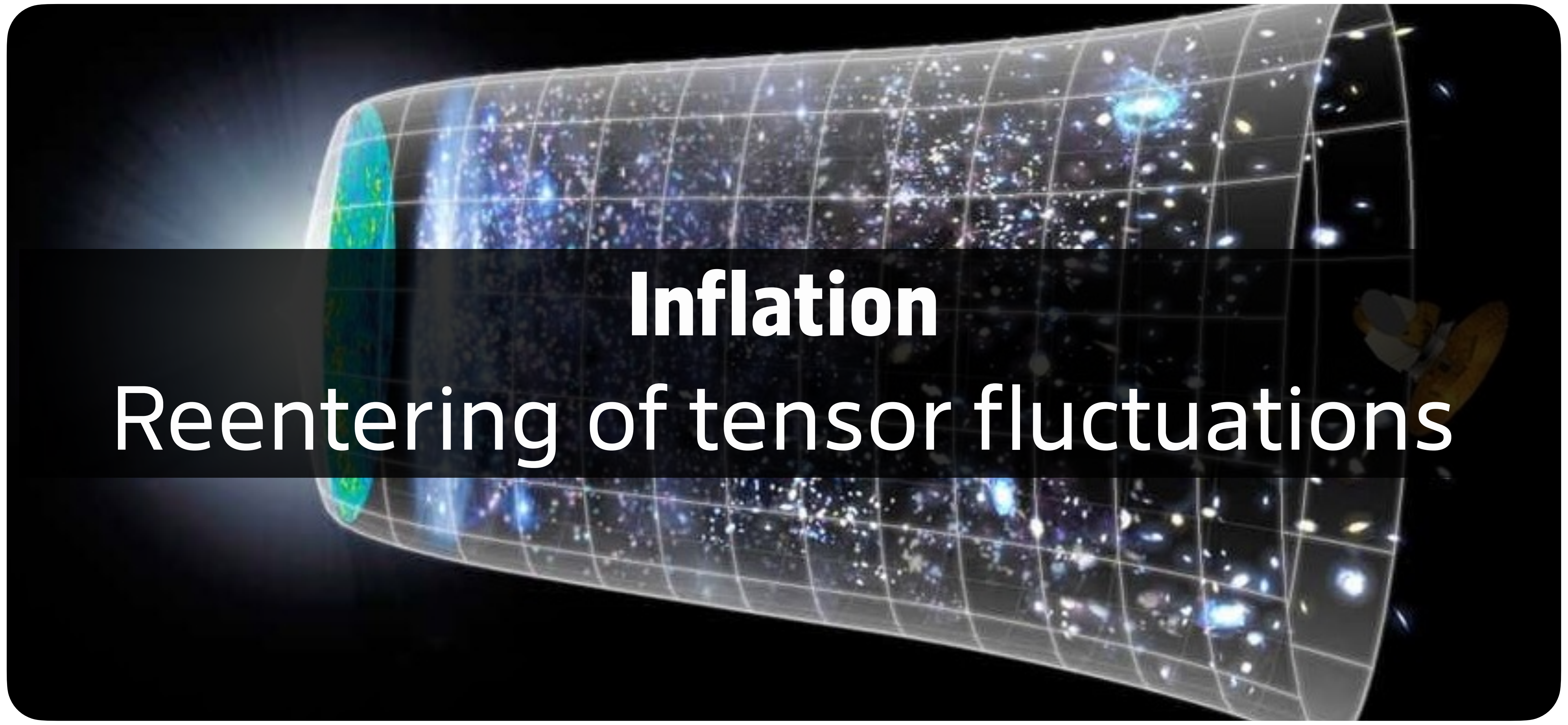

The impact of cosmic variance on PTA anisotropy searches.

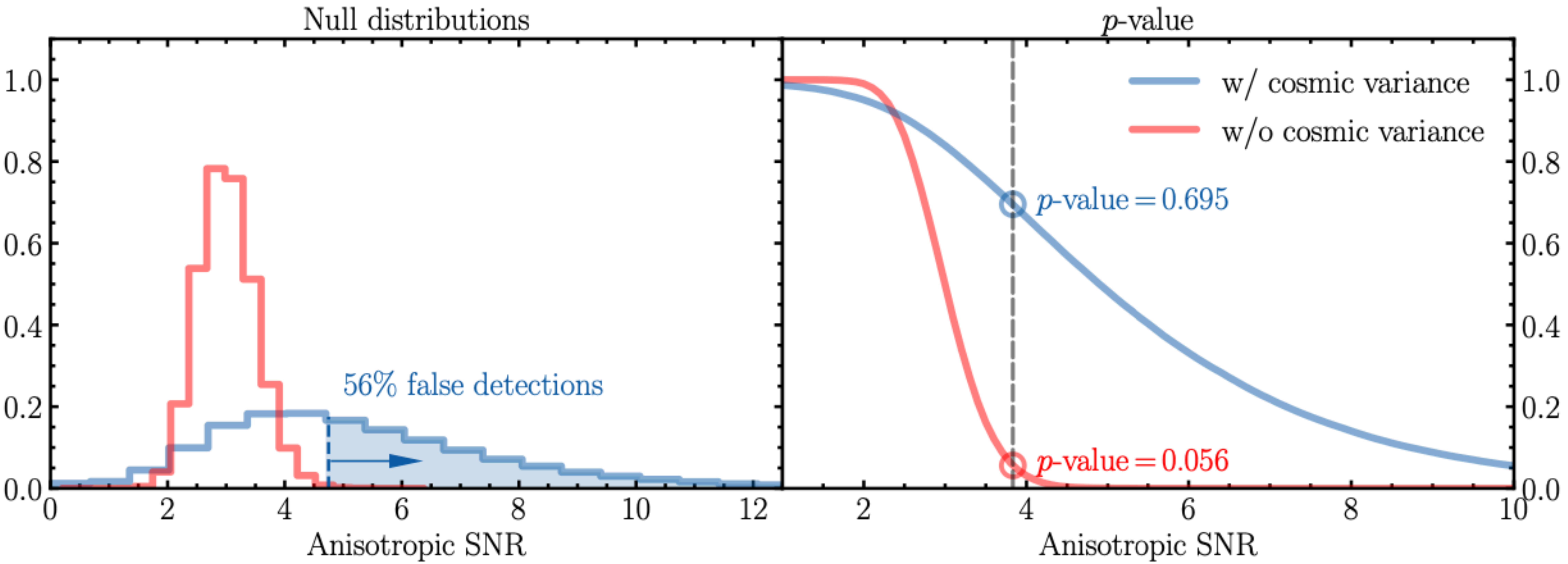

2408.07741, Konstandin, Lemke, Mitridate, Perboni

Gravitational waves from decaying sources in strong PTs.

$$\Omega_{\rm GW}(k) = 3\,\mathcal{T}_{\rm GW}\,\tilde\Omega_{\rm GW}\,(H_*/\beta)^2\,K^2_{\rm int}\;R_*\beta\;S(kR_*)\,, \tag{5.1}$$

where $S(k)$ denotes the shape function of the spectrum that is normalized to $\int d\ln k\, S(k) = 1$, and $K^2_{\rm int}$ is the integrated kinetic energy fraction K^2 over $\tilde t \equiv t\beta$, such that it reduces to $K^2\tau_{\rm sw}\beta$ when K is constant, being $\tau_{\rm sw}$ the GW source duration. Therefore, Eq. (5.1) is a generalization of the parameterization used in the stationary UETC assumption previously tested with numerical simulations [40, 50, 52] and usually assumed for sound-wave sourcing of GWs [22, 51, 54, 59, 91, 92, 99] that predicts a linear growth with the GW source duration when K does not decay with time.

The most robust results (i.e., an almost independent value of $\tilde\Omega_{\rm GW}$ with the PT parameters) are obtained when the typical bubble separation R_*, which determines the length scale of fluid perturbations, is given by the front of the expanding bubbles [22]

$$\beta R_* = (8\pi)^{1/3}\max(v_{\rm w}, c_{\rm s})\,, \tag{5.2}$$

where $1/\beta$ parameterizes the duration of the PT, $v_{\rm w}$ is the wall velocity, and $c_{\rm s}$ the speed of sound. This way, the residual dependence on the wall velocity in $\tilde\Omega_{\rm GW}$ is quite limited and we estimate from our numerical simulations values for the GW efficiency $\tilde\Omega_{\rm GW} \sim \mathcal{O}(10^{-2})$ for a range of PTs [see Fig. 7 and Eq. (4.9)],

$$10^2\,\tilde\Omega_{\rm GW} = \begin{cases} 1.04^{+0.81}_{-0.67}\,, & \text{for} \quad \alpha = 0.0046\,;\\ 1.64^{+0.29}_{-0.13}\,, & \text{for} \quad \alpha = 0.05\,;\\ 3.11^{+0.25}_{-0.19}\,, & \text{for} \quad \alpha = 0.5\,, \end{cases} \tag{5.3}$$

$$K^2_{\rm int}(b, \tau_{\rm sw}) \to \mathcal{K}_0^2\,\beta\, t_*\,\frac{(1+\tau_{\rm sw}/t_*)^{1-2b} - 1}{1-2b}\,, \tag{5.6}$$

when one uses the power-law fit for $K(\tilde t)$ and assumes that the GW production roughly starts at the time $\tilde t_* \simeq \tilde t_0 \simeq 10$ (note that the actual value of $\tilde t_0$ only appears as a consequence of our particular fit). It is unclear what should be the final time of GW sourcing in these cases, as the simulations seem to already be modelling the non-linear regime, so we leave $\tilde\tau_{\rm sw}$ as a free parameter. We note that this is an indication that the GW spectrum might still grow once that non-linearities develop in the fluid, such that the use of Eq. (5.5) would in general underestimate the GW production. We compare in Fig. 8 the numerical dependence of the GW amplitude with the source duration $\tilde\tau_{\rm sw}$ found in the simulations to the one obtained using Eq. (5.6), extending the analytical fit beyond the time when the simulations end.

As a final remark on the integrated GW amplitude, we note that so far Universe expansion has been ignored, which is not justified for long source durations. Taking into account that the fluid equations are conformal invariant after the PT if the fluid is radiation-dominated, we can apply the results from our fluid simulations in Minkowski space-time to an expanding Universe, as long as the PT duration is short ($\beta/H_* \gg 1$) even if the GW source duration is not short (see discussion in Sec. 2.6). Then, as a proxy to estimate the effect of the Universe expansion, we can use the following value for $K^2_{\rm int}$ [see Eq. (2.23)]

$$K^2_{\rm int} \to \mathcal{K}_0^2\,\Upsilon_b(\tau_{\rm sw})\,(\beta/H_*)\,, \tag{5.7}$$

which generalizes the suppression factor $\Upsilon = H_*\tau_{\rm sw}/(1+H_*\tau_{\rm sw})$ when the source does not decay [89, 91] to any decay rate b using Eq. (2.24) for the presented power-law decay fit of $K(\tilde t)$. We also compare in Fig. 8 the expected evolution of the GW amplitude with the source

2409.03651, Caprini, Jinno, Konstandin, Roper Pol, Rubira, Stomberg

Detecting GW anisotropies from SMBHBs.

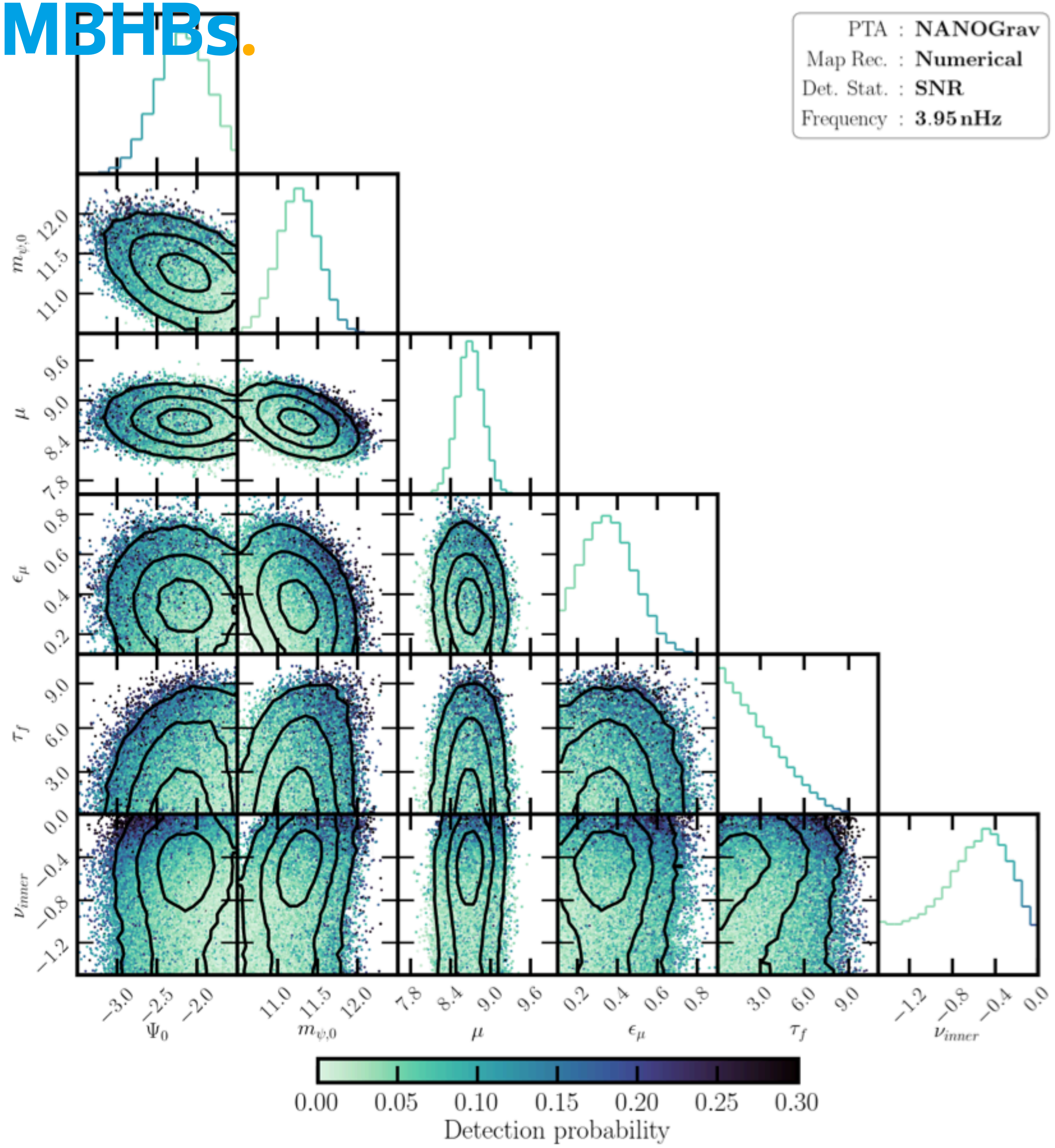

We find that a PTA with the noise characteristics of the NANOGrav 15-year data set had only a 2% – 11% probability of detecting SMBHB-generated anisotropies, depending on the properties of the SMBHB population. However, we estimate that for the IPTA DR3 data set these probabilities will increase to 4% – 28%, putting more pressure on the SMBHB interpretation in case of a null detection. We also identify SMBHB populations that are more likely to produce detectable levels of anisotropies. This information could be used together with the spectral properties of the GWB to characterize the SMBHB population.

2407.08705, Lemke, Mitridate, Gersbach

Turn up the volume.

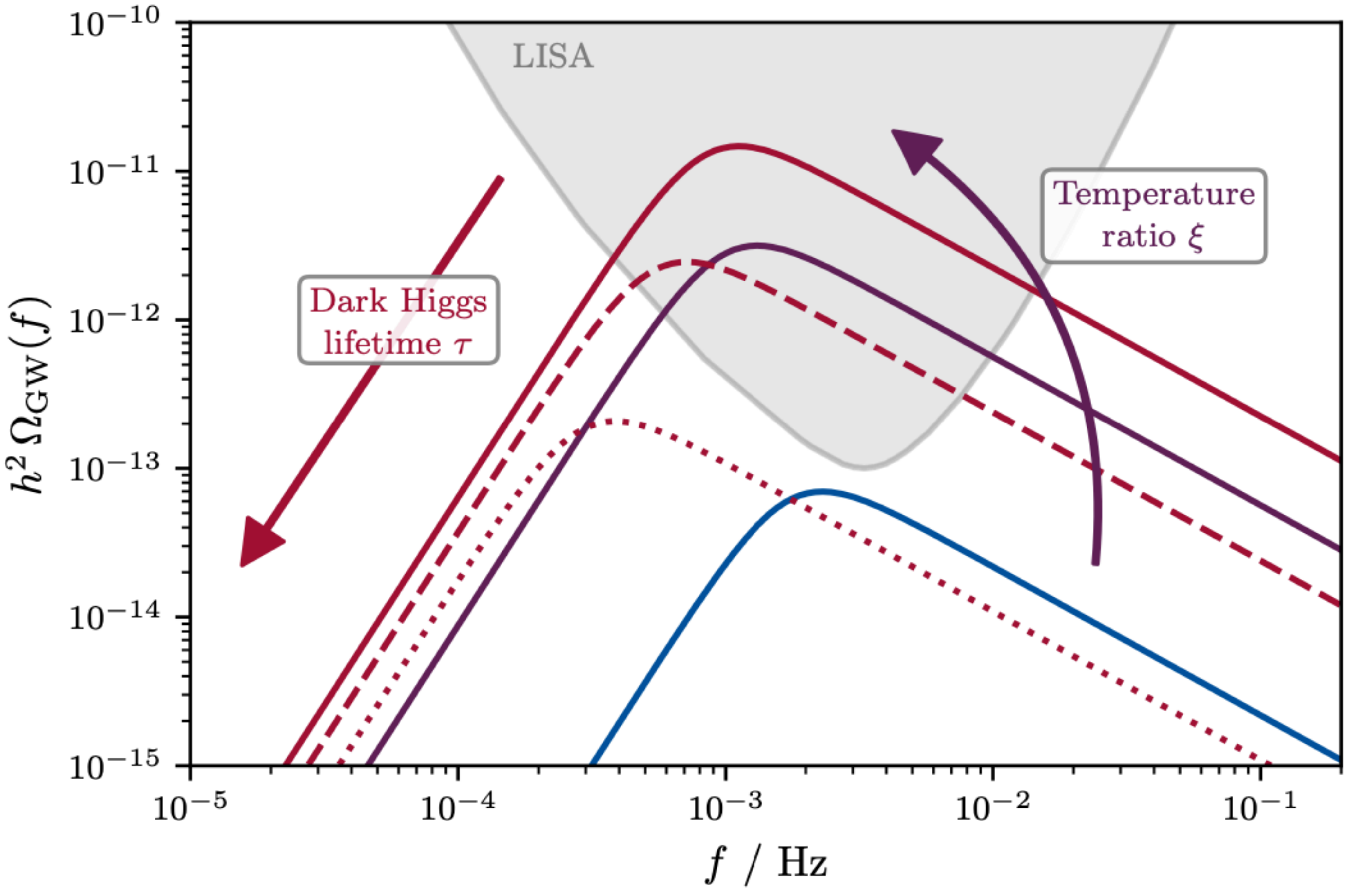

2109.06208, Ertas, Kahlhöfer, CT

Turn up the volume.

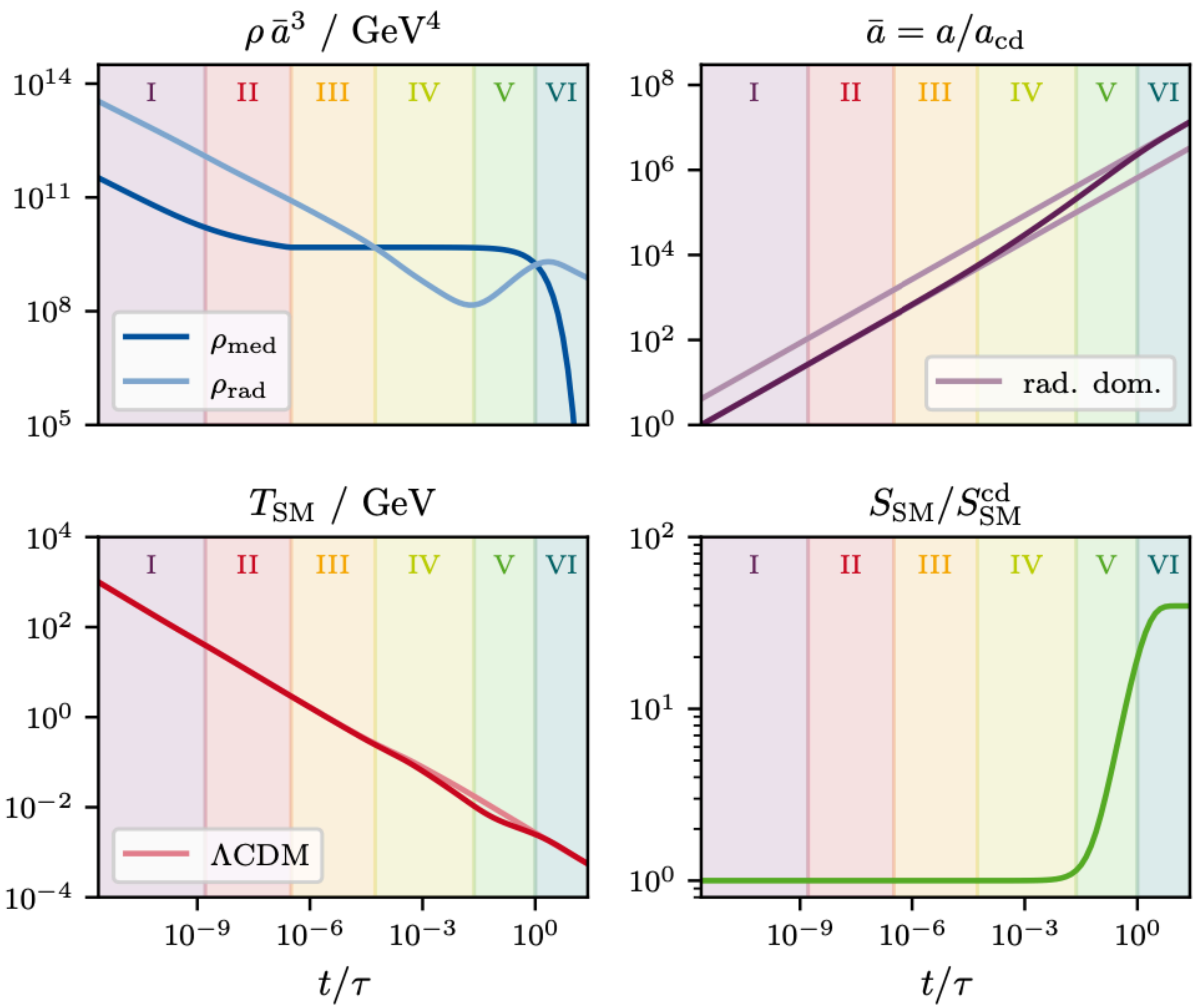

Figure 5. Time evolution of the comoving energy densities $\rho\,\bar{a}^3$ of the mediator species and the SM radiation (top-left), the normalized scale factor $\bar{a}$ (top-right), the temperature $T_{\rm SM}$ of the SM bath (bottom-left), as well as its entropy $S_{\rm SM}/S_{\rm SM}^{\rm cd}$ (bottom-right). The evolution can be divided into the following phases: relativistic mediator (I), cannibalism (II), non-relativistic mediator (III), early matter domination (IV), entropy injection (V), and decay (VI). See text for details.

2109.06208, Ertas, Kahlhöfer, CT

Turn up the volume.

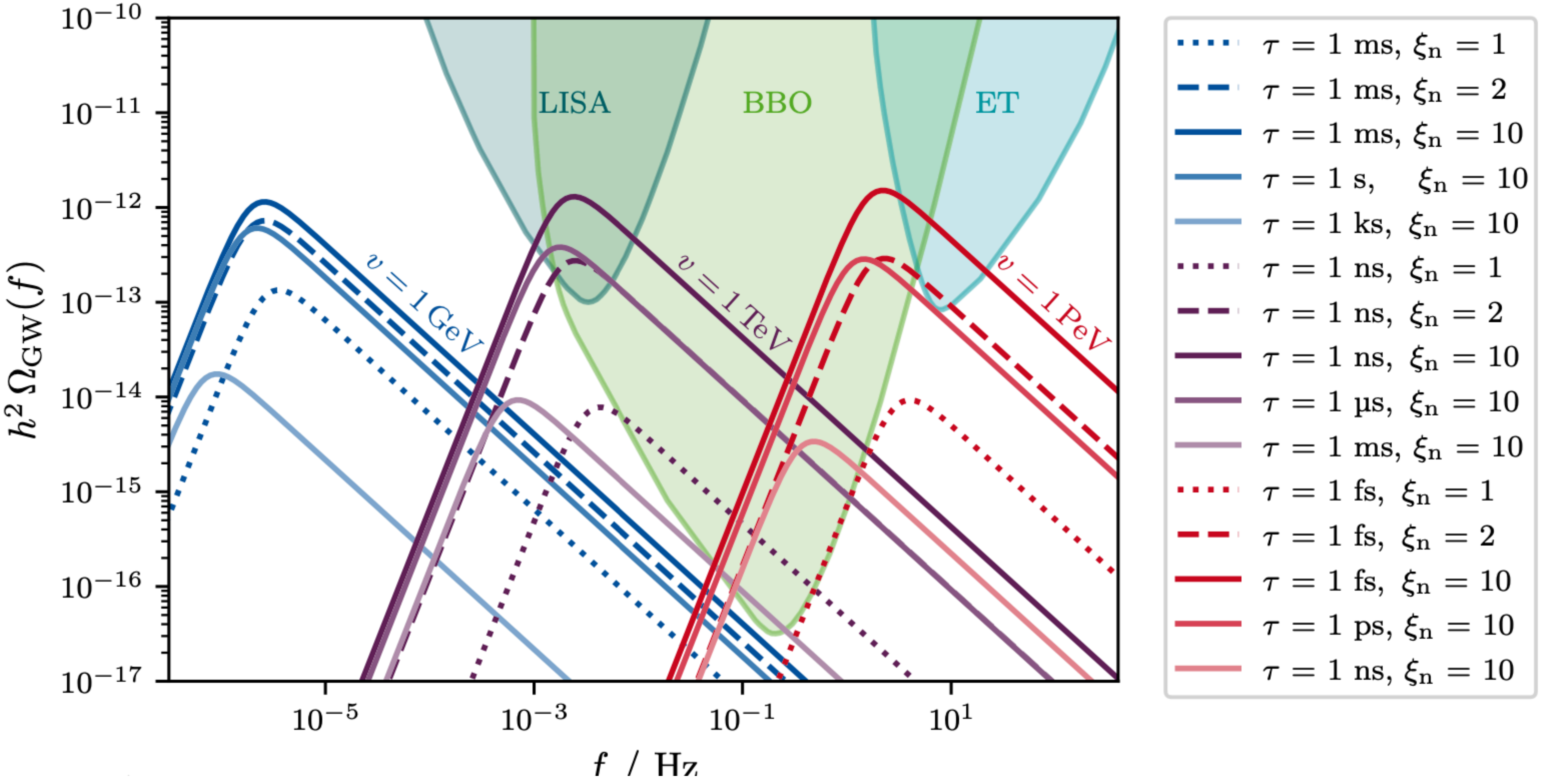

2109.06208, Ertas, Kahlhöfer, CT

Turn up the volume.

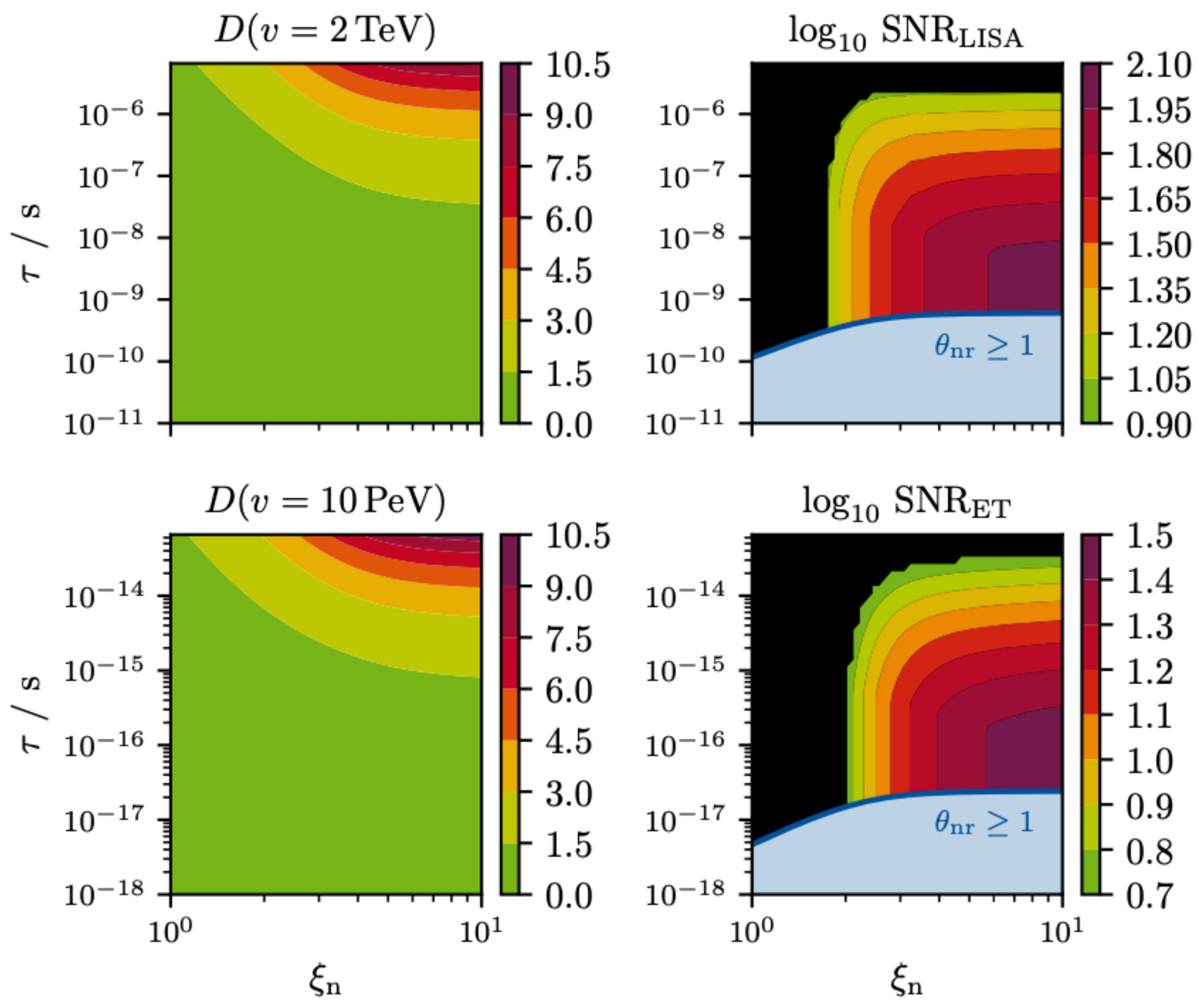

2109.06208, Ertas, Kahlhöfer, CT

Do PTAs observe a dark sector phase transition?

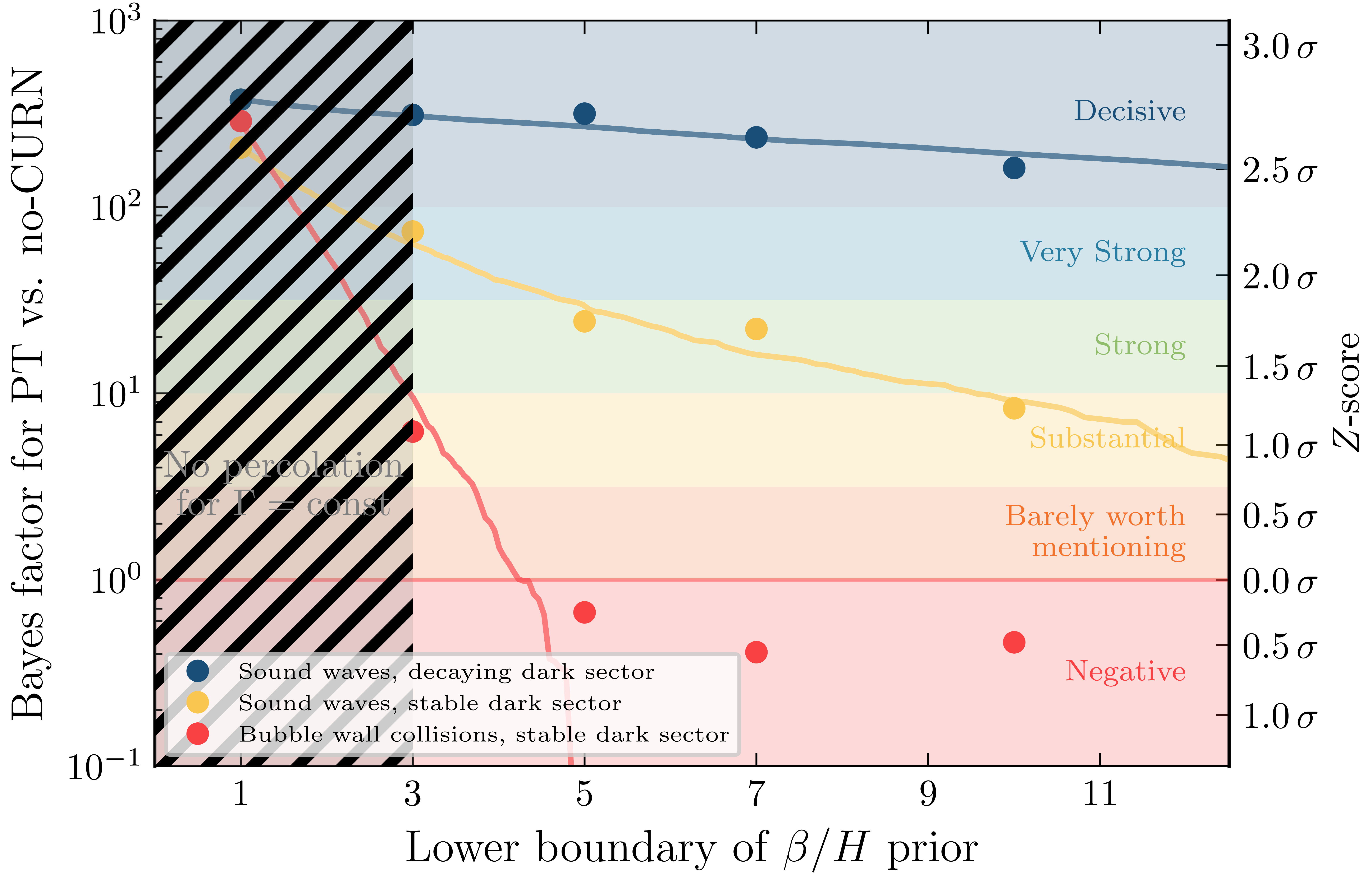

2306.09411, Bringmann, Depta, Konstandin, Schmidt-Hoberg, CT

Do PTAs observe a dark sector phase transition?

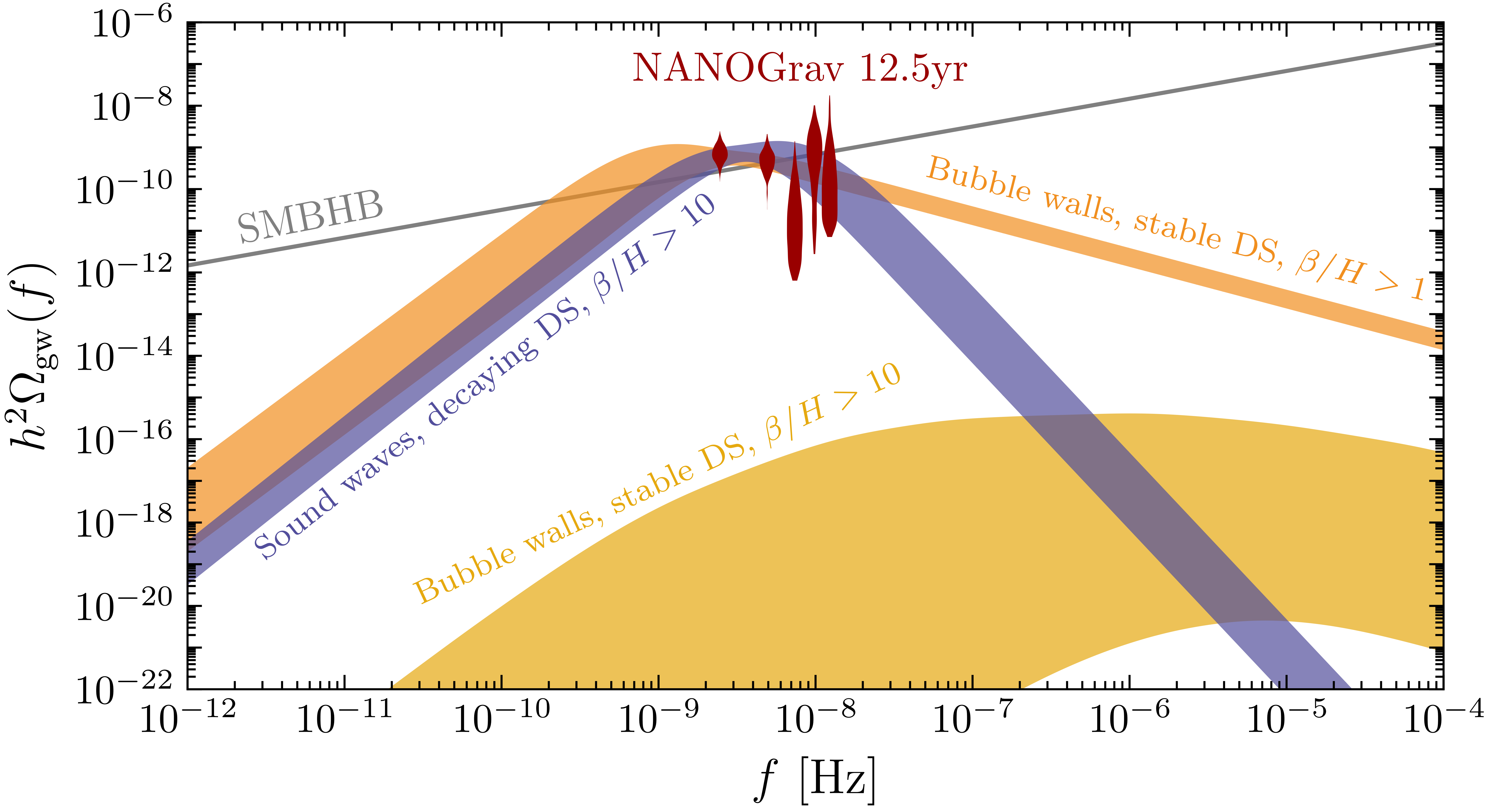

2306.09411, Bringmann, Depta, Konstandin, Schmidt-Hoberg, CT

Number of effective degrees of freedom at BBN.

$$\rho_\nu + \rho_{\rm extra} \equiv N_{\rm eff} \times \frac{7}{8}\left(\frac{4}{11}\right)^{4/3} \rho_\gamma \,, \tag{2.29}$$

such that the extra energy can be expressed as[7]

$$\rho_{\rm extra} = \Delta N_{\rm eff} \times \frac{7}{8}\left(\frac{4}{11}\right)^{4/3} \rho_\gamma \quad \text{where} \quad \Delta N_{\rm eff} \equiv N_{\rm eff} - N_{\rm eff}^{\rm SM} \,. \tag{2.30}$$

$$T_{\rm f} \simeq \left(\frac{\pi^2}{45}\right)^{1/6} \left[1 + \frac{7}{8}\left(\frac{4}{11}\right)^{4/3} N_{\rm eff}\right]^{1/6} \frac{1}{(G_{\rm F}^2 m_{\rm Pl})^{1/3}} \,.$$

BBN limits on MeV-scale electromagnetic scalar decays.

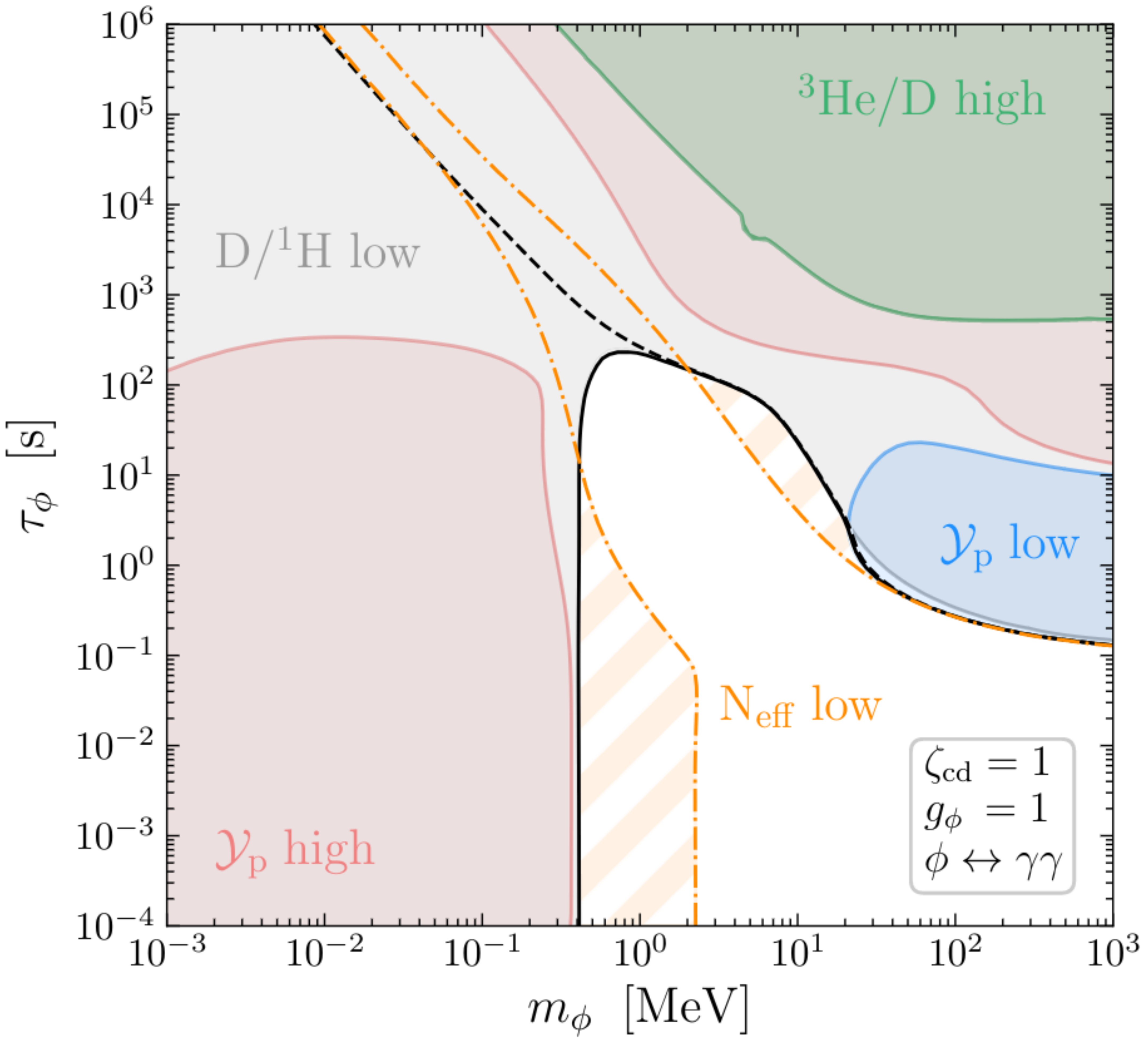

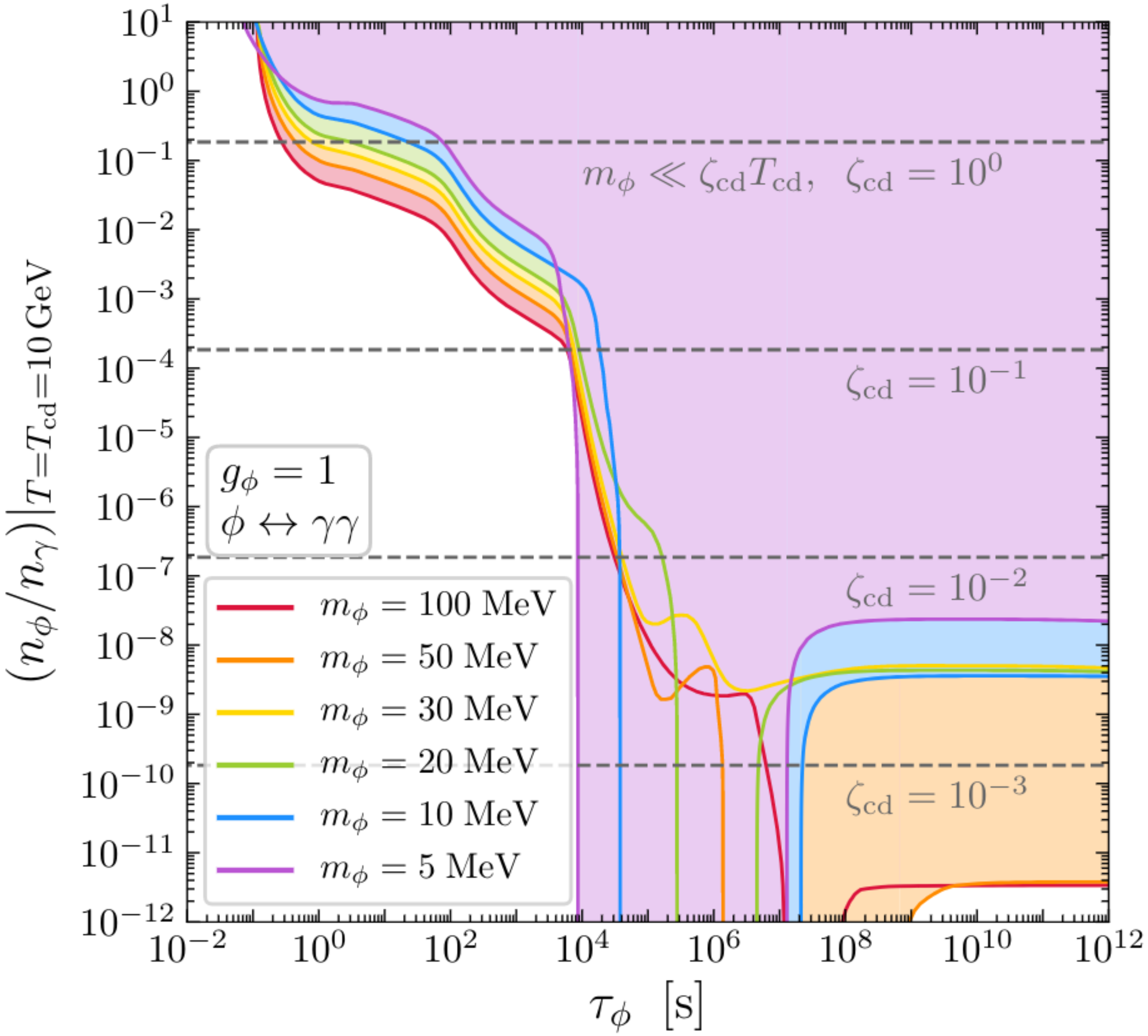

[Paul Frederik Depta]

Quo vadis pulsar timing?

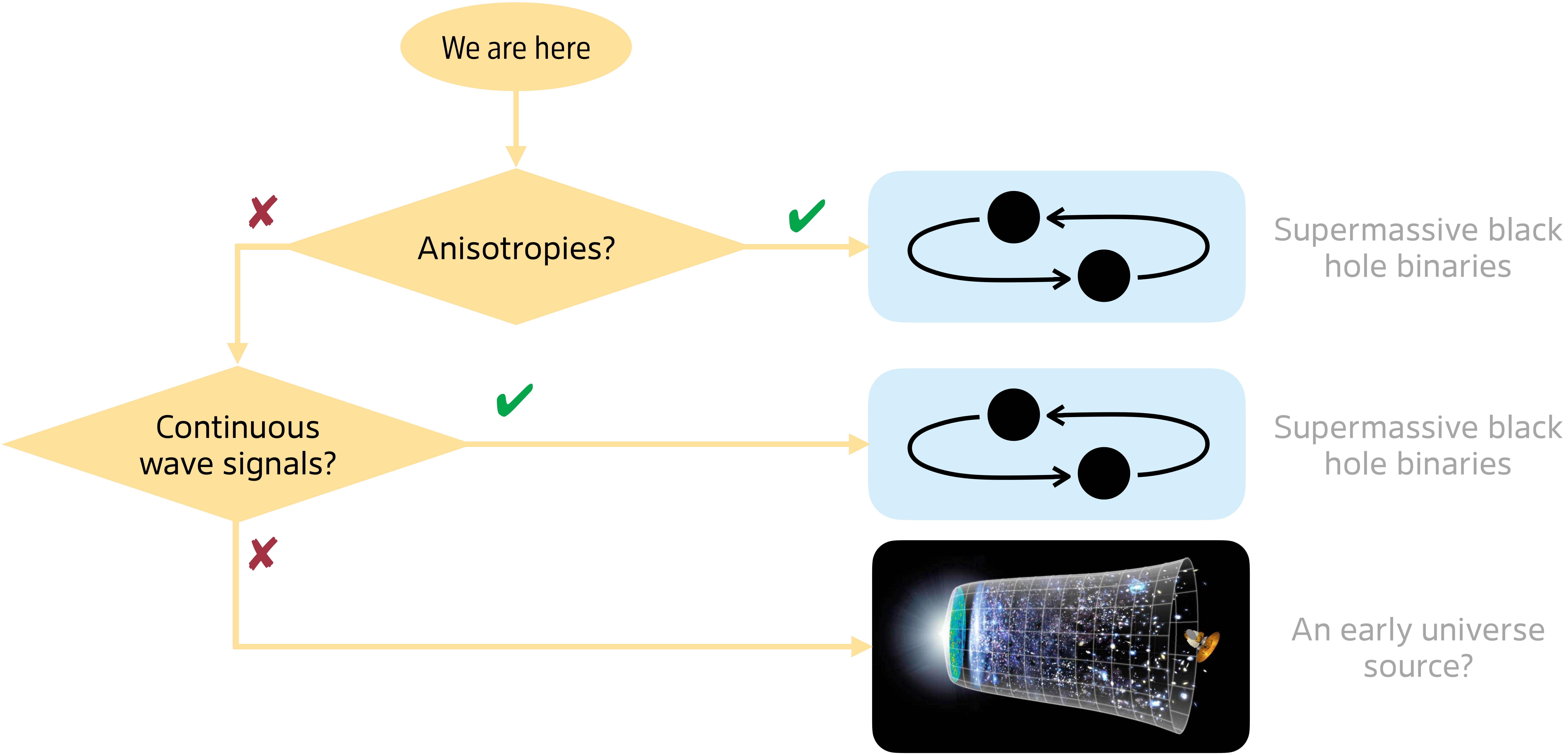

Polarization of a GW.

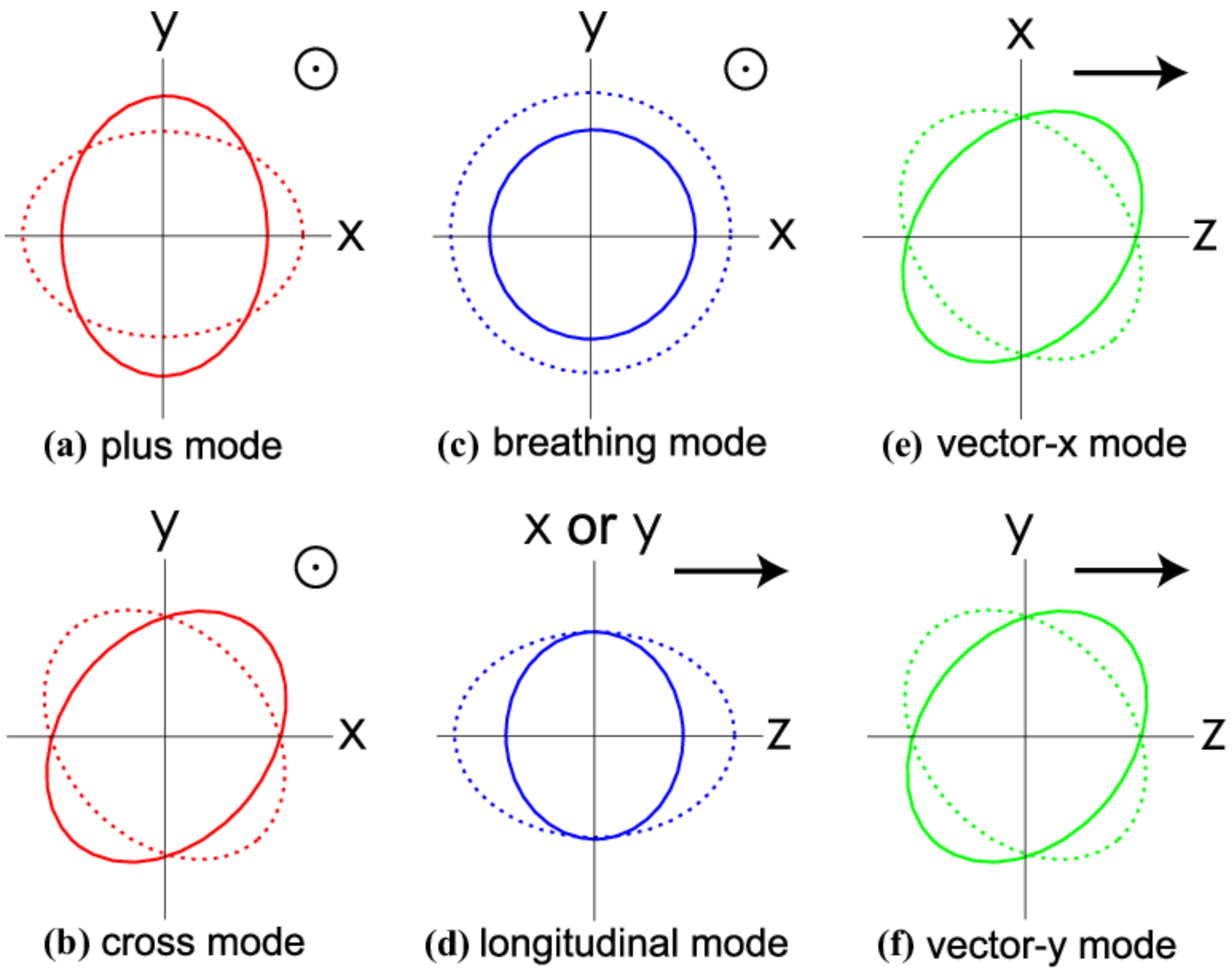

[Stephen Taylor et al., 2019]

Cosmological perturbation theory.

$$\Delta\Phi - 3\mathcal{H}\left(\Phi' - \mathcal{H}\Psi\right) = -2\frac{a^2\delta\rho}{m_{\mathrm{Pl}}^2}\,, \quad \Delta\left(\Phi + \Psi\right) = -\frac{a^2\Delta\sigma}{m_{\mathrm{Pl}}^2}\,,$$

$$\Delta\Xi_i = -\frac{2a^2 S_i}{m_{\mathrm{Pl}}^2} \quad \text{and} \quad \left(h_{ij}^{\mathrm{TT}}\right)'' + 2\mathcal{H}\left(h_{ij}^{\mathrm{TT}}\right)' - \Delta h_{ij}^{\mathrm{TT}} = \frac{2a^2\sigma_{ij}^{\mathrm{TT}}}{m_{\mathrm{Pl}}^2}\,.$$

Conversion of different GW spectra.

$$h^2\Omega_{\rm gw}(f) = \frac{4\pi^2}{3H_{100}^2} f^3 S_h(f) = \frac{2\pi^2}{3H_{100}^2} f^2 h_{\rm c}^2(f)$$

$$S_h(f) \simeq 10^{-36} \left(\frac{\rm Hz}{f}\right)^3 \frac{h^2\Omega_{\rm gw}(f)}{\rm Hz}$$

$$h_{\rm c}(f) \simeq 10^{-18} \left(\frac{\rm Hz}{f}\right) \sqrt{h^2\Omega_{\rm gw}(f)}$$

NANOGrav 15yr new physics analysis.

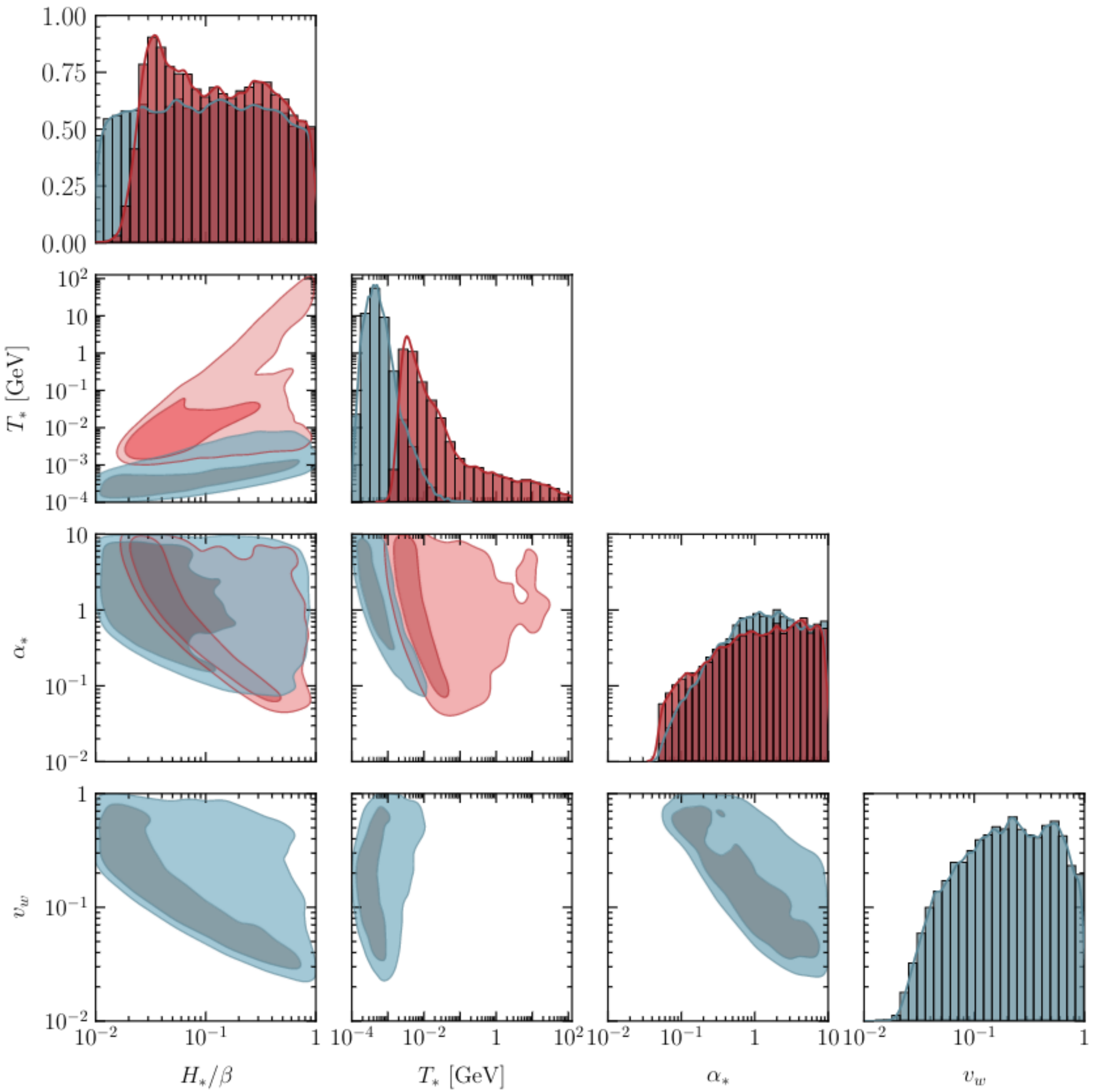

NANOGrav 15yr with BBN and CMB limits.

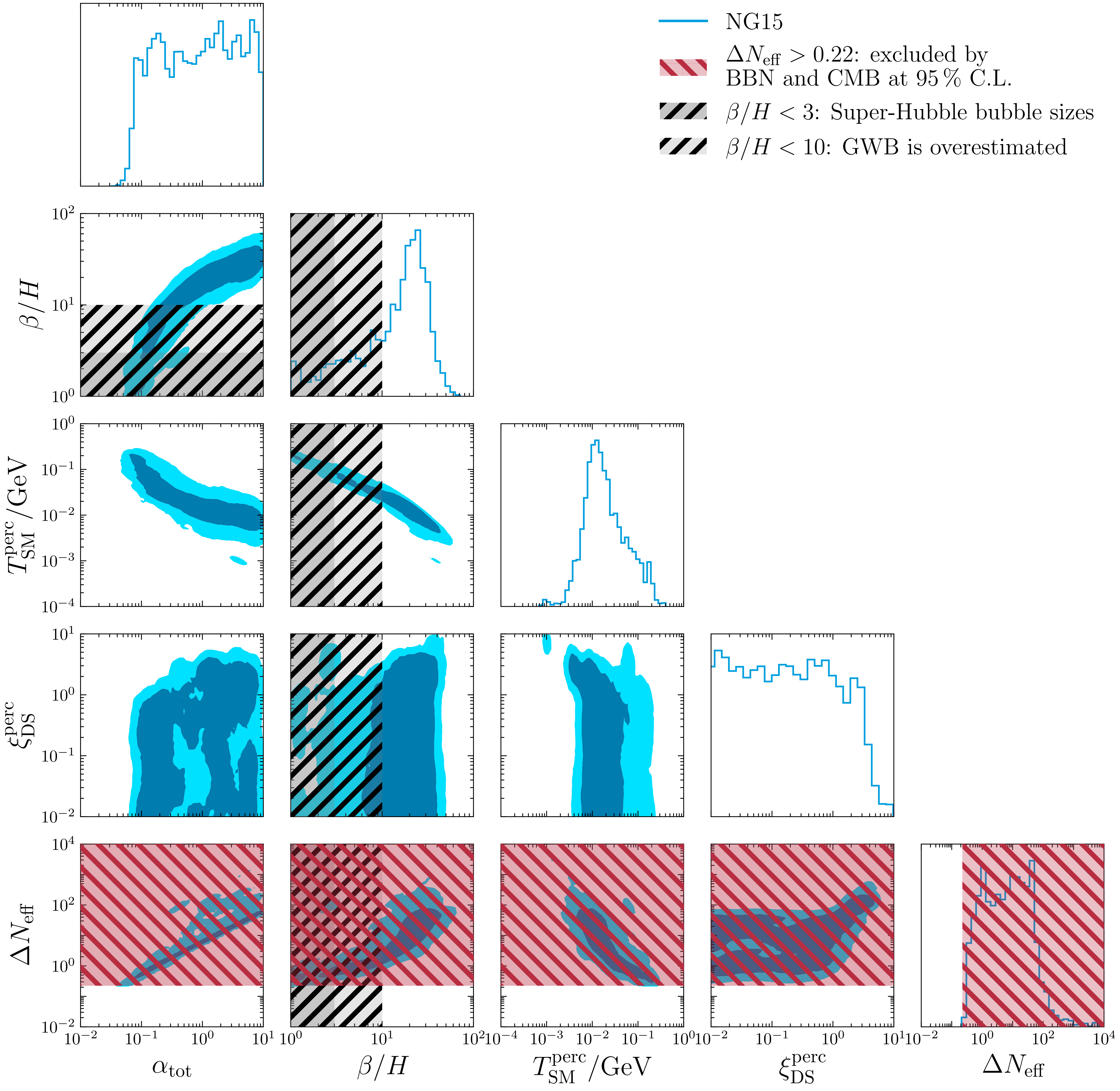

First-order phase transitions vs. cross-overs.

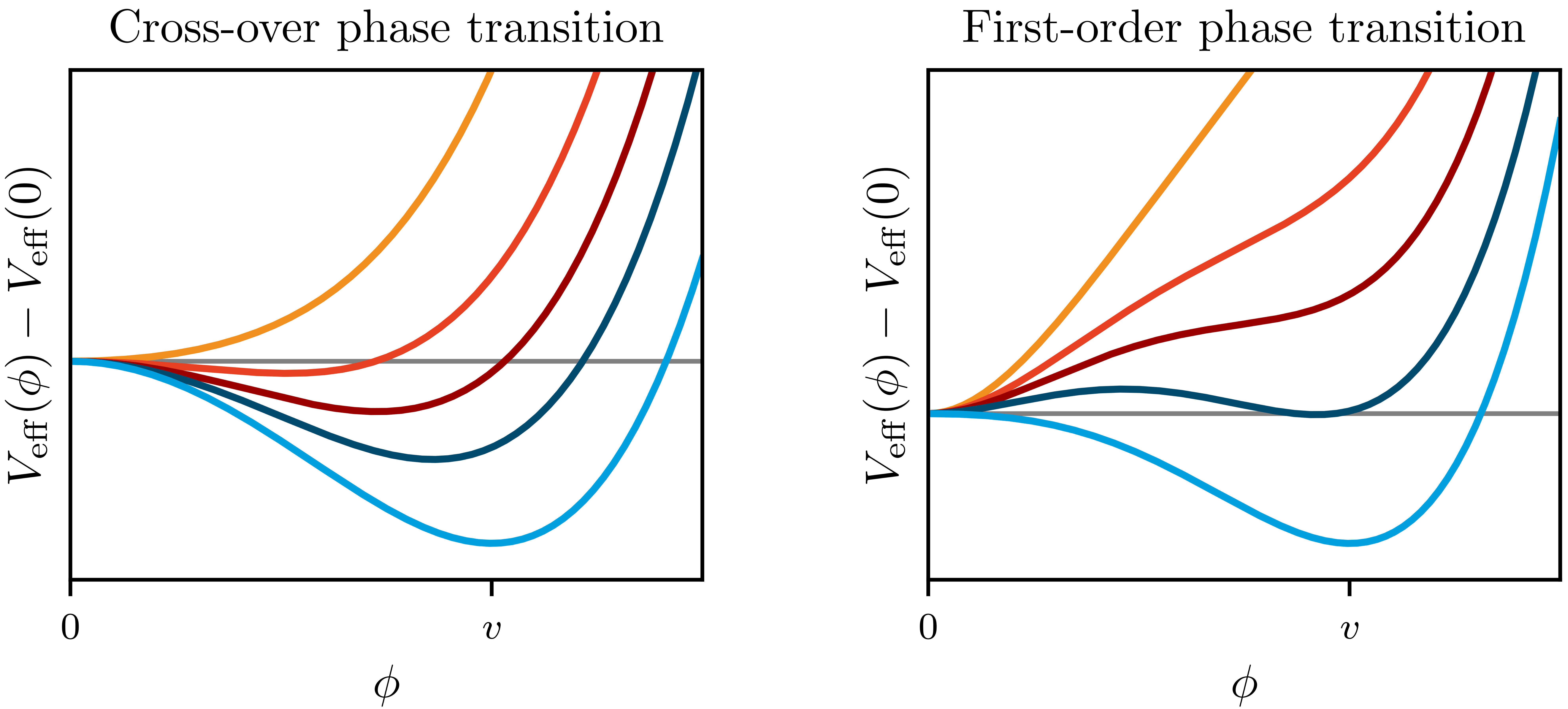

Einstein Telescope science case.

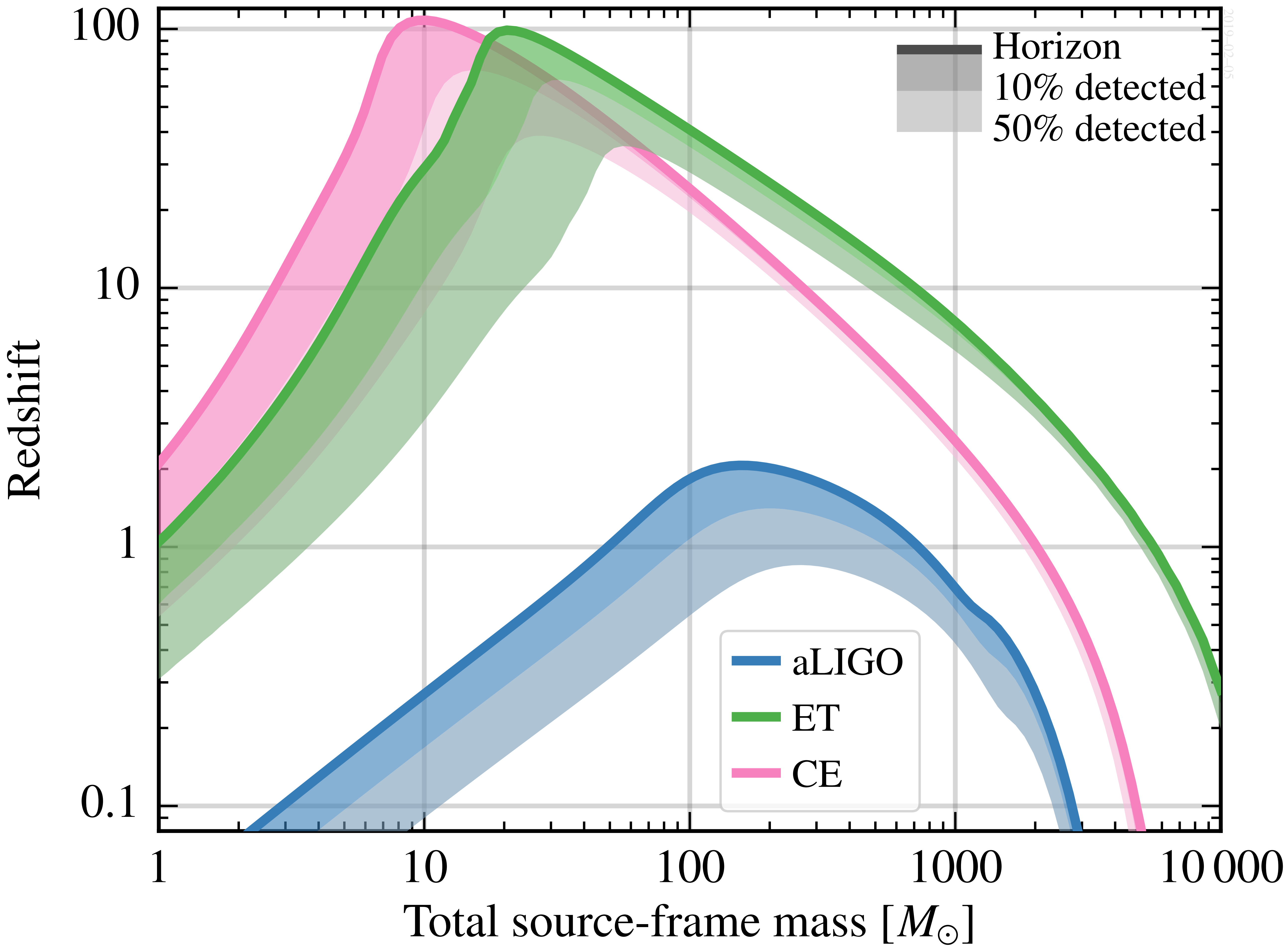

GW spectrum in characteristic strain.

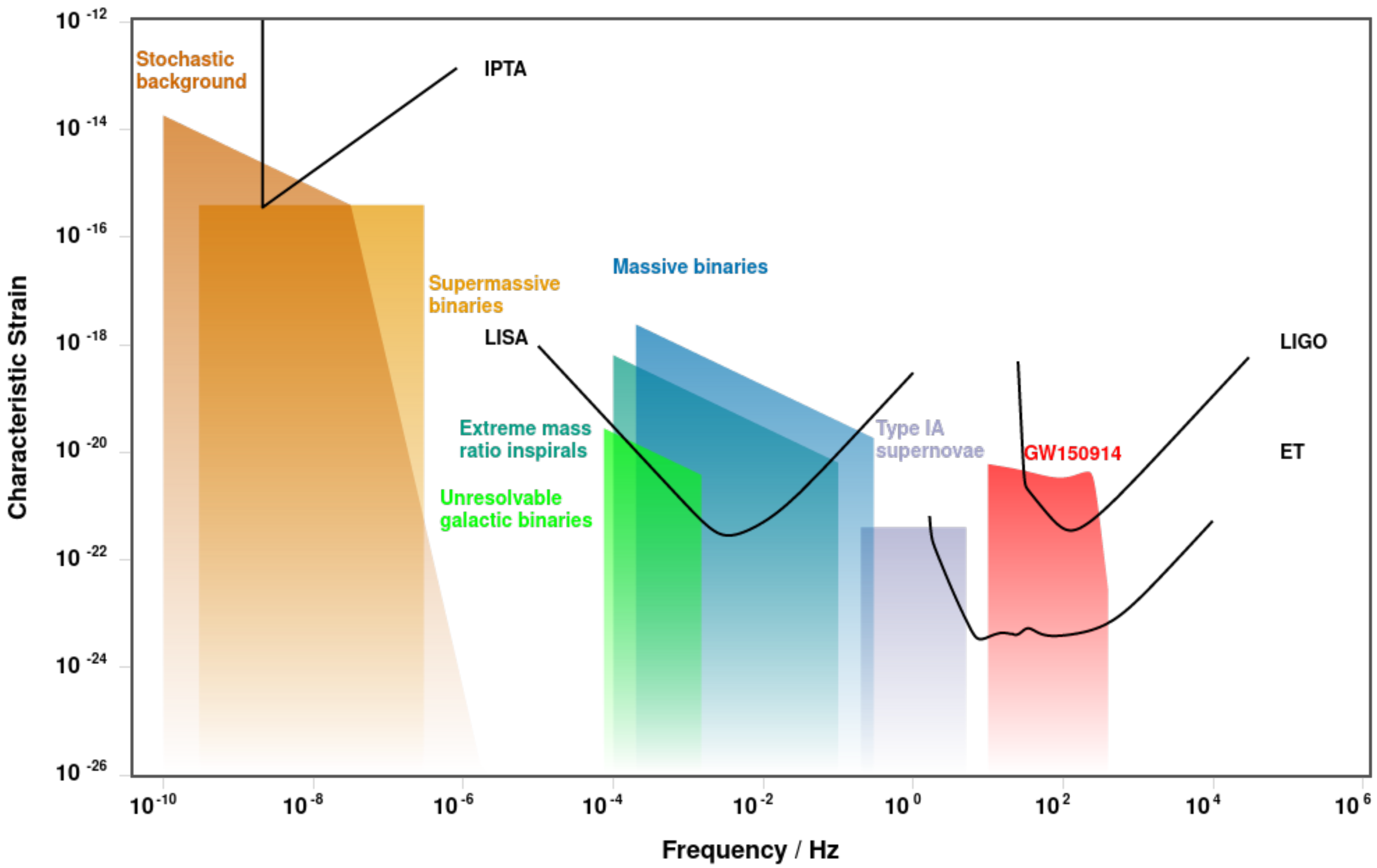

New physics interpretation of the NANOGrav 15yr data.

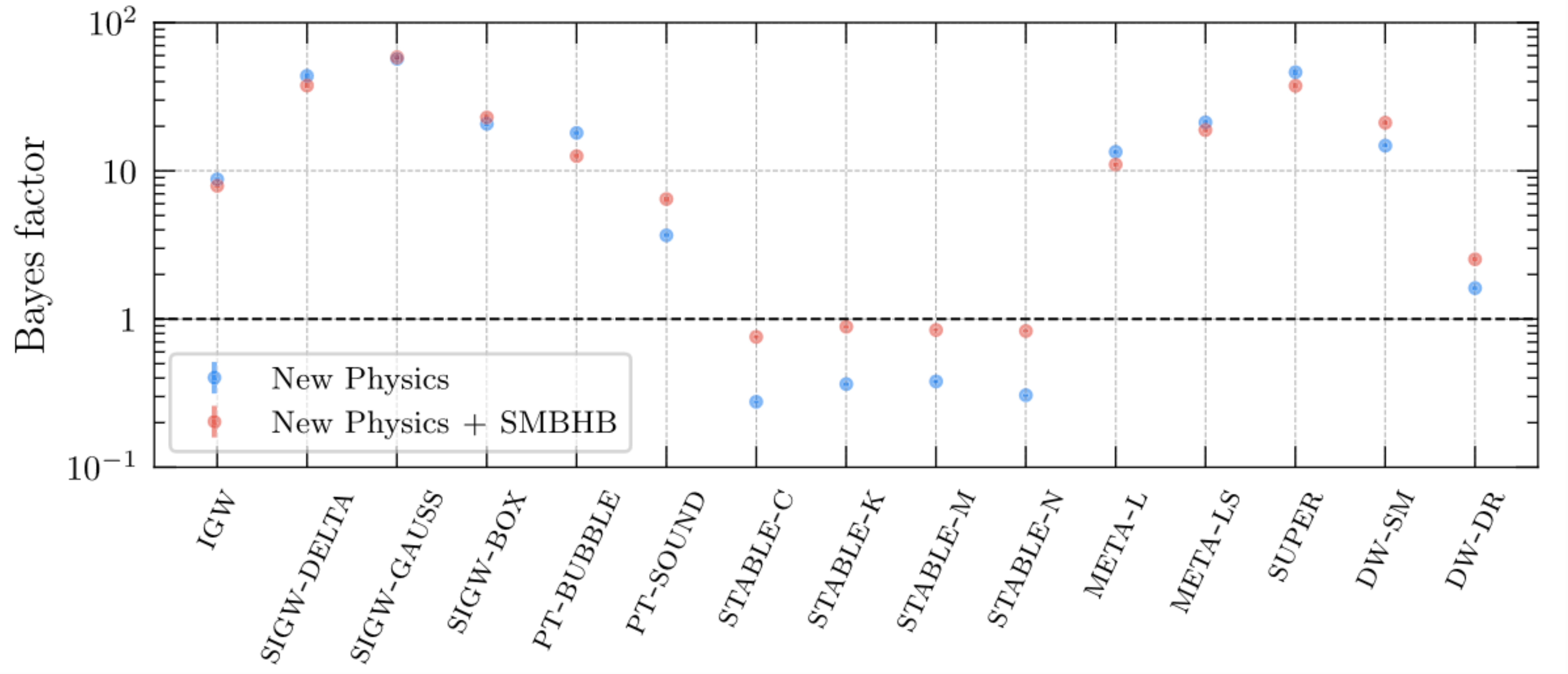

Cosmological constraints have not been included in the analysis.

Influence of eccentricity on SMBHB signals.

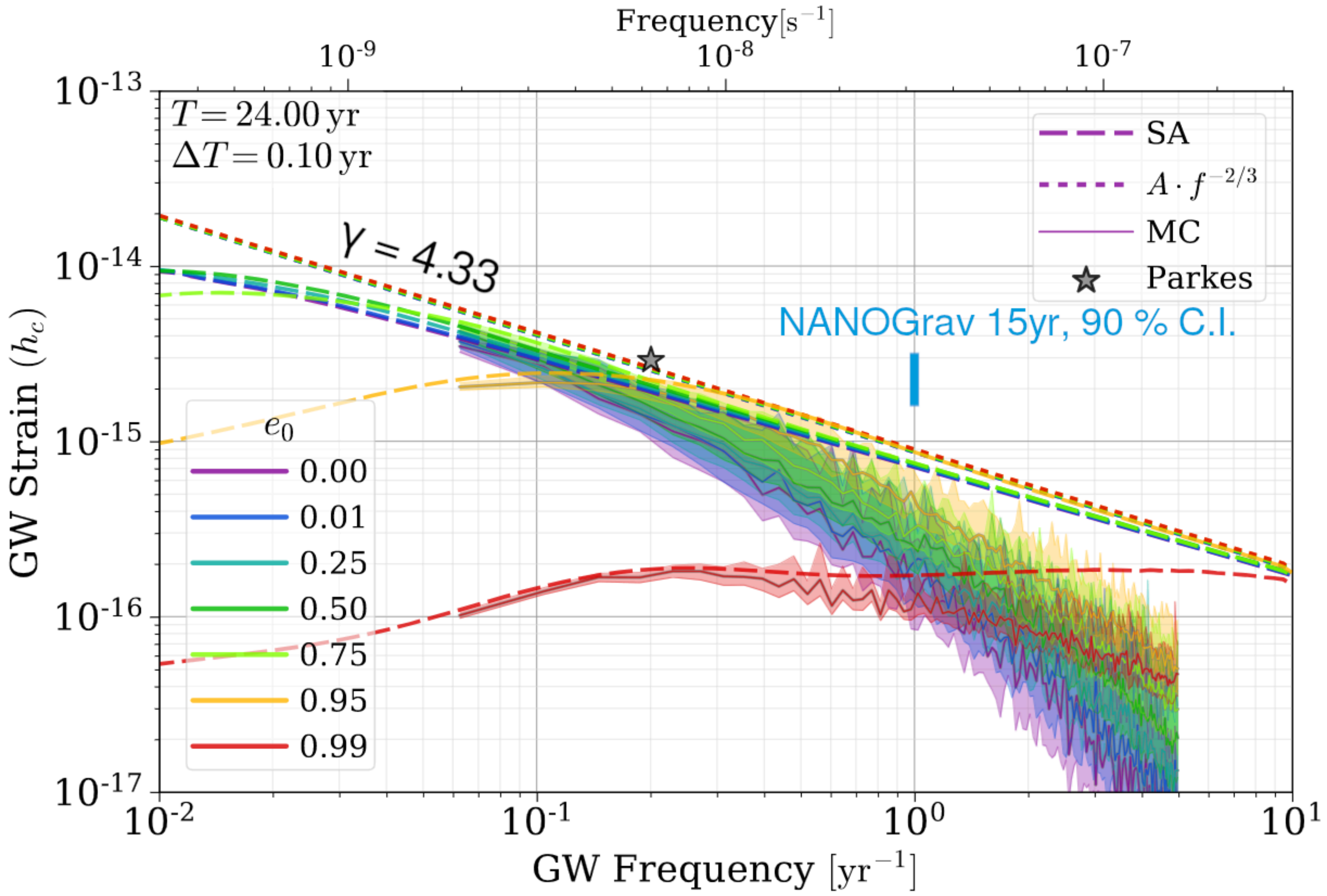

[Adapted from: Kelley+, 1702.02180]

NANOGrav 15yr data analysis.

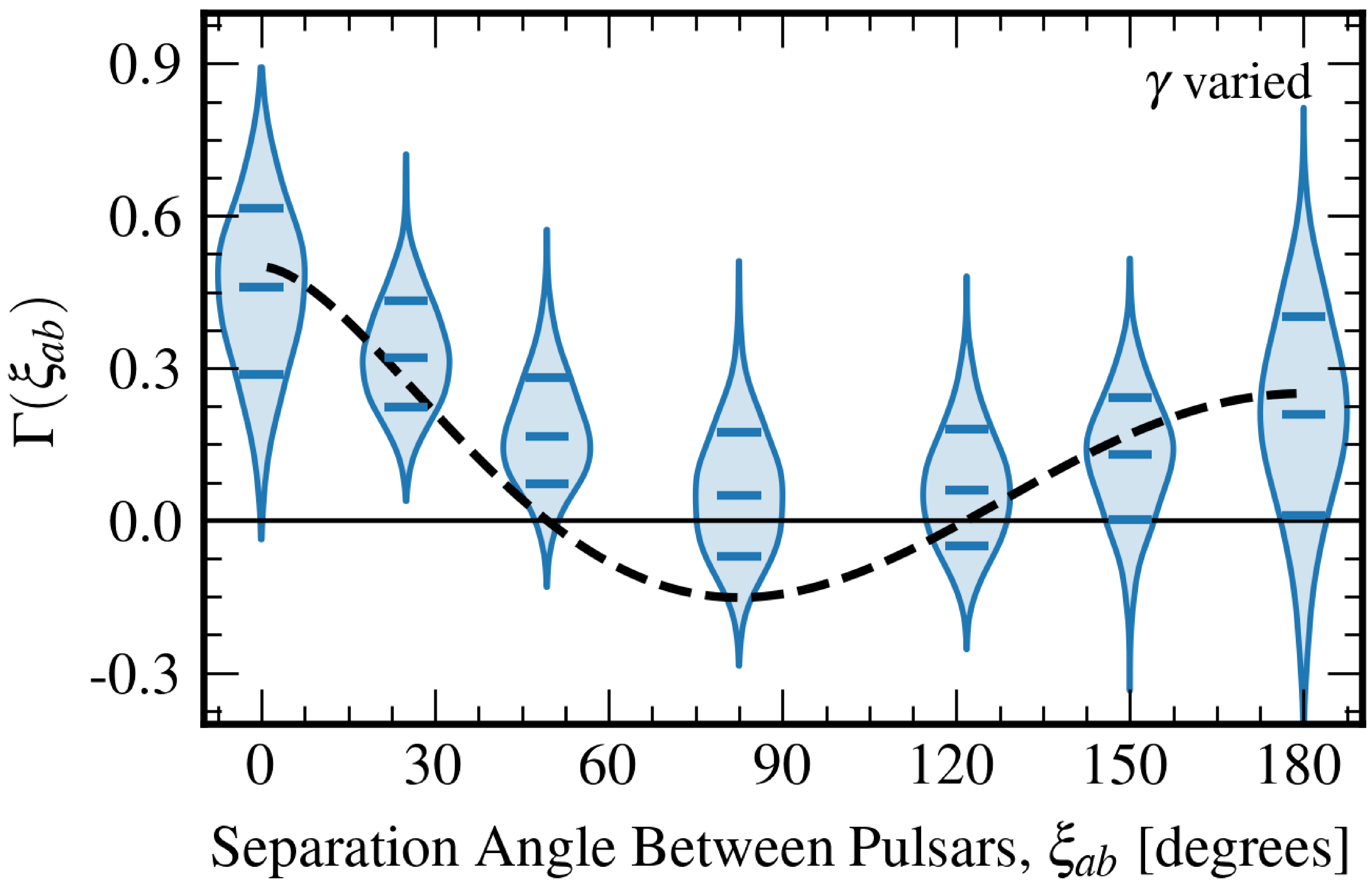

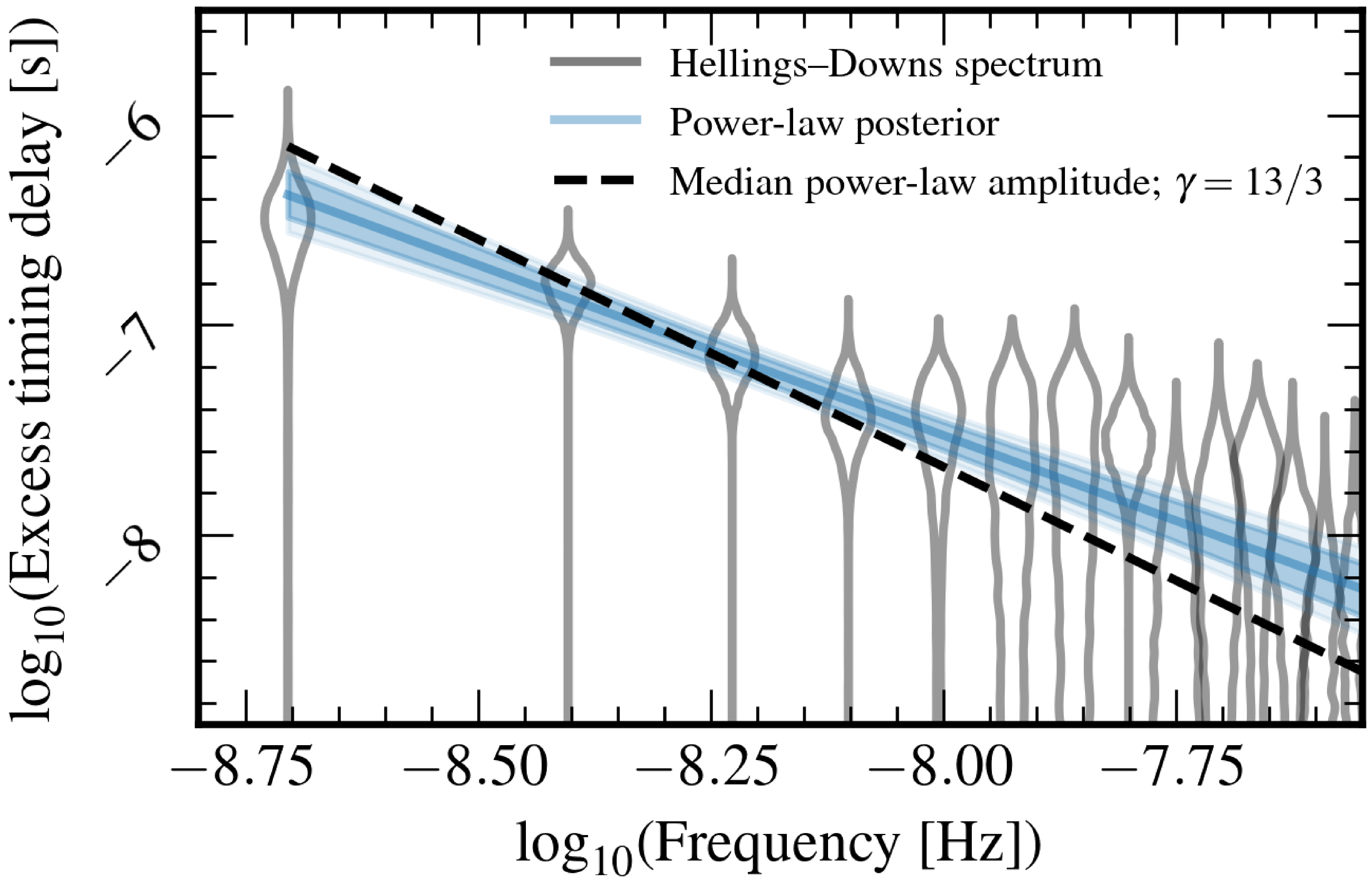

Daisy-improved effective potential.

SUMMARY Summing all discussed terms together, we obtain the one-loop, daisy-resummed effective potential of the QFT defined by the Lagrangian in eq. (4.6) [170]

$$V_{\text{eff}}(\phi, T_{\text{d}}) = V_{\text{tree}} + V_{\text{CW}} + V_{\text{ct}} + V_T + V_{\text{daisy}} \tag{4.22}$$

with the individual contributions

$$\begin{aligned}
V_{\text{CW}}(\phi) &= \sum_{a=\phi,\varphi,A',\chi} \eta_a n_a \frac{m_a^4(\phi)}{64\pi^2}\left[\ln\frac{m_x^2(\phi)}{v_\phi^2} - C_a\right],\\
V_{\text{T}}(\phi, T_{\text{d}}) &= \frac{T^4}{2\pi^2}\sum_{a=\phi,\varphi,A',\chi} \eta_a n_a\, J_{\eta_a}\left(\frac{m_a^2(\phi)}{T_{\text{d}}^2}\right),\\
V_{\text{daisy}}(\phi, T_{\text{d}}) &= -\frac{T_{\text{d}}}{12\pi}\sum_{b=\phi,\varphi,A'_{\text{L}}} n_b\left[\left(m_b^2 + \Pi_b(T_{\text{d}})\right)^{3/2} - \left(m_b^2\right)^{3/2}\right],\\
V_{\text{ct}}(\phi) &= -\frac{\delta\mu^2}{2}\phi^2 + \frac{\delta\lambda}{4}\phi^4
\end{aligned}$$

$$\begin{aligned}
\text{with}\quad \Pi_\phi = \Pi_\varphi &= \left(\frac{\lambda}{3} + \frac{y^2}{12} + \frac{g^2}{4}\right)T_{\text{d}}^2\,, \quad \Pi_{A'} = \frac{3}{4}g^2 T_{\text{d}}^2\,,\\
\delta\mu^2 &= \left[\frac{3}{2\phi}\frac{\mathrm{d}V_{\text{CW}}(\phi)}{\mathrm{d}\phi} - \frac{1}{2}\frac{\mathrm{d}^2 V_{\text{CW}}(\phi)}{\mathrm{d}\phi^2}\right]\Bigg|_{\phi=v_\phi},\\
\text{and}\quad \delta\lambda &= \left[\frac{1}{2\phi^3}\frac{\mathrm{d}V_{\text{CW}}(\phi)}{\mathrm{d}\phi} - \frac{1}{2\phi^2}\frac{\mathrm{d}^2 V_{\text{CW}}(\phi)}{\mathrm{d}\phi^2}\right]\Bigg|_{\phi=v_\phi}.
\end{aligned} \tag{4.23}$$

As above, n_a are the dofs of the fields coupled to ϕ, η_x is $+1$ (-1) for bosons (fermions), $C_a = 3/2$ $(5/6)$ are the renormalization constants for scalars and fermions (gauge bosons), and J_{η_a} are the thermal functions as defined in eq. (4.15).

Computation of the bounce.

$$\Gamma(t) = A(T_\mathrm{d}) \exp\left[-\frac{S_3(T_\mathrm{d})}{T_\mathrm{d}}\right]$$

$$S_3\left(T_\mathrm{d}\right) \equiv S_3\left[\phi_\mathrm{b}(\boldsymbol{x}; T_\mathrm{d})\right] = \int \mathrm{d}^3x \left[\frac{(\nabla\phi_\mathrm{b})^2}{2} + V_\mathrm{eff}(\phi_\mathrm{b}, T_\mathrm{d})\right]$$

$$\frac{\partial^2\phi}{\partial r^2} + \frac{2}{r}\frac{\partial\phi}{\partial r} = \frac{\mathrm{d}V_\mathrm{eff}(\phi, T_\mathrm{d})}{\mathrm{d}\phi} \equiv V'_\mathrm{eff}(\phi, T_\mathrm{d})\,.$$

$$\left.\frac{S_3(T_\mathrm{d})}{T_\mathrm{d}}\right|_{T_\mathrm{d,n}=\xi_\mathrm{n} T_\mathrm{n}} \simeq 146 - 2\ln\left(\frac{g_*(T_\mathrm{n})}{100}\right) - 4\ln\left(\frac{T_\mathrm{n}}{100\,\mathrm{GeV}}\right)$$

$$I(T) = \frac{4\pi}{3} v_\mathrm{w}^3 \int_T^{T_\mathrm{c}} \mathrm{d}T' \frac{\Gamma(T')}{T'^4\, H(T')} \left(\int_T^{T'} \frac{\mathrm{d}T''}{H(T'')}\right)^3$$

GWs from PBH mergers.

$$\Omega_{\rm gw}(f) = \frac{f}{\rho_{\rm crit}} \int_0^{t_0} {\rm d}t_{\rm r} \left(R(t_{\rm r} + \tau_{f_{\rm r}}) \frac{{\rm d}E^{\rm r}_{\rm gw}}{{\rm d}f_{\rm r}} \right)_{f_{\rm r}=(1+z)f}$$

$$\frac{{\rm d}E^{\rm r}_{\rm gw}}{{\rm d}f_{\rm r}} \simeq \frac{(\pi G)^{2/3} m_{\rm PBH}^{5/3}}{3 \times 2^{1/3}} \begin{cases} f_{\rm r}^{-1/3} & f_{\rm r} < f_1 \\ \frac{f_{\rm r}^{2/3}}{f_1} & f_1 \leq f_{\rm r} < f_2 \\ \frac{f_{\rm r}^2 f_4^4}{f_1 f_2^{4/3} [4(f_{\rm r} - f_2)^2 + f_4^2]^2} & f_2 \leq f_{\rm r} < f_3 \\ 0 & f_3 \leq f_{\rm r} \,. \end{cases} \quad (7.3)$$

$${\rm d}n_3(x,y) = \frac{n_{\rm PBH}}{2} \, {\rm e}^{-N_{\rm PBH}(y)} \, (4\pi n_{\rm PBH} \delta_{\rm dc})^2 \, x^2 \, y^2 \, {\rm d}x \, {\rm d}y$$

$$R(t_{\rm r}) = \int_0^{\tilde{x}} {\rm d}x \int_x^{\infty} {\rm d}y \, \frac{\partial^2 n_3}{\partial x \, \partial y} \, \delta(t_{\rm r} - \tau(x,y))$$

$$= \frac{9 \, \tilde{N}_{\rm PBH}^{53/37}}{296\pi \, \delta_{\rm dc} \, \tilde{x}^3 \, \tilde{\tau}} \left(\frac{t_{\rm r}}{\tilde{\tau}} \right)^{-34/37}$$

$$\times \left(\Gamma \left[\frac{58}{37}, \tilde{N}_{\rm PBH} \left(\frac{t_{\rm r}}{\tilde{\tau}} \right)^{3/16} \right] - \Gamma \left[\frac{58}{37}, \tilde{N}_{\rm PBH} \left(\frac{t_{\rm r}}{\tilde{\tau}} \right)^{-1/7} \right] \right)$$

Expected number of PBH pairs contributing to GWB.

$$\bar{N}(f_-, f_+) = \int_{f_-}^{f_+} \frac{\mathrm{d}f}{f} \int_0^\infty \mathrm{d}z \, \frac{8}{3} \, \tau_{f_\mathrm{r}} \, \frac{4\pi \left[d_c(z)\right]^2}{H(z)} \, R(t_\mathrm{r}(z) - \tau_{f_\mathrm{r}})$$

Evidence in favor of a stochastic GW background.

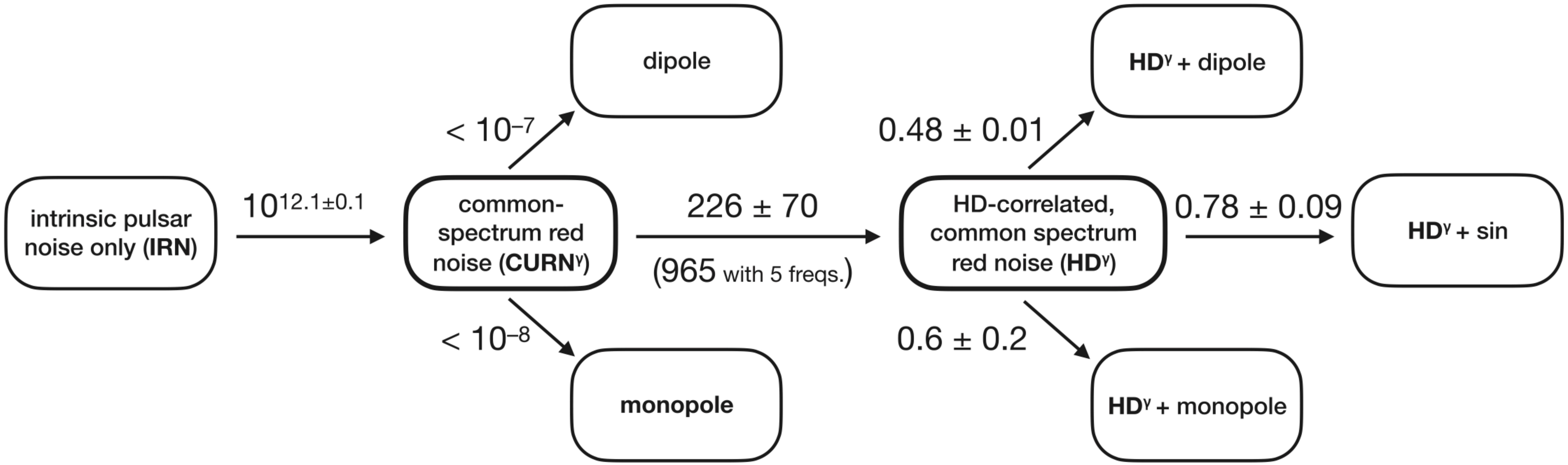

Figure 2. Bayes factors between models of correlated red noise in the NANOGrav 15 yr data set (see Section 5.3 and Appendix B). All models feature variable-γ power laws. CURN$^\gamma$ is vastly favored over IRN (i.e., we find very strong evidence for common-spectrum excess noise over pulsar intrinsic red noise alone); HD$^\gamma$ is favored over CURN$^\gamma$ (i.e., we find evidence for Hellings–Downs correlations in the common-spectrum process); dipole and monopole processes are strongly disfavored with respect to CURN$^\gamma$; adding correlated processes to HD$^\gamma$ is disfavored. While the interpretation of "raw" Bayes factors is somewhat subjective, they can be given a statistical significance within the hypothesis-testing framework by computing their background distributions and deriving the p-values of the observed factors, e.g., Figure 3.

Modeling SMBHBs.

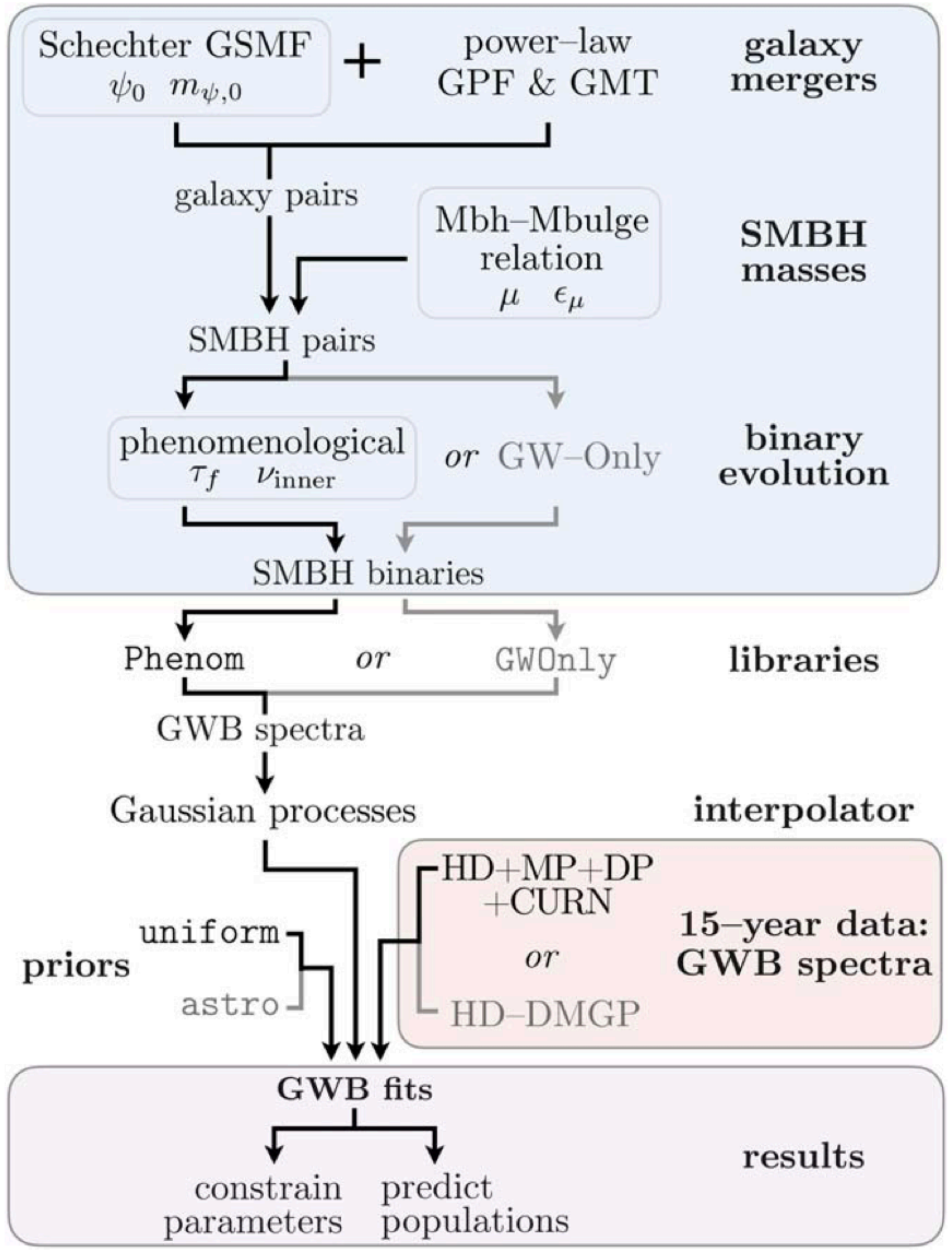

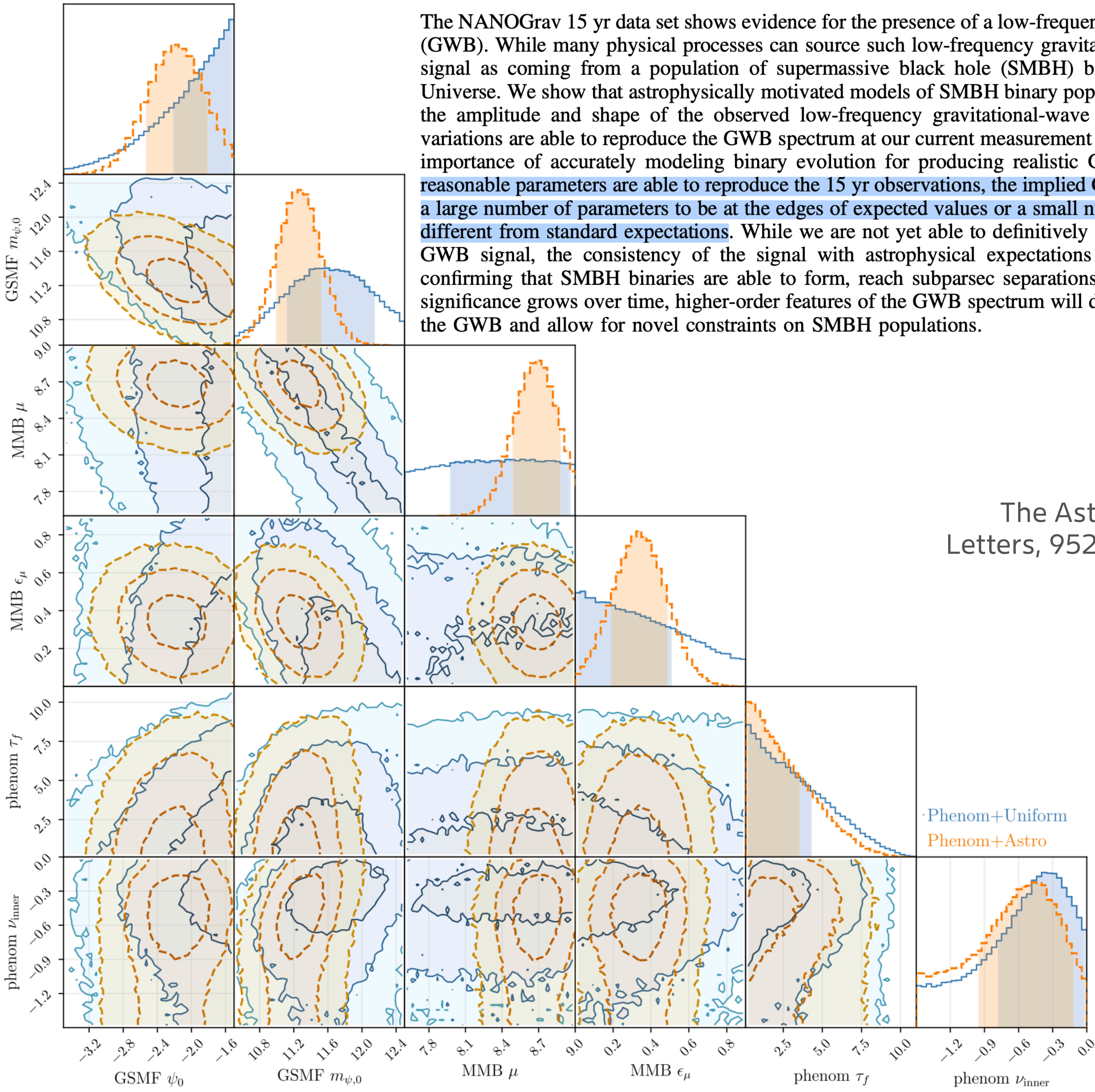

Abstract

The NANOGrav 15 yr data set shows evidence for the presence of a low-frequency gravitational-wave background (GWB). While many physical processes can source such low-frequency gravitational waves, here we analyze the signal as coming from a population of supermassive black hole (SMBH) binaries distributed throughout the Universe. We show that astrophysically motivated models of SMBH binary populations are able to reproduce both the amplitude and shape of the observed low-frequency gravitational-wave spectrum. While multiple model variations are able to reproduce the GWB spectrum at our current measurement precision, our results highlight the importance of accurately modeling binary evolution for producing realistic GWB spectra. Additionally, while reasonable parameters are able to reproduce the 15 yr observations, the implied GWB amplitude necessitates either a large number of parameters to be at the edges of expected values or a small number of parameters to be notably different from standard expectations. While we are not yet able to definitively establish the origin of the inferred GWB signal, the consistency of the signal with astrophysical expectations offers a tantalizing prospect for confirming that SMBH binaries are able to form, reach subparsec separations, and eventually coalesce. As the significance grows over time, higher-order features of the GWB spectrum will definitively determine the nature of the GWB and allow for novel constraints on SMBH populations.

The Astrophysical Journal Letters, 952:L37 (30pp), 2023 August 1

Uncertainties of the GWB amplitude from SMBHBs.

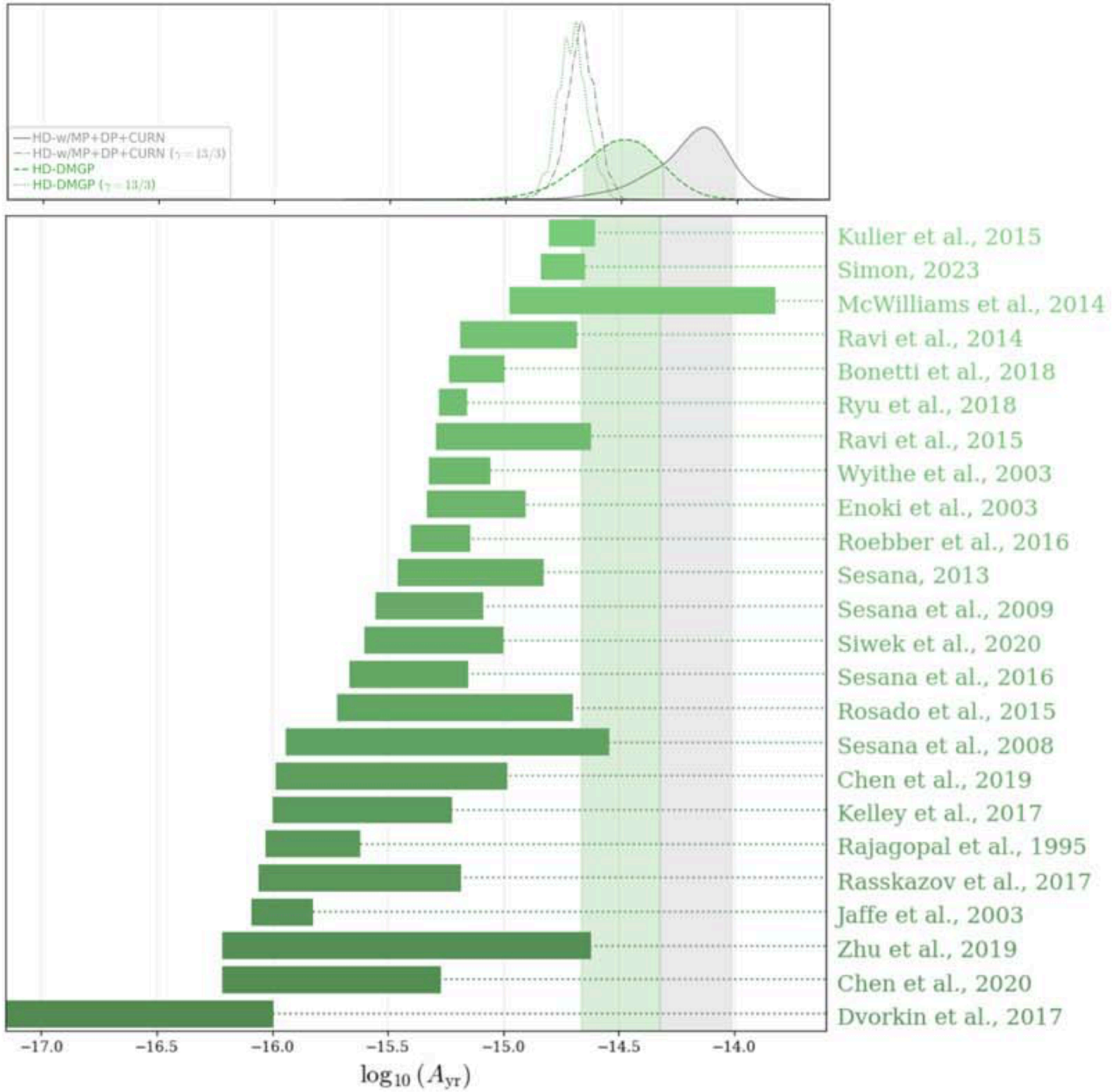

The Astrophysical Journal Letters, 952:L37 (30pp), 2023 August 1

Continuous waves in the NANOGrav 15yr data set.

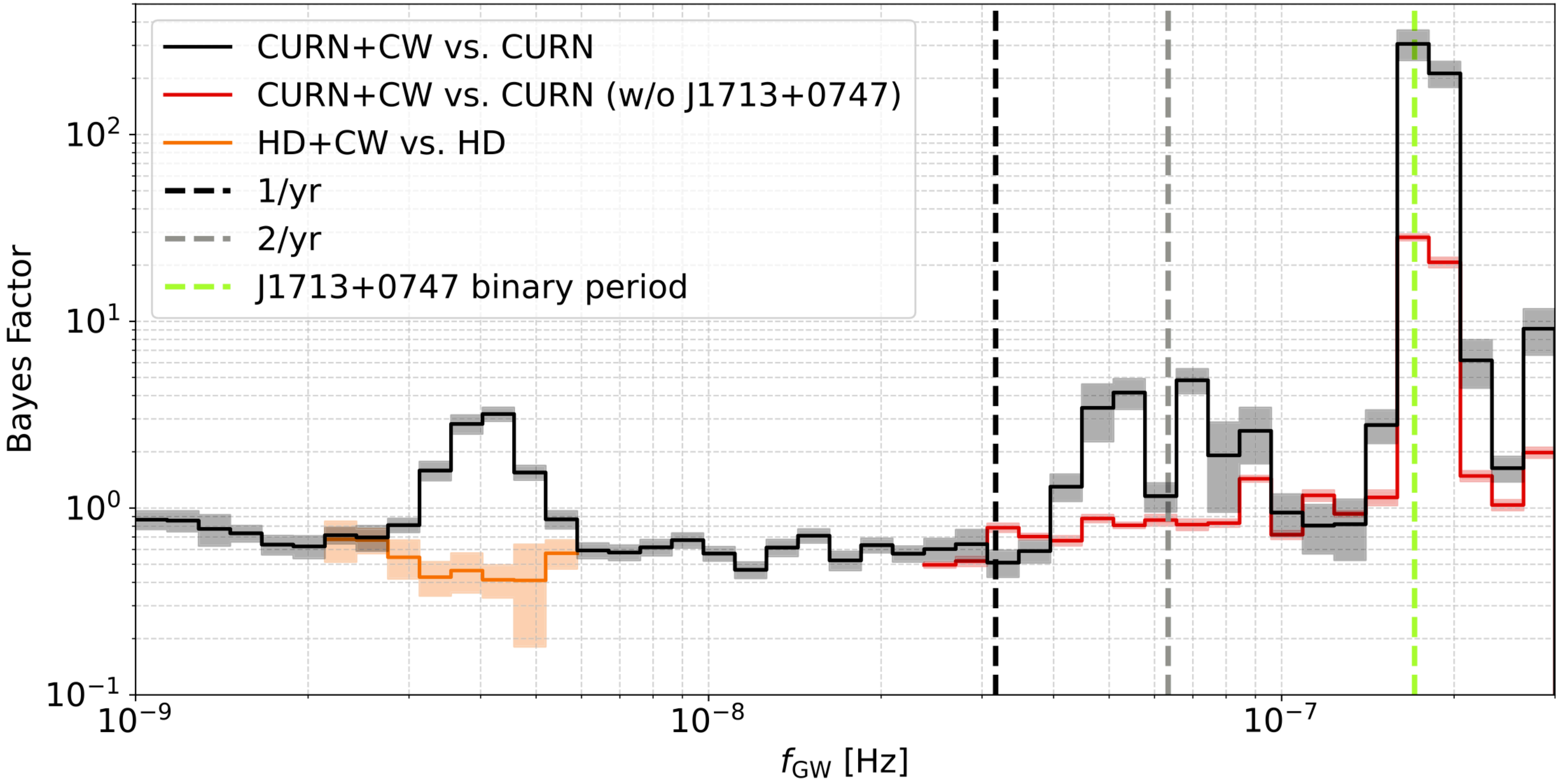

Astrophys.J.Lett. 951 (2023) 2, L50

Figure 1. Savage-Dickey Bayes factors for the CW+CURN model vs. the CURN model as a function of frequency (black). Also shown are Bayes factors when excluding PSR J1713+0747 (red, only computed for $f_{GW} > 24$ nHz) and Bayes factors based on a resampled posterior that takes into account the presence of HD correlations in the common red noise process, i.e., CW+HD vs. HD (orange, only computed for 2.1 nHz $< f_{GW} <$ 5.9 nHz). Shaded regions show the 1σ uncertainties.

NANOGrav 15yr data limits on anisotropy.

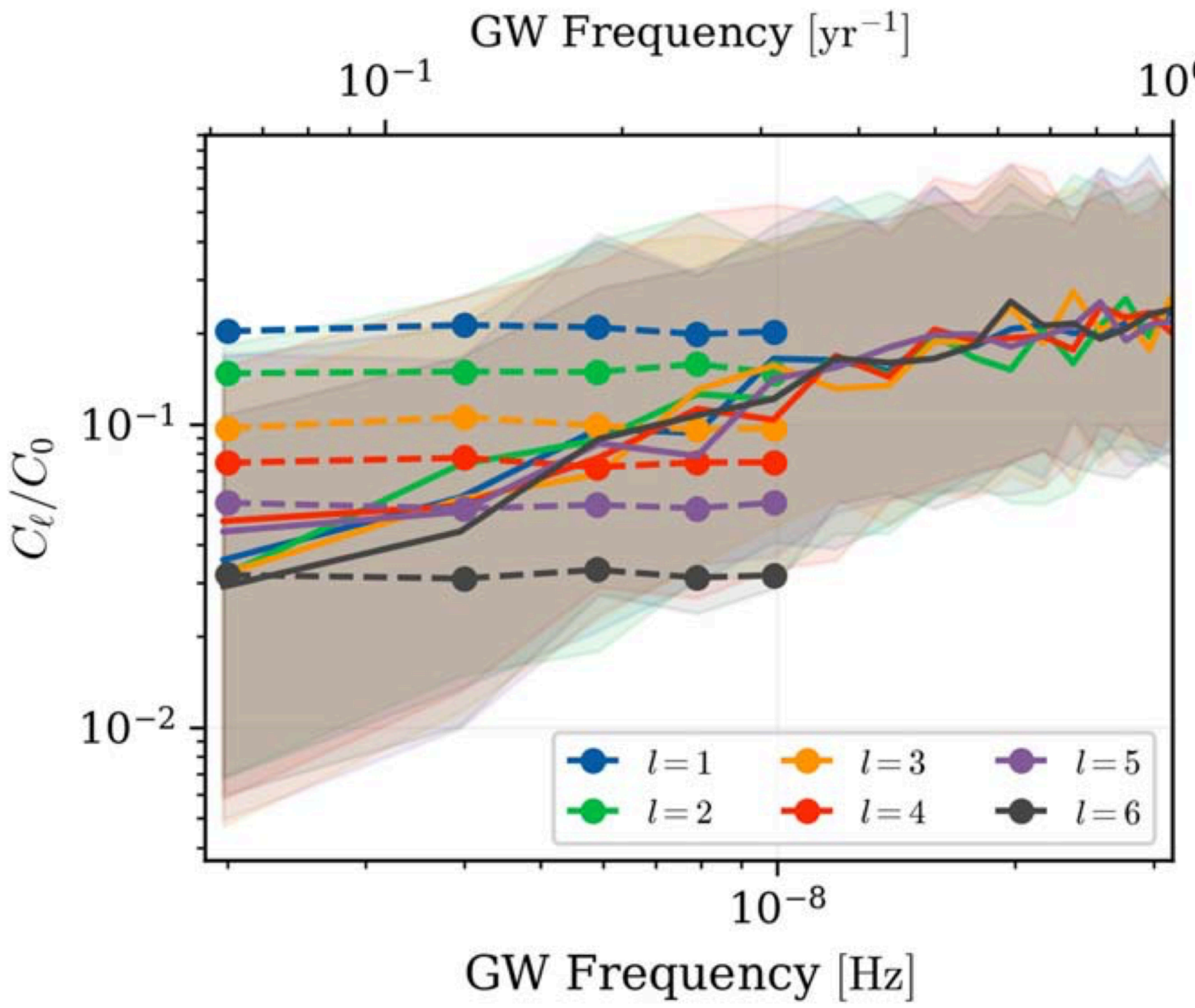

Figure 11. Normalized spherical-harmonic coefficients C_l/C_0 of the gravitational-wave sky as produced by simulated populations of SMBHBs, filtered by consistency with the 15 yr isotropic gravitational-wave background estimation (Agazie et al. 2023b). The different colors correspond to individual harmonics from $l=1$ to $l=6$. The solid lines represent the median realization of the median samples, and the shaded regions represent the 68% confidence intervals across all samples' median realizations. The circles connected by dashed lines represent the Bayesian upper limits as in Figure 5.

Abstract

The North American Nanohertz Observatory for Gravitational Waves (NANOGrav) has reported evidence for the presence of an isotropic nanohertz gravitational-wave background (GWB) in its 15 yr data set. However, if the GWB is produced by a population of inspiraling supermassive black hole binary (SMBHB) systems, then the background is predicted to be anisotropic, depending on the distribution of these systems in the local Universe and the statistical properties of the SMBHB population. In this work, we search for anisotropy in the GWB using multiple methods and bases to describe the distribution of the GWB power on the sky. We do not find significant evidence of anisotropy. By modeling the angular power distribution as a sum over spherical harmonics (where the coefficients are not bound to always generate positive power everywhere), we find that the Bayesian 95% upper limit on the level of dipole anisotropy is $(C_{l=1}/C_{l=0}) < 27\%$. This is similar to the upper limit derived under the constraint of positive power everywhere, indicating that the dipole may be close to the data-informed regime. By contrast, the constraints on anisotropy at higher spherical-harmonic multipoles are strongly prior dominated. We also derive conservative estimates on the anisotropy expected from a random distribution of SMBHB systems using astrophysical simulations conditioned on the isotropic GWB inferred in the 15 yr data set and show that this data set has sufficient sensitivity to probe a large fraction of the predicted level of anisotropy. We end by highlighting the opportunities and challenges in searching for anisotropy in pulsar timing array data.

The Astrophysical Journal Letters, 956:L3 (15pp), 2023 October 10

Different models for the GW spectrum from a FOPT.

	IR	UV	References
Envelope	3	−1	[16, 27]
Bulk flow	1	−3	[17, 28]
Scalar lattice	3	−1.5	[38]

	IR	Intermediate	UV	References
Sound shell	9	1	−3	[22, 23]
Scalar + fluid lattice	—	1	−3	[18, 20, 21, 29]
Hybrid	[2,4]	[−1,0]	[−4,−3]	[30]
Higgsless	3	1	−3	This work

JCAP02(2023)011, Jinno, Konstandin, Rubira, Stomberg

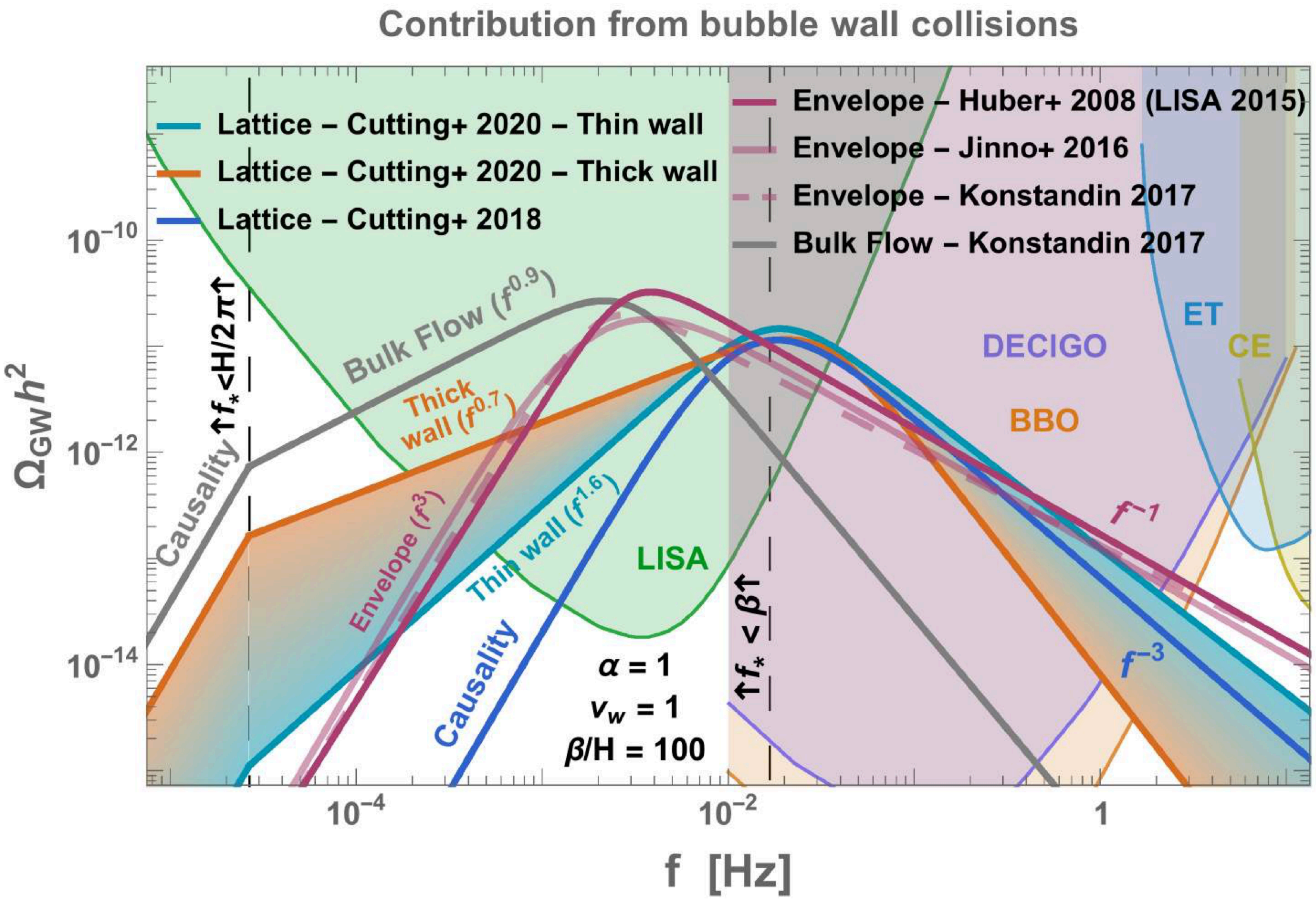

Yann Gouttenoire: Beyond the Standard Model Cocktail